Calreticulin Overexpression: A Mouse Model of Human Hemangioendothelioma

By
Melanie Merle Durston

A Thesis
Submitted to the Faculty of Graduate Studies
In Partial Fulfillment of the Requirements
For the Degree of

MASTER OF SCIENCE

Department of Biochemistry and Medical Genetics
Faculty of Medicine
University of Manitoba
and the Institute of Cardiovascular Sciences
St. Boniface General Hospital Research Centre
Winnipeg, MB

THE UNIVERSITY OF MANITOBA

FACULTY OF GRADUATE STUDIES

*****

COPYRIGHT PERMISSION

Calreticulin Overexpression: A Mouse Model of Human Hemangioendothelioma

BY

Melanie Merle Durston

A Thesis/Practicum submitted to the Faculty of Graduate Studies of The University of Manitoba in partial fulfillment of the requirement of the degree

MASTER OF SCIENCE

ABSTRACT

Blood vessel development is a tightly regulated process that involves growth factors, proteases, coagulation factors and the role they play in endothelial and vascular smooth muscle cell proliferation and migration. Blood vessel remodeling is critical during many physiological as well as pathological conditions such as: embryonic development, wound healing, the female reproductive cycle, development of cancer, vascular tumors and cardiovascular disease. Calreticulin (CRT) is an ER resident protein, which plays a role in calcium handling, protein folding and cell adhesion. CRT is highly expressed in the vascular wall during embryonic development and in the adult. Gene targeted deletion of *Crt* is embryonic lethal due to defects in cardiovascular development. These defects in the cardiovascular system could result as a consequence of altered extracellular matrix (ECM) composition, as *Crt* deletion results in altered expression and activity of matrix metalloproteinases (MMP)-2 and -9. Exogenously applied CRT has also been demonstrated to reduce intimal hyperplasia after arterial injury in rats, to inhibit endothelial cell (EC) migration *in vitro*, and to play an inhibitory role in tumor angiogenesis. These observations suggest a regulatory role for CRT in angiogenesis and vascular remodeling. Therefore, we have developed a mouse model of CRT overexpression in vascular smooth muscle cells (termed as *SMCRT* mice) to determine the role of endogenous CRT in vascular remodeling and function.

Adult male *SMCRT* mice developed skin lesions and defects in the cardiovascular system: including increased coronary angiogenesis, coronary

aneurysm, platelet aggregation, altered vessel wall mechanics and dilated cardiomyopathy. However, the major defect in the *SMCRT* mice is the development of an aggressive vascular tumor mainly associated with the arteries of the heart and lungs. The pathology of the *SMCRT* mice is very similar to a rare human vascular tumor, called hemangioendothelioma.

Our results demonstrated that CRT overexpression in the vascular smooth muscle cells resulted in decreased ECM components, increased activity of MMP-2 and MMP-9, and decreased expression of connexins 40 and 43. These structural changes in the blood vessel wall likely resulted in the proliferation and migration of EC which led to the and development of an endothelial derived vascular tumor similar to hemangioendotheliomas in humans. This study describes a novel role for CRT in blood vessel development and a unique animal model for human hemangioendothelioma.

ACKNOWLEDGEMENTS

I would first like to acknowledge my supervisor Dr. Nasrin Mesaeli for supporting my decision to go back to school, and allowing me the opportunity to complete my Master's in her laboratory. Thank you so much for your guidance and encouragement. I owe my success in this laboratory to your supervision, assistance and mentorship.

I would also like to thank my committee members Dr. Jeff Wigle and Dr. Hope Anderson for their collaboration, guidance, and finally for their kind support and encouragement. I would also like to thank the members of the Wigle and Anderson Labs who have become such great friends, and who provided support when I really needed it. I would like to give special thanks to Lam for helping me so much with my project, and to Josette for your constant support and help!

I am grateful to all the members of the Mesaeli Lab past and present who have made my time in the lab so rewarding. I would like to thank Tina, Lise, Lori, Pooran, Shahrzad, Anton, and Azadeh for their friendship, and support. I would especially like to thank Mike, Min, Maliheh and Behzad for their help and contributions to this work. A special thank you also to the members of the R.O. Burrell Animal Holding Facilities at SBRC, without your help I would never have been able to complete this work.

Most importantly, I would like to thank my parents and Steve for supporting my decision to go back to school, and helping me get through it all. To Steve thank you so much for helping me get through the long hours and frustrating times, your support has meant the world to me!!

TABLE OF CONTENTS

LIST OF FIGURES

LIST OF TABLES

LIST OF ABBREVIATIONS

Ang	Angiopoietins
BL-CFC	Blast Colony Forming Cells
CAM	Chorioallatoic Membrane Assay
COUP-TF	Chicken Ovalbumin Upstream Promoter-Transcription Factor
CRT	Calreticulin, protein
Crt	Calreticulin, gene
CSA	Cross section Area
DAB	Diaminobenzidine
DIC	Disseminating intravascular coagulopathy
DMEM	Dulbecco Minimum Essential Medium
E	Embryonic Day
EC	Endothelial Cells
ECM	Extracellular Matrix
EDHF	Endothelial-Derived Hyperpolarizing Factor
ER	Endoplasmic Reticulum
ES	Embryonic Stem Cells
ET-1	Endothelin-1
FBS	Fetal Bovine Serum
FGF-2	Fibroblast Growth Factor -2
GLUT-1	Glucose Transporter-1
GPF	Green Fluorescent Protein
GPI	Glycosylphosphatidyl Inositol
H&E	Hematoxylin & Eosin Stain
HA	Hemaglutannin-tag
HAE	Hemangioendothelioma
HC	Hematopoietic Cells
HPF	High Powered Field
IL-12	Interleukin-12
IP-10	Inducible protein-10
IP_3	Inositol 1,4,5 triphosphate
KMS	Kasabach-Merritt Syndrome
LeY	Lewis Y- Antigen
MEF	Mouse Embryonic Fibroblasts
MEF2C	Myocyte Enhancer Factor 2C
MLC	Myosin light chains
MLC2v	Ventricular Myosin Light Chain 2
MLCK	Myosin light chain kinase
MLCP	Myosin light chain phosphatase
MMP	Matrix Metalloproteinases
MT-MMP	Membrane Type-Matrix Metalloproteinase

NF-AT	Nuclear Factor of Activated T-cell
NO	Nitric Oxide
PA	Plasminogen Activator
PAF	Platelet activating Factor
PBS	Phosphate Buffered Saline
PCNA	Proliferating Cell Nuclear Antigen
PDGF	Platelet Derived Growth Factor
PDGFR	Platelet Derived Growth Factor Receptor
PDI	Protein Disulfide Isomerase
PGH2	Prostaglandins
PGI2	Prostacyclin
RBC	Red Blood Cells
RD	Rhabdomyosarcoma cells
RPE	Retinal Pigment Epithelial Cells
RTK	Receptor Tyrosine Kinases
SERCA	Sarcoplasmic/Endoplasmic Reticulum Ca^{2+} ATPase
SMαA	Smooth Muscle Alpha Actin
SMC	Smooth Muscle Cells
SMCRT	Calreticulin overexpressing transgenic mice
SR	Sarcoplasmic Reticulum
TF	Tissue Factor
TFPI	Tissue Factor Pathway Inhibitor
Tg	Transgenic
TIMP	Tissue Inhibitors of MMPs
tPA	Tissue Plasminogen Activator
uPA	Urokinase Plasminogen Activator
VEGF	Vascular Endothelial Growth Factor
VSMC	Vascular Smooth Muscle Cells
vWF	von Willebrands Factor
wt	Wild type mice

A. REVIEW OF LITERATURE

I. Blood Vessel Development

I.1. Introduction

The circulatory system consists of the heart, blood cells and an intricate network of blood vessels that are responsible for the distribution of essential nutrients and oxygen to support the tissues, and for the removal of the byproducts of metabolism from the tissues. Additionally, the blood vessels serve as conduits for signaling molecules and cells of the immune system. The importance of the circulatory system is underlined by the fact that it is the first functional organ system to develop in the embryo, with the blood vessels distributing blood and nutrients to the embryonic tissues even before the heart starts pumping [1, 2]. Once the presumptive vasculature has been formed in the embryo, the vessels undergo processes of remodeling to strengthen and enlarge existing vessels, and branching (angiogenesis) to expand the vascular network [3]. In adulthood, angiogenesis plays a vital role in wound healing, the female reproductive cycle and in the development of diseases [4, 5]. Angiogenesis is a multi-step process that is regulated by many stimulatory and inhibitory factors that are maintained in a tightly regulated counterbalance [4, 5]. Disruption of this strict balance of regulators leads to the development of pathologies including hemangiomas [5], cancers, inflammatory and ischemic diseases [4]. Therefore, by studying the stages of blood vessel development and the factors that regulate them it may be possible to develop novel treatments for disease.

I.2. Blood Vessel Structure

All blood vessels are made up of 3 concentric layers, called tunics, which are composed of different cell types that serve distinct functions. These layers arranged from the vessel lumen outward, are the tunica intima, tunica media and the tunica adventitia [6]. Assembly of these layers into a mature blood vessel is a stepwise process that begins with mesoderm development and will be described in detail in the following sections.

I. 2.i. Tunica Intima and the Endothelium

The tunica intima is the innermost layer of the blood vessel, which faces the vessel lumen and is solely comprised of the endothelium. The endothelium is a monolayer of endothelial cells (EC) that lines the entire cardiovascular and lymphatic systems [6, 7]. In culture, EC have a flattened polygonal shape, and form tight monolayers described as having a "cobblestone" appearance [8-10]. *In vivo* however, EC show heterogeneity in their structure, cellular connections and functions which varies with the size of vessels and the organs in which they are located [7, 11]. For instance, EC in large arteries have the characteristic polygonal shape of cultured cells, whereas EC lining micro-vessels tend to be more elongated and flattened. Tight, continuous endothelium is characteristic of organs such as the brain and retina where maintenance of a strict barrier is required. In organs such as the kidney and glands however, the endothelium is a discontinuous layer of cells with intracellular fenestrations or gaps allowing for efficient nutrient and gas exchange between the tissues and blood [7, 11]. The

tightness of the connections between EC can also be modulated under different conditions by various regulatory factors. For instance, Vascular Endothelial Growth Factor (VEGF) increases the permeability EC layers prior to angiogenesis [12-14]. The endothelium of all blood vessels is supported by a basement membrane composed of collagen (type IV) [15], proteoglycans and fibronectins and laminin, which are produced and secreted by the EC [16, 17].

I. 2.i.a. Endothelial cell markers

Despite EC heterogeneity, there are several proteins that are used as universal markers for the identification and characterization of EC *in vivo* and *in vitro*. EC contain a unique vesicular organelle called the Weibel-Palade bodies which function in the storage and regulated secretion of factors involved in hemostasis and inflammation [18]. These organelles appear as small cigar shaped structures in the EC using electron microscopy [7, 18]. One of the major protein components of the Weibel-Palade bodies, von Willebrands Factor (vWF), is an important regulator of hemostasis as it is involved in the recruitment of platelets to the sites of injury, and acts as a chaperone for the coagulation Factor VIII. vWF is considered to be a universal protein marker for blood EC. Another common marker for EC is CD31, also called Platelet Endothelial Cell Adhesion Molecule-1 (PECAM-1). CD31 is a 130 kDa glycoprotein belonging to the immunoglobulin (Ig) superfamily of cell adhesion molecules and is expressed only in cells of the vascular system such as platelets, white blood cells, and EC [19]. CD31 is a useful marker for EC as it is expressed in the endothelial precursors (angioblasts) in early development and in adult endothelium of the

blood and lymphatic vasculature [19]. CD34 is another cell surface glycoprotein that is commonly used as a marker for blood EC. This glycoprotein is expressed on hematopoietic stem cells [20], endothelial precursor cells [21] and EC of blood vessels [22, 23]. CD34 has been demonstrated to play significant roles in hematopoiesis [20, 24], immune response [23] and blood vessel development [20]. The above proteins are just a brief list of the many markers used to identify EC for *in vivo* and *in vitro* study.

I. 2.i.b. Endothelial cell function

Historically the endothelium was viewed to function as an inert barrier between the circulation and surrounding tissues, but it is now known that the endothelium is a dynamic organ that has many functions [11]. First of all, the endothelium serves as a barrier that actively regulates the movement of molecules and the migration of cells into and out of the circulating blood. Another key function of the endothelium is the regulation of vascular tone via the secretion of vasoactive molecules that act directly on vascular smooth muscle cells. These include both factors that promote smooth muscle cell relaxation, including nitric oxide (NO), prostacyclin (PGI2) and the Endothelium-Derived Hyperpolarizing Factor (EDHF), or promote constriction such as endothelin-1 (ET-1), Platelet Activating Factor (PAF) and prostaglandins (PGH2) [11, 25]. Two key functions of the endothelium that are of interest to us are its role in blood vessel development, which we will discuss in the following sections, and its role in hemostasis.

Blood coagulation can be separated into the primary cellular response, which involves platelet activation, and secondary hemostasis, which refers to the classical coagulation cascade of soluble circulating clotting factors that generate the fibrin clot. The endothelium plays a key role in both of these stages of coagulation as the ECs produce and secrete a number of factors that regulate platelet aggregation and activation of thrombin, the protease that initiates fibrin clot formation from fibrinogen [26, 27]. Intact healthy endothelium has a smooth surface that is not conducive for platelet adhesion. EC also express factors such as tissue factor pathway inhibitor (TFPI), which binds tissue factor (TF) and factors VIIa and Xa thereby preventing their ability to activate thrombin, and thrombomodulin which binds and inactivates thrombin directly [11, 28]. PGI2 which is secreted by EC as a vasodilator also strongly inhibits platelet aggregation [28]. Damage or inflammation converts the endothelium to a pro-thrombotic state. These insults induce TF, which initiates the coagulation cascade, and expose the sub-endothelial matrix to the plasma [11]. vWF secreted by the EC mediates platelet adhesion to the sub-endothelial matrix, which in turn, results in platelet aggregation and activation. The activated platelets release a number of factors which further stimulate the secondary coagulation cascade and fibrin clot formation [26]. It is important to note that some of the factors involved in the coagulation cascade and that are secreted by activated platelets, are important for angiogenesis since effective wound healing requires new blood vessel formation.

I. 2.ii.c. Endothelial cell attachments

EC attachment to the extracellular matrix (ECM) is important for cell survival, proliferation, migration and differentiation. A family of transmembrane glycoproteins that are expressed on the cell surface, called integrins, mediates these cell-matrix attachments [29]. Integrins are heterodimeric glycoproteins composed of α and β subunits. There are 18 known α and 8 β subunits, which assemble into 24 known distinct integrins. EC express many integrins including $\alpha1\beta1$, $\alpha2\beta1$, $\alpha3\beta1$, $\alpha6\beta4$, $\alpha5\beta1$, $\alpha v\beta3$, and $\alpha v\beta5$, all of which have different substrate specificities. Integrin $\alpha v\beta3$ binds a number of substrates such as fibronectin, thrombospondin, laminin, vWF and denatured collagen [29]. Integrin $\alpha v\beta3$ is implicated in blood vessel development [29-31] as it has been shown to be localized on newly developing vessels *in vitro* and *in vivo* [30, 31].

I. 2.ii. Tunica media and the vascular smooth muscle cell

The tunica media, the middle layer of the blood vessel is composed of mural cells, such as vascular smooth muscle cells (VSMC) and/or pericytes, elastin fibers and collagen. In larger caliber vessels such as arteries and veins the medial layer is composed of continuous layers of circumferentially arranged VSMCs [6], with arteries and arterioles generally having larger VSMC layers than veins. The VSMCs of the mature vessel are elongated spindle shaped cells containing one centrally located nucleus and criss-crossing networks of myofilaments in the myoplasm [32]. These contractile VSMCs are generally quiescent showing little division, migration or matrix production. VSMCs under

certain conditions (injury) can alter their phenotype to a more immature form, and these cells are capable of proliferation, migration and production of ECM such as collagen [33]. In smaller caliber vessels such as venules and capillaries the medial layer is small or almost non-existent. In these vessels the EC layer is often supported by pericytes instead of smooth muscle cells [33, 34]. Pericytes are elongated cells with long cytoplasmic extensions that wrap around the circumference of the capillary, are embedded in the basement membrane, and have direct contact with the endothelium. This pericyte layer unlike the smooth muscle cell layer is discontinuous [34].

I. 2.ii.a. Vascular smooth muscle cell markers

Smooth muscle specific isoforms of contractile proteins are the most commonly used markers for VSMCs [33]. One of the most extensively used markers is smooth muscle alpha actin (SMαA) [35-37]. SMαA makes up a large portion (40%) of total VSMC protein and is therefore a useful marker for these cells [33]. Pericytes have also been demonstrated to stain positive for this marker [34]. SMαA has been demonstrated to label VSMC precursor cells and mesoderm cells in close proximity to the developing endothelium [35]. SMαA was also shown to stain primitive cardiac and skeletal muscle cell types [35], which may limit its usefulness as a specific marker for VSMC precursors during development.

Another commonly used marker for SMCs is SM22α , which is a 22 kDa protein that is abundantly expressed in visceral and vascular SMC in the adult

[38, 39]. SM22α is a calponin related protein, which has been shown to co-localize with actin filament bundles and stress fibers, and has the ability to bind actin and tropomyosin [38-40]. The exact role of SM22α is not clear however, as *SM22α* deficient mice are viable and show no significant alterations of the vasculature or SMC containing tissues [40]. SM22α is expressed in all SMC precursors, and is transiently expressed in cardiac and skeletal cell precursors during embryonic development. Studies have revealed that the proximal 1344 bp of the *SM22α* promoter are sufficient to drive expression of a LacZ transgene in skeletal, cardiac and smooth muscle precursors during early development [39]. This same truncated promoter could only drive LacZ expression in vascular SMC, but not in visceral SMC in the adult. These studies indicate that gene expression in visceral and vascular SMC are regulated by distinct transcriptional regulatory pathways [39].

I. 2.ii.b. Vascular smooth muscle function

The major role of the tunica media is to maintain blood vessel tone, thus regulating the proper distribution of blood throughout the body. Contraction of the VSMCs reduces the size of the blood vessel lumen, which decreases blood flow and increases blood pressure, whereas VSMC relaxation results in decreased blood pressure due to increased blood flow [41]. VSMC contraction is controlled by changes in intracellular calcium (Ca^{2+}) levels that occur due to mechanical, electrical or chemical stimuli. An increase in free intracellular Ca^{2+} can result due to either the influx of Ca^{2+} through Ca^{2+} channels in the cell

membrane, or by release of Ca^{2+} from internal stores, namely the sarcoplasmic reticulum (SR) [41]. Free Ca^{2+} then binds to the Ca^{2+} binding protein called calmodulin, which in turn activates myosin light chain kinase (MLCK) [41]. This enzyme phosphorylates myosin light chains (MLC) in the presence of ATP leading to cross-bridge formation between the myosin heads and the actin filaments resulting in smooth muscle contraction [41]. Dephosphorylation of MLC by myosin light chain phosphatase (MLCP) inactivates the contractile apparatus resulting in muscle relaxation. A number of endothelial derived factors such as ET-1, PAF and PGH2 activate vasoconstriction by inducing an increase in intracellular Ca^{2+} of the VSMC [42, 43]. Nitric oxide produced by EC causes VSMC relaxation by mediating protein kinase G activation of MLCP [44]. Endothelial secreted PGI2 activates cAMP production, which causes Ca^{2+} uptake back into the SR inactivating the calmodulin mediated muscle contraction [41]. It has also been demonstrated by several groups that pericytes express proteins of the contractile apparatus, and may also play a role in regulating vascular tone in some micro-capillary beds [34, 45].

In addition to regulating vascular tone VSMCs also play an important role in the maintenance of vascular wall integrity. Initially both VSMCs and pericytes play an important role in stabilizing the vessel wall by inhibiting EC proliferation [37], migration [3, 37, 46], and then by producing the ECM components of the blood vessel wall during development [33, 47]. VSMCs produce many types of ECM components, which make up their basement membranes and the interstitial matrix of the tunica media. Collagens and elastins predominate in the interstitial

matrix of the blood vessel wall. The relative ratio of these proteins varies greatly with the vessel type (more in arteries vs. veins) [6, 33]. Elastin fibers of the media are arranged in a net like structure that extends circumferentially and provides support to distended vessels allowing them to recoil back to their normal caliber [47]. Collagen fibers found in this layer are of the Types I, II and III which are arranged circumferentially with the smooth muscle cells and serves mainly as a point of attachment for these cells [6, 47]. Other components of the media ECM produced by the VSMCs include fibronectin, fibrillin, proteoglycans and glycoproteins such as thrombospondin [6, 33].

I. 2.iii. Tunica Adventitia-the extracellular matrix

The outermost lining of the blood vessel wall is the tunica adventitia. This layer is composed primarily of ECM components such as collagens, elastins, fibronectin, proteoglycans, glycosaminoglycans and the fibroblast cells that produce them. Collagen of the adventitia is predominantly type I collagen, which forms longitudinal bundles that provide structural support [6].

I. 2.ii.a. Extracellular Matrix degrading Proteinases

Degradation of components of the ECM is important in angiogenesis, cardiovascular diseases [3], and cancer progression [48]. This degradation is carried out by the cooperative action of two families of proteases, the plasminogen activators and the matrix metalloproteinases.

The plasminogen activator (PA) family of serine proteases includes plasmin and the enzymes responsible for its activation from plasminogen, tissue-type PA (t-PA) and the urokinase-type PA (u-PA). Plasminogen is a single chain glycoprotein, which circulates in the plasma of blood at high levels. Plasminogen contains specialized structures called lysine-binding sites that mediate its specific binding to fibrin [49]. Cleavage of plasminogen at Arg560-Val561 (human) peptide bond produces the active plasmin, a two-chain trypsin like serine protease [50]. The classical substrate of plasmin is the fibrin clot produced by blood coagulation, but it can cleave a broad spectrum of ECM components such as elastin, collagen, fibronectin, and laminin [49]. Plasmin can also activate members of the matrix metalloproteinase (MMP) family such as MMP-1, MMP-3, MMP-9 and MMP-10 resulting in further ECM degradation [51].

t-PA is a serine protease that is secreted as an active enzyme with negligible activity [49]. t-PA has finger domains at its N-terminal end which allow for high affinity binding of fibrin clots and this binding results in increased activation of plasminogen to plasmin [50]. The primary role of t-PA, which is produced by EC [49], is to activate plasmin for clot dissolution [3]. u-PA is secreted as an inactive enzyme that is cleaved by plasmin, or by coagulation factors yielding the active from of the enzyme [49]. u-PA (and pro-u-PA) have a growth factor domain at its amino terminal end that directs binding to cellular receptors called u-PARs [49, 50] that hold the enzyme at leading edge of migrating cells such as VSMC [50], and EC [49]. In addition to its ability to cleave

and activate plasmin, u-PA has been demonstrated to directly activate MMP-2 [51].

MMPs, also called matrixins, are a family of structurally and functionally related Ca^{2+} dependent zinc-containing endopeptidases [52]. There are 23 members of the MMP family which are divided into 6 types; the collagenases, gelatinases, stromelysins, matrilysins, membrane-type MMPs (MT-MMP), and other MMPs, based on sequence homology, organization of their functional domains and substrate specificities (Table 1) [52, 53]. MT1-MMP and the gelatinases, MMP-2 and MMP-9, have been shown to play critical roles in angiogenesis [54], cardiovascular diseases [55-58], and in cancer [48].

Structurally MMPs are comprised of a signal peptide (that is removed in the endoplasmic reticulum [ER]), a propeptide domain, catalytic domain, and a C-terminal hemopexin-like domain. There are several MMPs that have additional functional domains such as the MT-MMPs, which either have transmembrane domains like MT1-MMP or glycosylphosphatidylinositol (GPI) anchors holding them at the plasma membrane [52]. The Gelatinases (MMP-2 and MMP-9) have three fibronectin-type II domains inserted in their catalytic domain, which enhances their ability to bind gelatin and collagens [59].

Table 1. MMP Family and their Common Substrate Specificities [52, 53]

MMP	Type	Common Substrates
	Collagenases	
MMP-1	Type 1	
MMP-8	Type 2	Col I, II, III, gelatin
MMP-13	Type 3	
MMP-18	(*Xenopus*)	
	Gelatinases	
MMP-2	Type A	Gelatin, Col I, II, III, IV, laminin
MMP-9	Type B	
	Stromelysins	
MMP-3	Type 1	Col IV, laminin, fibronectin,
MMP-10	Type 2	activate pro-MMPs
MMP-11	Type 3	
	Matrilysins	
MMP-7	Type 1	Gelatin, Fibronectin, laminin,
MMP-26	Type 2	fibrinogen.
	Membrane	
MMP-14	MT1-MMP	
MMP-15	MT2-MMP	
MMP-16	MT3-MMP	Gelatin, fibronectin, laminin,
MMP-17	MT4-MMP	Col I, II, III
MMP-24	MT5-MMP	
MMP-25	MT6-MMP	
	Other	
MMP-12	Macrophage metalloelastase	Elastin, fibronectin, Col IV
MMP-19	-	Aggrecan, elastin, fibrillin, Col IV, gelatin
MMP-20	Enamelysin	Aggrecan
MMP-21	XMMP	Aggrecan
MMP-23	-	Gelatin, casein, fibronectin
MMP-27	CMMP	Unknown
MMP-28	Epilysin	Unknown

MMPs are synthesized and secreted as inactive zymogens (or pro-MMPs) that require activation before they are able to cleave components of the ECM [59, 60]. The propeptide domain has a unique PRCGXPD sequence that contains a conserved cysteine residue that stabilizes the inactive pro-MMP [60, 61]. The catalytic domain is characterized by a Met-turn structure and conserved zinc-binding motif (HEXGHXXGXXH) that mediate binding of a Zn^{2+} molecule [59]. In the pro-MMP the Zn^{2+} of the catalytic site forms a bond with the conserved cysteine residue in the propeptide holding it in an inactive configuration. Disruption of this bond with subsequent binding of a water molecule to the Zn^{2+} ion switches the Zn^{2+} into an active configuration and results in partial activation of the proenzyme. This mechanism of MMP activation is commonly referred to as the "cysteine switch" [60]. Destabilization of the cysteine switch occurs predominantly by proteolytic cleavage, but can also occur via chemical modification of the sulfhydryl group of the cysteine residue by chemical reagents (Sodium dodecylsulfate, N-ethylmaleimide, sodium thiocyanate, heavy metals, oxidized glutathione, chaotropic agents or reactive oxygen species) *in vitro* [60]. Full activation of the enzyme requires complete cleavage of the prodomain either by the partially active pro-MMP or by other proteases [60, 61].

The hemopexin-like domain, as demonstrated by x-ray crystallography, has a squat cylinder shape with a 4 bladed β-propeller structure comprised of 4 antiparallel β-strands and an alpha helix in each propeller [62, 63]. This hemopexin domain mediates protein-protein interactions, and is required for

cleavage of the interstitial collagens (types I, II, and III) as it unwinds the triple helical structure [15, 59] allowing cleavage of individual chains to occur [64].

MMP activity is regulated by a family of four endogenous inhibitor proteins, called the Tissue Inhibitors of Metalloproteinases (TIMP-1, -2, -3, and -4). TIMP proteins are subdivided into N-terminal and C-terminal domains, with the N-terminal domain folding as a separate unit that has MMP inhibitory activity [52]. TIMPs act as a wedge that fits into the catalytic site of active of the MMP rendering it inactive by chelating the catalytic Zn^{2+} [52, 62]. All 4 TIMPs have been shown to inhibit all MMPs at a ratio of 1:1, although some show greater affinity for certain MMPs over others [52]. For instance, TIMP-1 acts as a direct inhibitor of MMP-9 but is a poor inhibitor of MT1-MMP, and TIMP-2 is an inhibitor for both MMP-2 and MT1-MMP [52, 59].

As mentioned previously, pro-MMP-2 and pro-MMP-9 can be activated by members of the PA family of proteases [51]. MT-MMPs, including MT1-MMP, are activated intracellularly by furin proteases prior to insertion in the plasma membrane. The majority of MT-MMPs including MT1-MMP have been demonstrated to activate pro-MMP-2 [52]. Activation of pro-MMP-2 by MT1-MMP requires the formation of a trimolecular complex with TIMP-2 [65]. TIMP-2 and MT1-MMP bind at the cell membrane through their N-terminal inhibitory and catalytic domains respectively. The C-terminal domain of TIMP-2 binds with high affinity to the hemopexin domain of the pro-MMP-2, forming a trimolecular complex of MT1-MMP/TIMP-2/pro-MMP-2 [65], which is responsible for MMP-2 activation [52, 65, 66].

MMP activity is also regulated by a variety of other factors including a variety of ECM components [16, 67-69] and cell adhesion molecules [70, 71]. For instance, mice deficient in thrombospondin-2, an ECM glycoprotein, exhibit abnormal collagen fibril structure, reduced cell adhesion, increased EC proliferation and vascularization of the skin, which may result from elevated levels of MMP-2 [67, 72]. It appears that under normal conditions thrombospondin-2 may control MMP activity by acting as a clearing agent for both the pro and active forms of MMP [67]. Collagen type IV and type I have also been demonstrated to upregulate MMP-2 activation in different cancer cell lines [68, 69]. Hofmann *et al.* (2000) demonstrated that increased levels of active MMP-2 and MT1-MMP correlated with $\alpha_v\beta_3$ expression in human melanoma cell lines [71]. Thrombin a component of the coagulation pathway has also been demonstrated to regulate MMP activation in both VSMC and EC possibly mediating the migratory ability of these cells [73, 74]. MMPs are also regulated at the transcriptional level by a variety of signaling factors including intracellular Ca^{2+} [75, 76], Ras/Raf/MEK [77-79], PI 3 Kinase/Akt dependent pathways [77-79], and NFkB and activator protein-1[80].

I. 3. Mesoderm development

During early development, cells of the embryonic epiblast migrate inward through the primitive streak (gastrulation) setting up the three primitive germ layers of the embryo. The first cells to migrate through the primitive streak give rise to the endoderm, followed by the cells that will become the mesoderm. The

ectoderm of the embryo is derived from the cells that do not migrate inward but remain in the epiblast layer [2, 81]. The presumptive mesoderm then specializes into several regions each of which eventually gives rise to different organ systems. One of these regions, the lateral plate mesoderm is split horizontally by the growing coelome into the dorsal somatic mesoderm, which underlies the ectoderm, and the ventral splanchnic mesoderm that resides just above the endoderm. The primitive vascular system originates from a subset of cells, the hemangioblast, which differentiate from the splanchnic mesoderm via the process of vasculogenesis [1, 2].

I. 4. Vascular development

Development of the vasculature is a multistage process that includes the process of vasculogenesis, angiogenesis and vessel maturation. Vascular development requires the coordinated action of a variety of cell types (EC and VSMC/pericytes), signaling proteins, such as vascular endothelial growth factor (VEGF), angiopoietins (Ang), and platelet-derived growth factors (PDGF), coagulation factors, and proteases, such as the MMPs.

I. 4.i. Vasculogenesis

Vasculogenesis is a two-stage process that results in the formation of the first blood vessels of the embryo [2, 82]. The first stage involves the differentiation of the angioblast (the EC precursors), and hematopoietic cells, (HC, blood precursor cells) from the splanchnic mesoderm. Differentiation of

these cells from the splanchnic region of the lateral plate mesoderm is induced by signals derived from the endoderm beneath the mesoderm [2]. It has been demonstrated using explant cultures that only mesoderm cultures grown in the presence of endoderm form angioblasts and HC, and that the signal responsible for this induction may be fibroblast growth factor-2 (FGF-2) [83].

The close association of HC and angioblasts during development led to early speculation that they are derived from a common precursor called the hemangioblast [2, 84, 85]. Both angioblasts and HC have been demonstrated to have many markers in common for example QH-1 and MB-1 (in quail) [86], CD31 and CD34 in mouse as well as receptor tyrosine kinase receptors (RTK) Flk-1 (VEGFR2), Flt-1(VEGFR1), Tie1 and Tie2. Further evidence came from the Flk-1 knockout mice, which die *in utero* (E8.5-9.5) due to defects in the development of HC and endothelial cells [87] suggesting a common precursor cell. The clearest evidence for the role of the hemangioblast came from work done by Choi *et al.* (1998) with embryonic stem (ES) cells. Choi and colleagues demonstrated that when the ES differentiated they produced a unique population of cells, the blast colony-forming cells (BL-CFC). These BL-CFCs were demonstrated to express Flk-1 and develop into both HC and angioblasts following treatment with VEGF [88].

The second stage of vasculogenesis involves the development of blood islands from aggregates of hemangioblast cells [2, 82, 85]. The cells towards the centre of the blood islands become the HC, and those towards the periphery become the angioblasts [2, 82, 85]. The angioblasts flatten as they differentiate

into EC forming primitive vesicular structures, which fuse forming into long tubes or vessels that develop into the primitive vascular network or plexus [2, 5]. This primary vascular plexus is expanded to develop the entire circulatory system of the embryo by vessel branching, or angiogenesis.

I. 4.ii. Angiogenesis

Angiogenesis is the process of new blood vessel development from pre-existing blood vessels [82]. There are two types of angiogenesis that occur during embryonic development: sprouting and non-sprouting (or intussusception) angiogenesis [82]. Sprouting angiogenesis requires the proteolytic breakdown of the ECM by the MMPs resulting in the release of growth factors, which induce EC proliferation and migration into new vascular sprouts. Intussusception involves the splitting of larger preexisting vessels into smaller vessels by structures of EC called transcapillary pillars [82]. This type of angiogenesis is more common in the growth of vessel networks within specific organs such as the lungs [82]. New blood vessels will then undergo maturation and remodelling stage, which involves the recruitment of mural cells to the nascent vessel wall and the formation of the ECM by the EC and mural cells. This maturation/stabilization stage is required otherwise vessels will regress [3, 82].

I. 4.ii.a. Growth factors and their receptor tyrosine kinases (RTK)

The VEGF family of growth factors has several members of which VEGF-A is the most frequently studied. VEGF-A has 5 isoforms that result from

alternative splicing events. VEGF165 is considered the most biologically active isoform [13], and is found both in soluble form and bound to the ECM [13, 82, 89]. All VEGF isoforms bind and activate two RTKs, the VEGFR-1 (Flt-1) and VEGFR-2 (Flk-1-mice/KDR-human), which are expressed almost exclusively in EC [13, 82]. VEGF promotes vasculogenesis and angiogenesis by increasing vessel permeability, inducing EC proliferation, survival, differentiation and chemotaxis. Mice deficient for VEGF die *in utero* due to defects in blood vessel development in the yolk sac and in the embryo [12, 14]. VEGF plays a dose-dependent role in the regulation of blood vessel development as the absence of a single allele is embryonic lethal [12, 14]. Gene deletion studies showed that *Flk-1* is the first receptor expressed in blood vessel development as it is expressed in the blood island precursor cells (hemangioblasts) [87]. Mice deficient for this receptor die starting at embryonic day (E)8.5 because they are unable to form blood islands, and lack both angioblasts and haematopoietic stem cells [87, 90]. The Flt-1 receptor is required for organization of the embryonic vasculature but not EC differentiation, as *Flt-1* knockout mice develop both EC and haematopoietic cell normally. These mice, however still die at E8.5, as the EC do not assemble into organized or functional blood vessels [90]. Thus VEGF is required for vasculogenesis and angiogenesis and Flk-1 mediates its role in EC formation, whereas Flt-1 mediates its effects in vessel formation and maturation.

The angiopoietins are another major family of growth factors that help regulate blood vessel development. The best characterized members of this

family are Ang-1, and Ang-2. They are both ligands for the RTK Tie2 (also called Tek) which is expressed only in EC and haematopoietic stem cells [91]. Studies with *Tie2* deficient mice demonstrate that this receptor is required for vessel stabilization and maturation as these mice die at E9.5-E10.5 due to severe hemorrhaging from leaky vessels [92]. Ang-1 mediates this role of Tie2 in vessel stabilization as *Ang-1* knockout mice also die *in utero* from underdeveloped vessel networks [93]. Vessels in these mice have reduced numbers of mural cells associated with them and have poorly elaborated ECM [93]. Recent studies have demonstrated that Ang-1, which is expressed by mural cells of the blood vessels [94], stabilizes vessels by promoting EC survival via the PI 3 Kinase survival pathway upon activation of the Tie2 receptor [91]. EC will undergo apoptosis without mural cell contact [46]. Ang-2 however, acts as an antagonist for Ang-1 by inhibiting its binding to the Tie2 receptor and preventing receptor activation (autophosphorylation) [95]. Mice overexpressing Ang-2 in the blood vessels die between at E9.5-E10.5 due to leaky discontinuous vessel networks, and the absence of major vessels such as the cardinal veins [95]. More recently it has been demonstrated that Ang-2 may play dual roles. For instance, in the presence of VEGF, Ang-2 acts to destabilize vessels promoting vessel sprouting, but when the VEGF survival signal is absent Ang-2 may promote vessel regression [91]. Tie1 receptor is a RTK that is structurally related to Tie2 but to date it has no known ligand [96]. Finally, Ang-2 deficient mice are seen to die shortly after birth, with a small number surviving to adulthood. These mice have major lymphatic vessel defects resulting from improper SMC support of lymphatic

EC [97]. Mice deficient for the Tie1 receptor die at E13.5-E14.5 from edema/aneurysms of the microvasculature leading to widespread hemorrhage, which is not manifested until E13 [96]. These mice undergo vasculogenesis and early angiogenesis normally, thus the Tie1 receptor promotes survival and integrity of angiogenic EC in later development [96].

The Platelet-derived Growth Factor (PDGF) family of proteins regulate growth, differentiation, chemotaxis and ECM production of SMCs and fibroblasts [98-100]. This family consists of 4 different polypeptide chains PDGF-A, -B, -C, and –D which are encoded by separate genes [100]. These 4 chains have been shown to form 5 separate dimers: PDGF-AA, AB, BB, CC and DD [100]. These dimers act via two RTK PDGFR-α, which binds PDGF-AA, -AB, -BB, and –CC, and PDGF-β that binds PDGF-BB and DD chains [98, 100]. PDGF-B and its receptor PDGFR-β have been demonstrated to play critical roles in pericyte and SMC recruitment during blood vessel development in the embryo [37]. In the developing embryo PDGF-B is produced by the EC, and PDGFR-β is produced by VSMC and pericytes [100, 101]. PDGF-B and PDGFR-β knockout mice die just prior to birth due to microaneurysms and hemorrhaging leading to severe tissue edema [99]. Further examination revealed that the EC in the vessels of these knockouts, exhibit abnormal morphology associated with increased EC number in the vessel walls, and decreased EC contacts [98, 99]. The vasculature of these animals was dilated and more permeable due to lack of supporting mural cells and increased VEGF expression [98, 99]. Benjamin *et al.* (1998) demonstrated that in the absence of VEGF expression the VSCM/pericytes

prevent EC apoptosis and migration [46]. PDGF-C is expressed by many cell types during embryogenesis, including mesenchymal precursor cells, cardiomyocytes, and VSMC of some major arteries [100]. PDGF-C was demonstrated to be a potent stimulator of angiogenesis using the CAM and mouse corneal pocket assays [102]. It was shown to mobilize EC and VSMC precursor cells from the bone marrow resulting in stable vessel formation [102].

I. 4.ii.b. Matrix metalloproteinases

The role of MMPs in angiogenesis is to degrade ECM components allowing EC to migrate. Cleavage of the ECM also releases sequestered growth factors such as, VEGF and Fibroblast Growth Factor-2 (FGF-2), that mediate EC proliferation and migration [103]. For instance, angiogenesis and tumorigenesis are induced in a mouse model of pancreatic cancer by the release of VEGF from the ECM by MMP-9 [103]. MMP-2 and MMP-9 have been demonstrated to expose cryptic binding sites upon cleavage of collagen IV that are required for $\alpha v\beta 3$ mediated EC migration required for angiogenesis. MT1-MMP is important in angiogenesis, as it is associated with plasma membrane allowing it to activate pro-MMP-2 and cleave the ECM in a locally restricted manner [48, 65, 104]. MT1-MMP deficient mice are the only lethal MMP-knockout, with mice dying after birth at 3-12 weeks of age [104]. These mice had skeletal defects, which occurred due to the inability to cleave collagens leading to impaired vascular invasion of cartilage. *In vivo* corneal micro-pocket angiogenesis assays in these mice also demonstrated a defect in angiogenic response to FGF-2 [105]. The

hemopexin domain of MMP-2 tethers it at the plasma membrane by binding to αvβ3 integrin and mediates its functions in angiogenesis [30, 31]. A cleavage fragment of this hemopexin domain called PEX inhibits angiogenesis by binding to αvβ3 and preventing the binding of active MMP-2 at the cell surface. TIMP-2 and -3 are secreted by perivascular cells (VSMC and pericytes) and have been demonstrated to inhibit MMP-2 activation by MT1-MMP on EC [106].

I. 4.ii.c. Coagulation system

The coagulation system is intimately involved in angiogenesis. In the initial stages of angiogenesis VEGF stimulates vessel permeability leaking plasma into the sub-endothelial matrix. This results in activation of platelets and secondary coagulation cascade ending with fibrin clot formation [13]. Activated platelets release many factors that upregulate the coagulation cascade, but they also release a number of proangiogenic growth factors including VEGF, PDGF, and FGF-2 [26, 107]. TF, which is not normally expressed on quiescent ECs, is upregulated by VEGF, and in a positive feed back loop TF may upregulate VEGF expression [107]. TF has been demonstrated to play a role in angiogenesis and vessel stabilization [108]. TF knockout mice are embryonic lethal due to defects in yolk sac vessel development [108]. Furthermore, it has been demonstrated that overexpression of TF in a sarcoma cell line resulted in larger more vascularized tumours, whereas smaller less vascularized tumours resulted when the sarcoma cells were transfected with antisense DNA for TF [109]. Thrombin, the protease that cleaves fibrinogen to produce fibrin, is a potent platelet

activator inducing VEGF secretion [107]. As mentioned previously, thrombin activates MMPs resulting in ECM degradation, and upregulated EC migration and proliferation [73, 74, 107]. Finally fibrin, the end product of the coagulation cascade, provides a provisional matrix upon which EC can attach as they migrate to form new vessels [13, 17, 107]. Fibrin also stimulates tPA to cleave plasminogen to plasmin, which in turn activates MMPs upregulating angiogenesis [13, 17, 73, 74].

II. Vascular Tumours

Vascular tumours are a spectrum of complex vascular proliferations commonly composed of EC that are frequently misdiagnosed or mischaracterized [110]. These include hyperplastic lesions of benign nature such as the hemangiomas of infancy and low grade or borderline malignant tumours such as Kaposiform hemangioendotheliomas (HAE) and epitheliod HAE [111-115].

II. 1. Infantile Hemangiomas

Hemangiomas are the most common soft tissue tumours of infancy and childhood, developing in anywhere from 10 to 12% of children by their first birthday. Hemangiomas develop more frequently in female infants than male infants at rates of between 3 to 5:1 [114, 115]. There is also increased incidence of hemangiomas in premature or low birth weight (less then 1000g) neonates (30%) [114,115]. Most hemangiomas begin to develop within three months of

birth. A large proportion of these tumours (60%) develop on the head or neck, with the remainder associated with the body (25%) and extremities (15%) [116]. Hemangiomas can develop cutaneously, subcutaneously or at visceral locations. Hemangiomas present as single lesions in 80% of affected infants, with the remaining 20% demonstrating multiple tumours at varying locations in the body. Infants with multiple hemangiomas of the skin are at higher risk of having visceral hemangiomas, which can associate with almost any organ, but most commonly appearing in the liver [116].

Despite the overall benign nature of hemangiomas their size and or location can lead to serious complications particularly if they compromise the function of vital structures [114, 115]. One frequent complication of hemangiomas is ulceration, which results due to necrosis in deep rapidly proliferating tumours. Ulceration can be very painful, and it carries the risk of hemorrhage, infection and scarring [114, 115]. Hemangiomas of the face and neck are of concern as they may obstruct critical functions. For instance, hemangiomas of the periorbital region can obstruct vision or distort the growing eye resulting in amblyopia (lazy eye), nearsightedness, farsightedness, double vision, corneal damage and potentially blindness [114-116]. Hemangiomas in the neck region (subglottic) can compress the airway potentially leading to respiratory failure if left untreated [115, 116]. Other hemangiomas of regional importance include those in the lumbosaccral region that are commonly associated with tethered spinal cord or anorectal and urogenital abnormalities. These lesions are more at risk for ulceration and infection [114-116]. Finally, high-output congestive heart failure

may occur as the result of large cutaneous, or visceral hemangiomas such as those associated with the liver. The increased blood flow required by the extensive vascularization of the hemangioma places large demands on the heart resulting in cardiac failure [114, 116, 117].

Superficial hemangiomas may first appear as a patch of red or bruise coloured skin, telangiectasia (spider veins). Hemangiomas then undergo a rapid proliferative stage, generally lasting 4 to 8 months, in which the growth of the tumour outpaces the growth of the child [115]. Hemangiomas generally appear as deep red, tense, non-compressible masses with draining veins visible at the periphery [114], whereas subcutaneous tumours appear as pale blue or purple masses [114]. Following the rapid proliferative phase the hemangioma undergoes a lengthy involution phase in which the tumour regresses spontaneously over years. During this involution phase the lesions gradually lose their colour and firmness until they are completely resolved in 90% of the cases by 9 years of age [116]. Involution of the hemangioma may leave behind scarring, excess skin or telangiectasias [114, 116].

Histologically these tumours are composed of masses of plump rapidly proliferating EC with multilaminated basement membranes surrounding capillary like channels [114, 116]. In addition to ECs, hemangiomas contain pericytes, fibroblasts, mast cells and interstitial cells [118]. Immunohistochemical analysis of these hemangiomas verified the presence of EC (CD31 and vWF positive) and pericytes (SMαA positive) surrounding the vascular channels [118]. Additionally, high levels of several markers of angiogenesis were demonstrated during the

proliferative phase including; proliferating cell nuclear antigen (PCNA), MMP-2, FGF-2, VEGF, and u-PA [118]. As involution progresses, the vascular lumens dilate, EC flatten and fibrous tissues are deposited resulting in the lobular structure of these lesions [116]. The involution phase is characterized by upregulated expression of TIMPs [118] and by a 5-fold increase in apoptosis within the tumour [119]. Recently, it has also been shown that hemangiomas at all stages express GLUT-1, a glucose transporter, and the Lewis Y antigen (LeY), which are both associated with the placenta vasculature [120]. These markers are not normally associated with adult tissues, or other forms of vascular tumours including hemangioendotheliomas, and as such, may serve as novel markers for infantile hemangiomas [120]. It is interesting that hemangiomas stain positive for placental markers because there is a 10 fold increased risk of hemangioma development associated with chorionic villus sampling [121].

II. 2. Kaposiform Hemangioendotheliomas

Kaposiform HAE (also called Karposi-like HAE), which develops in infancy and childhood, but infrequently in adulthood, have in the past been mistaken for infantile hemangiomas. These tumours normally develop outside the cervicofacial region, most commonly on the trunk, extremities or associated with the retroperitoneum, and affect males and females equally [114, 115, 117]. Kaposiform HAE rapidly proliferate forming hard, purple coloured cutaneous lesions [114, 115] that may proliferate for 2 to 5 years [115]. They are commonly associated with dilated, fast flowing vessels that feed and drain the tumours

[117]. These are locally invasive, non-metastatic tumours that have a high rate of recurrence after surgical removal [117].

Histologically these tumours are characterized by sheets and irregular lobules of round and spindle shaped EC that are surrounded by a hyaline matrix, which infiltrates the dermis and subcutaneous fat [110, 114, 117]. These tumours may also contain discrete aggregates of epitheliod EC with hyaline or hemosiderin granules [110]. Microthrombi and hemosiderin deposits are common in these tumours, while pericytes and mast cells are rare [114, 117]. Kaposiform HAE stain positive for CD31, CD34, stain weakly for vWF and SMαA, and are negative for GLUT1 or LeY [110, 111].

Kaposiform HAE is often associated with Kasabach-Merritt Syndrome (KMS), which is a consumptive coagulopathy and bleeding disorder. KMS is characterized by sequestration of platelets and coagulation factors leading to disseminating intravascular coagulopathy (DIC) in which patients tend to form localized blood clots while having increased risk of bleeding. Patients with KMS frequently develop anemia and thrombocytopenia [111, 114, 115]. The invasive nature of the Kaposiform HAE and development of KMS puts a great deal of strain on the heart, which leads to congestive heart failure, organ failure and septicemia [115].

III. 3. Epitheliod Hemangioendotheliomas

Epitheliod HAE are borderline malignant tumours that develop in adults of both sexes usually in the 3rd and 4th decade of life. These tumours grow in the

soft tissues of many organs such as the lung, liver and bone [110, 112, 113] and rarely develop in the skin unless it involves the underlying bone of the upper and lower limbs [110]. Visceral HAE commonly arise and expand from the wall of medium to large sized veins and arteries often forming solid masses surrounding the vessels [110, 112, 113]. Epitheliod HAE are distinguished by histicoid or epitheliod-like EC that form solid cords and nests in a basophilic hyaline or myxoid stroma. The EC contain intracytoplasmic lumens that look like vacuoles [110, 112, 113]. Larger vascular channels are less obvious but are surrounded by cuboidal EC and contain red blood cells. These tumours stain positive with reticulin stains and the EC cells are immunopositive for CD34, CD31 and vWF [110, 112, 113].

II. 4. Mechanisms of hemangioma and hemangioendothelioma development

There is some literature describing the hemangioma development, but to date there is very little describing the specific mechanism underlying hemangioendothelioma development. Many investigators suggest that hemangiomas arise as a result of aberrant angiogenesis or defects in vasculogenesis [5, 115]. Hemangiomas generally develop sporadically, but a familial form of these lesions that demonstrate an autosomal dominant pattern of inheritance has been discovered in several families [122, 123]. Gene linkage studies carried out on 3 of these families showed linkage to the 5q31-33 locus [122, 123]. Candidate genes in this region included PDGFR-β, FGF-2 receptor, and the VEGF receptor Flt-4, all of which have demonstrated roles in

angiogenesis [122, 123]. Mutations in the *Flk-1* and *Flt-4* genes have been found in EC isolated from hemangiomas [123]. These studies suggest a potential role for VEGF signaling in vascular tumour development. In fact, it has been previously demonstrated that VEGF is upregulated in the proliferative phase of hemangioma development [118]. A transgenic rabbit model with increased hepatic expression of VEGF developed hemangioma associated with coagulopathy similar to the Kasabach-Merritt syndrome [89]. Yu *et al.* described upregulated Tie2 expression and increased migration in response to Ang-1 in EC isolated from human hemangiomas [124]. Another group studying EC isolated from a mouse model of hemangioma induced by the Polyoma Virus middle T oncogene found that aberrant regulation of Ang-2 expression was responsible for the upregulated EC growth in hemangiomas, and that blockade of Ang-2 resulted in decreased growth of these cells [125]. These studies suggest that altered regulation of growth factors and their receptors may lead to increased angiogenic potential of cells within vascular tumours.

III. Calreticulin

III. 1. Gene

The calreticulin (CRT) protein was first isolated in 1974 by Ostwald and McLennan, but little was known about the gene until the cDNA was cloned by two separate groups in 1989 [126-128]. To date, CRT cDNAs have been identified in mammals, insects, nematodes, and plants [129]. The CRT gene, which is located to the short arm of chromosome 19 in humans [130], and chromosome 8 in mice

[131], consists of 9 exons and 8 introns [130, 132]. There is greater than 70% homology between the human (3.6 Kb) and mouse (4.6 Kb) genes with the major differences found in introns 3 and 6, which are almost twice as long in the mouse [132]. The 1.9kb mRNA contains all 9 exons, and to date there are no known splice variants for the CRT gene. Recently one group discovered a novel isoform of CRT in humans and mice that is encoded by a separate gene (crt2), which is expressed only in the testis [133].

III. 2. Protein

CRT is a highly conserved protein, and has both an N-terminal cleavable ER signal sequence, and a C-terminal KDEL ER retention sequence. These sequences target, and retain the CRT protein in the ER/SR lumen [127, 128, 134]. ER localization of CRT has been demonstrated in a variety of cell types using immunohistochemical staining methods [135-137]. Much controversy still exists over whether CRT resides outside of the ER. For instance, CRT has been demonstrated to bind to the cytoplasmic tails of α-integrins [138] and to nuclear steroid receptors *in vitro* [139, 140]. For CRT to bind these proteins *in vivo,* it needs to be localized to both the cytoplasm and nucleus of the cell. Past studies have demonstrated both cytoplasmic [70, 141], and nuclear localization [135, 142] of the CRT protein, but observed nuclear localization has been attributed to an artefact of the antibody used [143], and to date there is no convincing evidence for the existence of cytosolic CRT [144, 145].

The mature CRT protein is 400 amino acids long and is highly conserved [129, 146]. CRT has a calculated molecular mass of 46 kDa, but it appears at 55-60 kDa polypeptide on SDS-PAGE gels due to its highly negative charge [147]. Based on amino acid sequence, functional and structural analysis CRT is divided into 3 putative domains; the N-terminal globular domain, the proline rich domain (P-domain) and the C-terminal Ca^{2+} binding domain [127, 128, 130] (Figure 1).

III. 2.i. N-domain

The N-domain, which consists of the first 186 N-terminal amino acids of CRT [128], is hydrophobic and has a predicted globular structure with a helix-turn-helix motif followed by 8 anti-parallel β-sheets [127, 146, 148]. This domain has the greatest sequence conservation between the different species, and contains 3 conserved cysteine residues (Cys88, Cys120, and Cys146). The Cys120 and Cys146 residues form an intramolecular disulfide bridge which results in a 25 amino acid loop that is required for proper protein folding [149]. CRT has Zn^{2+} binding capabilities (14 mol Zn^{2+}/mol protein), which is mediated by 5 important histidine residues in the N-domain [150]. Using fluorescence microscopy CRT has been shown to undergo Zn^{2+} dependent conformational changes and thus Zn^{2+} may play an important role in proper folding of the CRT proteins. Additionally interaction between CRT and protein disulfide isomerase (PDI) are potentially mediated by these histidine residues and were found to be Zn^{2+} dependent [151].

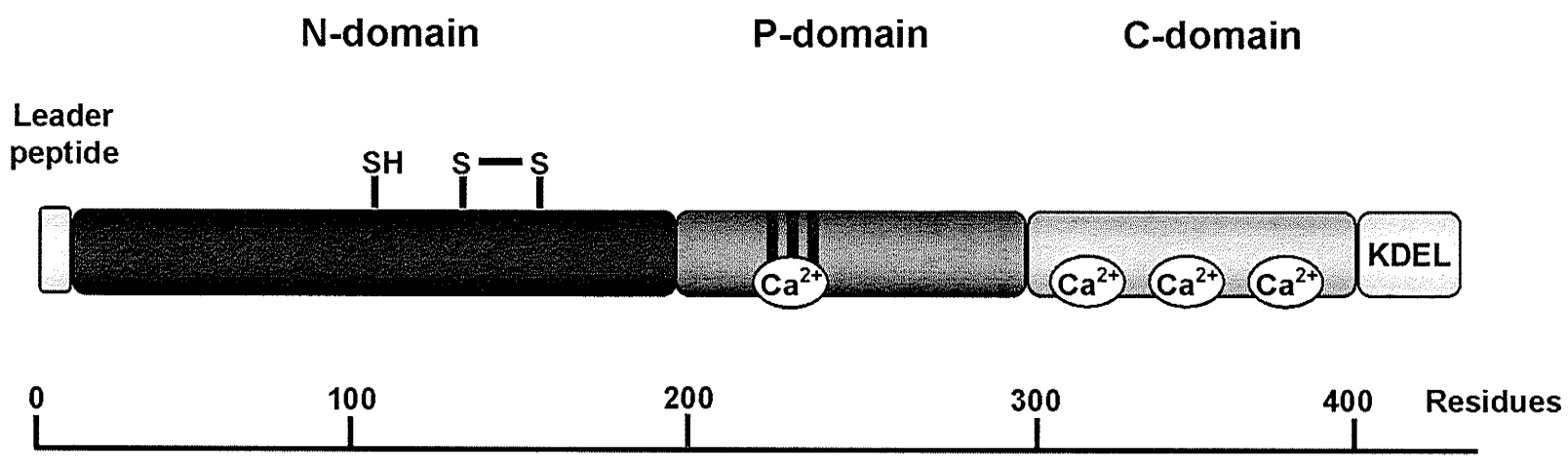

Figure 1: Schematic diagram of the calreticulin protein and its predicted functional domains. The protein is divided into 3 putative domains: the N-domain, P-domain and C-domain. The calreticulin protein has a cleaveable signal peptide. The N-domain contains three conserved cysteine residues two of which form a disulfide bridge. The P-domain consists of proline rich repeats and contains a high affinity, low capacity calcium binding domain. Together the N- and P-domains make up the chaperone region of the protein. The C-domain is highly acidic and contains a low affinity, high capacity calcium binding domain and it terminated in a KDEL ER retention sequence.

CRT is a lectin-like chaperone that binds preferentially to glycoproteins with Asparagine-linked oligosaccharides and enhances their folding [152]. Lectin binding is coordinated by 6 residues that reside in a cleft on the surface of the globular N-domain [153-155]. Another function of this domain is to be an inhibitor of angiogenesis. The N-terminal 180 amino acids (called vasostatin) has been demonstrated to inhibit EC migration and proliferation (see below for further details) [156]. Finally this domain interacted with the highly conserved sequence KXGFFKR present in the cytoplasmic domains of the α subunit of integrins [138, 139] and the DNA binding domain of nuclear steroid receptors *in vitro* [139, 157].

III. 2.ii. P-domain

The P-domain makes up the mid-region of the protein, and spans amino acids 187 to 286 [128]. It is highly homologous with the calnexin P-domain, another member of the ER lectin chaperones [158, 159]. The P-domain is so named because its amino acid sequence is comprised of multiple copies of two proline rich repeats, which contain 17 (type 1 repeat) and 14 (type 2 repeat) amino acids respectively [146, 158]. These repeats are arranged into two triplets, three type 1 repeats followed by three type 2 repeats [158]. Structurally the P-domain is arranged in a hairpin loop structure that extends into a curved arm-like structure connected to the N-domain [153, 158, 160]. The N-domain and P-domain together constitute the chaperone domain of the CRT protein [153, 160, 161]. The P-domain contains a high-affinity, low capacity Ca^{2+} binding site [134], which is capable of binding 1 mol Ca^{2+} per mol of protein [126, 134]. The proline

rich repeats, or the acidic nature of this domain may be responsible for its ability to bind Ca^{2+}, as it does not contain the classical EF-hand Ca^{2+} binding motif [134]. The thiol oxireductase ERp57 has been demonstrated to interact with CRT through binding to the tip of the P-domain arm complex and this interaction mediates its activity [155, 162]. This interaction may in part be regulated by Ca^{2+}-binding at the C-domain [163]. PDI also binds the P-domain, which results in a reduction in CRT ability to bind Ca^{2+} at its high affinity binding site [151].

III. 2.iii. C-domain

The C-domain consists of a short hydrophobic stretch of amino acids (residues 287-310) followed by a very acidic zone and ends with the KDEL sequence [128]. These acidic residues in addition to the KDEL sequence have been postulated to help retain the protein in the ER, since a number of ER chaperones have similar acidic residues in their C-terminal regions including PDI and BiP [134]. The C-domain contains a low-affinity high capacity Ca^{2+}-binding site [127, 128, 134], which is responsible for the Ca^{2+}- storage function of the CRT protein in the ER [161, 164]. Corbett *et al.* (1999) revealed that Ca^{2+}-binding at the C-domain of CRT modulates CRT interaction with chaperone proteins such as PDI and ERp57 [163]. The C-domain was also shown to bind to the vitamin K-dependent coagulation factors IX, X and prothrombin thus mediating antithrombotic effects in a canine electrically induced thrombosis model [165].

III. 3. Protein Functions

CRT was first isolated from rabbit skeletal muscle and was described as a high affinity Ca^{2+}-binding protein of the sarcoplasmic reticulum (SR) [126]. CRT is now known to also reside in the endoplasmic reticulum (ER) in non-muscle cells [137, 145], and was renamed to reflect its role in the ER as a major Ca^{2+}-handling protein [130]. In addition to its roles in Ca^{2+} homeostasis CRT functions as a molecular chaperone that modulates protein folding [146], modulates cell adhesion [144, 145, 147, 166] and plays a critical role in cardiovascular development [167-169].

III. 3.i. Chaperone

Newly synthesized glycosylated, secreted and membrane proteins must undergo maturation and folding in the ER in order to achieve the precise tertiary structure required for proper protein function. Molecular chaperones within the ER interact with nascent or misfolded proteins to prevent protein aggregation and support proper processing into their native confirmations [170]. CRT has been shown to act as a chaperone in the ER due to its ability to bind unfolded and heat denatured forms of ovalbumin with greater affinity, than for the native protein [171]. CRT interacts and helps in the folding of both non-glycosylated proteins by binding to hydrophobic peptides [172], and glycosylated proteins through its lectin domain [152, 172]. CRT was also found to bind and inhibit aggregation of unfolded glycosylated and non-glycosylated proteins, but does not bind to the

mature proteins [172]. CRT also mediates protein folding through the recruitment and binding of other chaperones such as PDI and ERp57 that catalyze the formation of intramolecular disulfide bridges [151, 155, 162, 163]. The interactions between these chaperones and CRT are Zn^{2+} and Ca^{2+} dependent [151, 163]. CRT is responsible for the proper folding for a variety of proteins including myeloperoxidase [173], laminin [174], vinculin [145], IgY antibody [172], HIV-1 envelope glycoprotein [159], and coagulation factors V and VIII [175].

III. 3.ii. Calcium Homeostasis

Ca^{2+} is a very important signaling molecule which regulates numerous cell functions, including cell motility, secretion, contraction-relaxation, proliferation, cell survival, and gene expression. Most cellular Ca^{2+} is stored in the lumen of the SR and/or ER where it is buffered by Ca^{2+} -binding proteins like CRT. Within the ER, Ca^{2+} is regulated by ER resident Ca^{2+}-binding proteins such as CRT, which has both high affinity, low capacity (P-domain) and low affinity, high capacity (C-domain) binding sites [126-128, 134]. CRT has been demonstrated to affect the amount of Ca^{2+} stored within the ER. Overexpression of CRT in mouse L-type fibroblasts and HeLa cells resulted in increased intracellular Ca^{2+} storage capacity of the ER [164, 176]. On the other hand, Liu *et al.* (1994) demonstrated that downregulation of CRT expression with antisense oligonucleotides in NG-108-15 neuroblastoma X glioma cells diminished Ca^{2+} release from inositol 1,4,5 triphosphate (IP_3) receptor channels upon stimulation with bradykinin (known stimulator of IP_3 receptor activity) [177]. Mouse embryonic fibroblast cells (MEF)

isolated from CRT deficient embryos (*crt* -/-) had depleted ER Ca^{2+} storage capacity and also showed no measurable Ca^{2+} release from the ER with bradykinin stimulation [161, 167]. Reintroduction of full length CRT or its P+C domains was able to restore the Ca^{2+} storage capabilities of the knockout cells [161]. This experiment demonstrates a direct role for CRT in Ca^{2+} buffering within the ER, which is mediated by the P and C-domains of the protein.

Ca^{2+} in the ER is also regulated at the level of the channels/transporters that release Ca^{2+} into the cytosol (IP_3 receptors), and those that uptake Ca^{2+} back into the ER (SR/ER Ca^{2+} -ATPase, or SERCA pump) [178]. CRT may play a role in the regulation of these membrane bound channels and pumps. CRT has been demonstrated to colocalize to the same compartments in the ER as does the IP_3 receptor [177]. Both the IP_3 receptor and SERCA-2b pump (predominant isoform of non-muscle cells) have glycosylation sites that are located on the protein domains within the ER lumen [179, 180]. CRT deficient embryos die due to defects in cardiac development [167], and cardiomyocytes derived from *crt-/-* embryonic stem cells *in vitro* have defects in myofibrillogenesis [169]. In both these systems IP_3 mediated Ca^{2+} release from the ER is defective, resulting in impaired nuclear localization of transcription factors such as, nuclear factor of activated T-cells (NF-AT) and Myocyte Enhancer Factor 2C (MEF2C) which are involved in cardiac gene expression [167, 169, 181]. Nuclear translocation of these transcription factors is dependent on dephosphorylation by the Ca^{2+}/calmodulin dependent phosphatase calcineurin [167, 181]. Comacho & Lechleiter (1995) demonstrated that CRT overexpression in *Xenopus* oocytes

resulted in reduced occurrence and frequency of IP_3 induced Ca^{2+} waves, and they suggested that this was the result of the CRT lectin-like interactions (P-domain interactions) with IP_3 receptor or SERCA pump [182]. CRT inhibition of Ca^{2+} oscillations in the *Xenopus* oocytes resulted due to altered Ca^{2+} uptake via the SERCA-2b pump. Site directed mutagenesis of the glycosylation site of the SERCA-2b pump restored normal Ca^{2+} uptake and rescued IP_3 mediated Ca^{2+} oscillations [180]. These observations suggest that CRT modulates Ca^{2+} signaling at the ER by controlling the IP_3 receptor and SERCA pump directly.

III. 3.iii. Cell Adhesion

Some of the controversy surrounding CRT localization outside the ER, result from its demonstrated role in modulating cell adhesion. It was shown that CRT bound to a highly conserved sequence KXGFFKR present on the cytoplasmic tail of the α-integrin subunit [70, 138, 147]. In fact *crt-/-* ES cells have compromised integrin mediated adhesion to laminin and fibronectin substrates, and decreased integrin-mediated extracellular Ca^{2+} influx [147]. Direct interactions and regulation of integrins in the cell membrane would require CRT to be localized to the cytoplasm, and to date there is not convincing evidence for localization of full length CRT in the cytoplasm. CRT may instead regulate cell adhesion by regulating the formation of focal contacts (cell-ECM contacts) and adherens junctions (cell-cell contacts) [144, 145, 166]. CRT has been shown to modulate adhesiveness by regulating the expression of vinculin, a cytoskeletal protein essential for cell-ECM and cell-cell attachments [144, 145,

166], and N-cadherin which is present in cell-cell adherens junctions [144, 183]. Cells overexpressing CRT have increased expression of vinculin and N-cadherin and were demonstrated to have more cell-cell contacts, adhere more strongly to the substratum (ECM), and to spread more than do control cells [144, 145, 166]. The opposite was seen to occur in cells in which CRT levels had been reduced [144, 145, 166]. Dual labeling experiments demonstrated that CRT did not co-localize at these contact sites with vinculin or integrins [145]. In addition, it was demonstrated that retinal pigment epithelial cells (RPE) expressing low levels of CRT migrated more quickly than those cells which overexpressed CRT [166]. CRT was also shown to modulate phosphotyrosine levels in cells, as protein phosphatase levels were seen to increase with an increase in CRT expression [144, 166]. Fadel *et al.* (2001) observed that decreased phosphorylation of adherens junction proteins led to greater stability of the junctional complex [144]. Microinjection of CRT into the cytosol or transfections with a leaderless CRT construct had no observable effect on cell adhesiveness or cell motility [145]. Thus CRT appears to modulate cell adhesiveness and motility from the ER by regulating gene expression, or folding of adhesive molecules, and by regulating protein-tyrosine phosphatases or kinases.

III. 4. CRT and the Cardiovascular System

Transgenic mice expressing a reporter vector containing a green fluorescent protein (GFP) under the control of the CRT promoter demonstrated that CRT is highly expressed in the cardiovascular system during mouse

embryonic development [167]. In early development (E9.5-E10.5) CRT expression was highest in the heart (ventricles and atria), dorsal aorta, and some smaller arteries. CRT expression in the heart peaks at approximately E14.5 and then slowly declines, and is almost undetectable in the hearts of 3 week old mice [167] and absent in the adult heart [136, 167]. CRT expression in the heart during development is essential as mice deficient for both alleles of the gene (*crt-/-* mice) die at E14.5-E16.5 due to defects in the ventricular wall [167, 168]. Furthermore, mice overexpressing CRT postnatally in the heart, exhibit decreased systolic function, chamber dilation and ventricular wall thinning. These mice die within 2-3 weeks of birth due to defects in the cardiac conduction system leading to heart block [184]. The reduced conduction between cardiomyocytes in the heart may be due in part to decreased expression of the connexin 40 and 43 proteins resulting in fewer conducting gap junctions. These observations suggest that CRT may be important in cardiac development and therefore its expression must be tightly regulated during embryogenesis and after birth.

III. 4.i. CRT in Cardiac Development

Regulation of *Crt* gene expression during cardiac development and after birth depends on the interaction of several transcription factors such as Nkx2.5, chicken ovalbumin upstream promoter-transcription factor 1 (COUP-TF1), and MEF2C [169, 181, 185]. The mouse *Crt* promoter contains three putative binding sites (CTCAAGTGT) for the homeobox transcription factor Nkx2.5, and these

sites were shown to increase CRT expression in transfected fibroblasts and cardiomyocytes [185]. Nkx2.5 is a transcription factor that is highly expressed during cardiomyogenesis, but is drastically down-regulated at birth which is similar to the expression of the *Crt* gene. This transcription factor is responsible for the activation of other cardiac specific genes including cardiac alpha actin [185], and the transcription factor MEF2C [186]. COUP-TF1 is a transcription factor that is expressed at a constant level throughout development. The DNA binding site (AGTTCA) of COUP-TF1 is similar to Nkx2.5 response elements. A recent report showed that when Nkx2.5 protein levels were low COUP-TF1 was able to bind Nkx2.5 binding sites in the CRT promoter and suppress transcription [185]. Therefore, it is likely that when Nkx2.5 levels are high early in embryonic development it binds preferentially to its response element activating CRT gene expression. While later in development and after birth when Nkx2.5 expression is drastically reduced, COUP-TF1 binds the sites inhibiting CRT expression [185].

As mentioned previously, CRT regulates Ca^{2+} dependent nuclear translocation of MEF2C and NF-AT3 transcription factors (see above discussion). NF-AT is a transcription factor that is important in cardiac development [167]. Reduced activation of this transcription factor to the nucleus via calcineurin could result in defects in the cardiac development program [167]. MEF2C is a transcription factor responsible for the activation of cardiac specific embryonic genes including ventricular myosin light chain 2 (MLC2v) [169]. *Crt-/-* cardiomyocytes from mutant mice or derived *in vitro* from *crt-/-* ES cells, have defects in myofibrillogenesis due to decreased expression and improper

arrangement of MLC2v in sarcomeric structures [169]. MEF2C knockout mice are embryonically lethal due to impaired ventricular development similar to that seen for *Crt* deficiency [187]. MEF2C has also been shown to activate the *Crt* promoter [181], and upregulate CRT expression. This positive feedback activation of *Crt* expression ensures that MEF2C is activated and translocated to the nucleus during myofibril development [181].

III. 4.ii. CRT and Angiogenesis

CRT is highly expressed in the heart and vascular wall of the developing mouse embryo [161]. In the adult, CRT expression remains high in the blood vessel wall and is expressed by both EC and VSMC [137]. Dai *et al.* (1997) demonstrated that treatment of rat femoral arteries with CRT prior to balloon angioplasty reduced intimal hyperplasia [188]. The N-terminal fragment (amino acids 1-180) of CRT, named vasostatin, can inhibit EC proliferation *in vitro* [156]. Vasostatin was also shown to inhibit angiogenesis in chorioallantoic membrane assays (CAM) [189] and in murine and rat models of corneal neovascularization [189, 190]. In these *in vivo* assays it was shown that vasostatin inhibited new vessel formation by inhibiting EC proliferation with no effect on pre-existing, quiescent vessels [189, 190]. Vasostatin was also shown to inhibit tumour angiogenesis, and growth of human Burkitt lymphoma, colon carcinoma and ovarian carcinoma when applied by subcutaneous injection during the induction of tumour formation in the nude mouse model of tumour growth [156, 191, 192]. Full length CRT was also demonstrated to inhibit Burkitt lymphomas tumour

angiogenesis [156]. Vasostatin when used in combination with interleukin 12 (IL-12) resulted in a significant decrease in tumour size and progression [191]. IL-12 has been demonstrated to target tumour vasculature through interferon inducible protein-10 (IP-10), and to induce necrosis in tumour cells [156, 191]. Lange-Asschenfeldt *et al.* (2001) found that tumour inhibiting doses of vasostatin in mice did not inhibit wound healing [192]. Gene therapy studies using vasostatin alone or in conjunction with immunotherapy have also shown positive outcomes with inhibition and regression of tumour growth in mice without significant side effects [189, 193].

The exact mechanisms of vasostatin's anti-angiogenic effect are not clearly understood. The anti-angiogenic activity of CRT and vasostatin has been pinpointed specifically to the amino acids 120-180 [156]. The anti-angiogenic effect of vasostatin may be due to the release of NO from EC in response to vasostatin binding [156]. Exogenously added CRT has been previously shown to bind to EC and to upregulate the production of endothelial derived NO [165], which has anti-thrombotic and anti-angiogenic effects [156, 165]. More recently it has been demonstrated that vasostatin may inhibit EC proliferation and migration by preventing EC from interacting with the ECM protein laminin [194]. Laminin proteins provide sites of attachment for EC allowing them to migrate, proliferate and form vessel sprouts [194]. Vasostatin can bind to laminin preventing EC attachment and thus inhibiting angiogenesis [194]. The breakdown of the ECM is an important regulator of angiogenesis. CRT may also control new blood vessel

growth by regulating the MMPs, which are responsible for ECM degradation during angiogenesis (see discussion below).

III. 4.iii. CRT and MMPs

It had been previously demonstrated that decreasing [70] CRT expression in human Rhabdomyosarcoma (RD) cells using antisense oligonucleotides inhibited pro-MMP-2 secretion resulting in a decrease in MMP-2 activation. This study also showed that CRT overexpression in the RD cell induced a 2.2 fold increase in pro-MMP-2 secretion, thus suggesting that CRT mediated this response through α3 integrin subunit signaling [70]. More recently, we demonstrated that target deletion of CRT in mouse embryonic fibroblast cells resulted in a significant decrease in MMP-9 activity [77]. This change was attributed in part to an alteration in the Ras/Raf/MEK pathway as treatment with the MEK inhibitor PD98059 resulted in an increase in MMP-9 expression in the *crt -/-* cells back to levels approximating those in *wt* cells. We also observed an increase in MMP-2 expression and activity, and increased expression of the MMP-2 activator MT1-MMP upon stimulation with insulin [77]. This up-regulation of MMP-2 expression was due in part to insulin-mediated activation of the PI 3-kinase dependent pathway. This observation is in agreement with findings in our laboratory that *crt-/-* cells have increased insulin receptor expression and activation of the PI 3-kinase/Akt pathway (Jalali & Mesaeli, manuscript under revision). These findings suggest that CRT does play a role in regulating MMPs, but that exact mechanism may differ depending on cell type.

B. RATIONALE

Blood vessel development is a complex process that is regulated by many positive and negative factors, which are maintained in a tightly regulated balance [4, 5]. Proper vessel development requires the coordinated action of growth factors and their receptors, proteases and coagulation factors to regulate extracellular matrix breakdown, endothelial cell proliferation, smooth muscle cell recruitment and vessel stabilization. CRT is an ER resident protein, which has been demonstrated to play a role in Ca^{2+} handling, protein folding and cell adhesion. Studies on developmental regulation of the CRT promoter showed that this protein is highly expressed in the heart and vasculature during early cardiovascular development [167, 168]. Gene deletion studies in mice confirmed that CRT plays a critical role in cardiovascular development as these mice died from defects in cardiac development and wound healing [167, 168]. These defects in cardiovascular development could result as a consequence of altered ECM composition, as we have previously shown CRT deletion results in altered expression and activity of MMP-2 and -9 [77]. CRT expression is maintained in the vessel wall after birth [137] and exogenous CRT has been demonstrated to alter vascular function; for example in adult rats, exogenous CRT acts as a vascular regulatory protein by reducing intimal hyperplasia after arterial injury [188]. Exogenously added CRT has also been shown to selectively inhibit EC migration *in vitro*, and to play an inhibitory role in tumour angiogenesis [156]. These observations suggest a regulatory role for CRT in angiogenesis and

vascular remodeling, but to date there have been no studies examining the effect of endogenous CRT on these processes. Thus our hypothesis was that **"endogenous CRT regulates role in the processes of vascular remodeling and angiogenesis".** The specific aims of this study were:

(1) to develop a transgenic mouse model that overexpressed CRT in the vascular smooth muscle cell layer of the blood vessel wall (*SMCRT* mice),

(2) to characterize the phenotype of these transgenic mice,

(3) to determine what, if any, role endogenous overexpression of CRT may play in vascular remodeling.

C. Materials and Methods

I. Materials:

Dulbecco Minimum Essential Medium (DMEM), Fetal Bovine Serum (FBS), Penicillin-Streptomycin antibiotic solution, Lipofectamine 2000, Insulin-Selenium-TransferrinA, *Taq* polymerase, restriction enzymes and pcDNA 3.1-Hygromycin plasmid vector were purchased from Invitrogen (Burlington, ON). pBluescript SKII plasmid vector was purchased from Fermentas (Burlington, ON). All primers for PCR were purchased from Sigma-Genosys (Oakville, ON). Maxiprep plasmid isolation and gel purification kits were obtained from Qiagen (Missassauga, ON). Proteinase K and Blocking Reagent were purchased from Roche Diagnostics (Laval, QC). The DC protein assay kit, pre-stained SDS-PAGE low range molecular weight standards and nitrocellulose membranes used for western blot analysis were obtained from BioRad Laboratories (Mississauga, ON). Primary antibodies used for western blot, immunocytochemistry and immunohistochemistry are: rabbit anti-hemaglutannin-tag (HA) obtained from Rockland Immunochemicals (Mississauga, ON), rabbit anti-actin, mouse anti-smooth muscle actin, and rabbit anti-MMP-9 obtained from Sigma-Aldrich (St. Louis, USA), rabbit anti-MMP-2 obtained from Medicorp (QC, Canada), rat anti-PECAM-1 (CD31) antibody from BD Biosciences (Mississauga, ON), rat-anti-CD34 antibody from Biolegend (Hornby, ON), rabbit anti-connexin 43 was a generous gift from Dr. Kardami (Department of Human Anatomy and Cell Science, University of Manitoba), and rabbit anti-connexin 40 was a gift from Dr.

Nagy (Department of Physiology, University of Manitoba). Peroxidase conjugated secondary antibodies were purchased from Jackson ImmunoResearch Laboratories (Medicorp distributor QC, Canada). Western Blotting Luminol Reagent kit was purchased from Santa Cruz Biotechnologies (Santa Cruz, CA). Cryostat embedding media Optimum Cutting Temperature (O.C.T.) was purchased from Cedarlane Laboratories (Hornby, ON). Immunohistochemical staining reagents including Vectastain ABC Kit, Diaminobenzidine and NovaRed peroxidase substrate were obtained from Vector Laboratories (Burlington, ON). Other chemicals and reagents were purchased from Fisher Scientific or Sigma-Aldrich and were of the highest Molecular Biology grade.

II. Generation of the smooth muscle specific transgene construct

The transgene targeting over-expression of CRT specifically to the vascular smooth muscle cell layer (*SMCRT*) construct was generated as using a truncated (1344bp) SM22α promoter (pXP1-1344SM22α plasmid), which was a generous gift from Dr. Eric Olson (Southwestern Medical Center, University of Texas). The expression pattern and characteristics of this promoter were previously described by Li *et al.* (1996) as driving expression exclusively to the vascular smooth muscle cell layer [39]. The pXP1-1344SM22α plasmid was digested using the restriction enzymes *BamHI* and *SalI* to excise the 1.3 Kb SM22α promoter. This 1.3 Kb SM22α promoter fragment was gel purified and ligated into pBluescript-SKII digested with the same enzymes to generate

pBluescript-SM22α. This plasmid was then transformed into *E. coli* DH5α and plated on LB-Ampicillin plates containing X-gal and IPTG substrates. Positive clones were isolated by blue/white screening. Next, the pcDNA-CRT-HA-KDEL CRT expression construct, a generous gift from Dr. Marek Michalak (University of Alberta), was digested with *HindIII* and *ApaI* to excise CRT-HA-KDEL. This fragment was then gel purified and ligated into the pBluescript-SM22α plasmid that had been linearized with *HindIII* and *ApaI*. Following transformation into the E. coli DH5α and screening, a positive clone was isolated and sequenced (University of Calgary) using T7 and T3 universal primers in pBluescript to verify the sequence of the plasmid.

To generate a mammalian expression vector containing a polyA tail the pBlue-SM22α-CRT-HA-KDEL construct was digested with *PVUII* to excise SM22α-CRT-HA-KDEL, which was then gel purified. In parallel the plasmid pcDNA3.1-Hygromycin plasmid was digested with *NruI* and *EcoRV* to excise the CMV promoter, followed by gel purification. The SM22α-CRT-HA-KDEL fragment was then ligated in the cut pcDNA3.1-Hygromycin resulting in the pcH-SM22α-CRT-HA-KDEL construct. This plasmid was then transformed into the *E. coli* DH5α and positive clones were screened by restriction enzyme digestion using *BamHI* or *PstI* to ensure the proper orientation of the insert. Large scale plasmid DNA was prepared using the Qiagen Maxi-prep isolation kit according to the manufacturers' instructions. The isolated plasmid was then digested with *PVUII* (present in the pcDNA3.1 vector) to remove bacterial vector sequences as they have been demonstrated to inhibit the expression of some genes *in vivo*

[195]. The digested DNA was then resolved on a 1% agarose mini-gel and the desired 3.6 Kb transgene fragment was gel purified and resuspended in sterile DNase free water. The purified transgene construct (renamed as *SMCRT*, Figure 2A) was used to develop the smooth muscle specific CRT over-expressing transgenic mice, which will be referred to as the *SMCRT* mice.

III. Generation and screening of *SMCRT* transgenic mice

III. 1. Generation of the SMCRT transgenic mice

The *SMCRT* mice were developed at the Fee for Service Transgenic Mouse Facility at the University of Alberta. The purified *SMCRT* transgene construct was used for pronuclear injection into a fertilized ovum and implanted into a pseudo-pregnant FVB/N female. Mice of the first generation (F0 founders) were screened for the presence of the transgene using PCR and for protein expression via western blot as described below. Animals determined to be transgenic were bred with wild-type (*wt*) FVB/N mice, to propagate separate breeding lines according to protocol guidelines. Briefly, transgenic males were placed in a cage with 1 or 2 *wt* FVB female mice, or a transgenic female was placed with one *wt* FVB male. Male mice were removed from the breeding cages following the observation of sperm plugs, which indicated a successful mating, or once the females appeared pregnant. All procedures involving mice were approved and followed the guidelines for the ethical care and treatment of animals set out by the Canadian Council of Animal Care.

III. 2. Screening mice for transgene expression

Mouse litters were screened for the presence and expression of the transgene construct by PCR and by western blot analysis using DNA and protein isolated from tail biopsies. Tail biopsies were divided in two pieces, one for protein isolation and the other for genomic DNA isolation as described below.

III. 2.i. Genomic DNA isolation and PCR analysis

Tail biopsies from individual mice were placed in 350 μl of lysis buffer (100mM NaCl, 50mM Tris-HCl (pH 8.0), 25mM EDTA, 0.5% SDS) and were digested with 5 μl of Proteinase K (10 mg/ml) at 37°C for 1 hour followed by an overnight incubation at 55°C. The remaining protein was precipitated on ice following the addition of a high salt solution (4 mg/ml NaCl) and centrifugation at 10,000 rpm for 10 min. Genomic DNA was isolated from the supernatant by phenol-chloroform extraction and ethanol precipitation, and was resuspended in TE buffer (10mM Tris, 1mM EDTA, pH 7.5-8.0).

The PCR reaction for genotyping was set-up using 150 ηg of genomic DNA isolated from tail biopsies as a template, 0.5 μg/μl of

SM-5: 5'- TGGCTGTAGTGGATTGAGCGTCTGAGGC -3' and

CR-3: 5'- TTGAAGTAGACGACGGGCTC -3' transgene specific primers, 10mM dNTPs, and *Taq* reaction buffer plus $MgCl_2$. The PCR reaction included a 15 min denaturing step prior to addition of the *Taq* DNA polymerase followed by 35 cycles consisting of a 45 sec denaturing step at 94°C, a 1 min annealing step at

65°C and an elongation step of 2 min at 72°C. An amplification product of 0.9 Kb was expected in samples positive for the transgene.

III. 2.ii. Protein isolation and western blotting

Tail biopsies taken for protein were homogenized on ice in RIPA lysis buffer (250mM NaCl, 10mM TRIS, 1mM EDTA, 1mM EGTA, 10mM $Na_4P_2O_7$*10 H_20, 30mM NaF, 0.5 % Na-Deoxycholate, 0.1 % SDS, 1 % Nonidet P-40, 1% Triton X-100 containing 0.5 μM PMSF and cocktail of protease inhibitors). Cell debris was removed by centrifugation at 7,000 rpm at 4°C for 10 min. Protein concentrations of the supernatant were determined using DC protein assay kit. 30-50 μg of protein was resolved on 10% SDS-PAGE gels, and transferred to nitrocellulose membranes. Nitrocellulose membrane was blocked for 30 minutes using a 5% milk powder solution in Phosphate buffered saline (PBS, 140mM NaCl, 2.7mM KCl, 8.1mM Na_2HPO_4, 1.5mM KH_2PO_4) followed by incubation with 1:5000 dilution of rabbit anti-HA in milk powder solution overnight and then with a peroxidase conjugated secondary antibody goat anti-rabbit (1:10,000) for 30 min at room temperature. The protein signal was detected via chemiluminescence using the Western Blotting Luminol Reagent Kit and visualized on a Fluor-S Max MultiImager (BioRad).

Descending aorta samples were collected from mice and homogenized in RIPA buffer as described above. Western blot analysis was carried out using different primary antibodies including: Rabbit anti-connexin 43 (1:5000, 2 hr

incubation), or Rabbit anti-connexin 40 (1:100, 1 hour incubation) followed by Rabbit anti-tubulin (1:2000, 1 hr incubation) as a loading control.

III. 3. Histopathological screening of SMCRT phenotype

Detailed histopathological analysis was carried out on *wt* and *SMCRT* transgenic mice following euthanization with an overdose of sodium pentobarbital (60 mg/Kg) injected intraperitoneally. This assessment included external examination, internal examination of macroscopic anatomy, pathology of all major organ systems, and microscopic analysis of tissues all of which was documented in writing and with digital photographs. Tissue samples were also collected for isolation of cells and for further analysis including western blot analysis, histological, and immunohistochemical analysis.

III. 3.i. Tissue Preparation and Sectioning

Tissues were fixed using 3 separate fixation methods necessary for different stains and antibodies. Tissues for histological staining were fixed in a 4% neutral buffered formalin (Fisher Scientific) for several days and then processed using an automatic tissue processor (ThermoShandon) and embedded in paraffin. Using a microtome, 4 μm sections were prepared in transverse for all tissues of interest. These sections were used for histological staining as described below.

For immunohistochemistry paraformaldehyde or zinc fixative was used. Tissues for frozen sections were fixed in 4% paraformaldehyde solution in PBS

for several hours to overnight depending on the tissue size, followed by incubation overnight in 30% sucrose solution with constant shaking at 4°C. The solution was then changed to 50% O.C.T. Medium in PBS for 8 hrs followed by an overnight incubation in 100% O.C.T. Medium at 4°C. The following day tissues were frozen in O.C.T using liquid nitrogen or dry ice slurry and stored in -80°C until cryo-sectioning. Tissue sections of 7 μm were prepared on a cryotome (-20°C,ThermoScientific) and stored at -80°C until used for immunohistochemistry, as described below.

Tissues were also fixed in a Zinc fixative solution (0.1M Tris-HCl, 3 mM $Ca(OAc)_2$, 22 mM $Zn(OAc)_2$, 36 mM $ZnCl_2$, pH 6.5-7.0) for 24-48 hours to retain tissue morphology similar to formalin fixed/paraffin embedded tissue while maintaining compatibility with certain antigens for immunohistochemistry. These tissues were prepared for tissue processing and paraffin embedding and then sectioned as described above for formaldehyde fixed tissues.

III. 3.ii. Histological Staining of Paraffin sections

Tissue sections were deparaffinized in xylene and hydrated through stepwise changes of alcohols (100%, 95% and 70%) to water and then stained using several methods. Sections were stained with hematoxylin/eosin (H&E), which differentially stains cytoplasm (pink) and nuclei (purple) to assess general tissue morphology. To examine for differences in connective tissue composition, sections were also stained using Masson's Trichrome staining method as previously described [196]. Briefly, deparaffinized sections were fixed in Bouin's

fixative overnight at room temperature. Tissue sections were then stained with Weigert's iron hematoxylin for 2 to 2.5 min and then stained using Biebrich's scarlet-acid fuchsin solution for 4 min with thorough washes with water in between. Finally tissue sections were differentiated with phosphomlybdic-phosphotungstic acid solution for 10 min and then counterstained with aniline blue for 10 min. To examine collagen disposition we stained tissue sections using the Picrosirius red staining method as previously described [197]. Briefly, sections were rehydrated to water and stained with the Picrosirius Red solution overnight with gentle shaking. Tissue was differentiated in two washes of acetic acid water. Collagen is seen to stain bright red with the cytoplasm staining a pale yellow with black nuclei.

III. 3.iii. Immunohistochemical Staining of frozen sections

For immuohistochemistry, frozen sections (7 μM) were first washed in PBS for 30 min to remove the O.C.T. Medium and then incubated in 0.3% Peroxide solution for 15 min at room temperature to block endogenous peroxidase activity. Tissue sections were blocked for 30 min in Roche Blocking Reagent to block any non-specific binding of antibodies. The primary antibodies rabbit anti-HA (1:500), MMP-9 (1:300), or rat anti-PECAM (1:250) were diluted in Roche blocking reagent and applied to the section for 1 hr at room temperature. Immunostaining with a mouse primary antibody such as mouse anti-MMP-2 (1:200) required an additional blocking step with Mouse IgG (overnight at 4°C) before incubation with the primary antibody. Following incubation with primary

antibodies sections were washed using the blocking reagent and incubated with the appropriate biotinylated secondary antibody for 1 hr at room temperature. Sections were then washed with PBS, and were incubated with Vectastain ABC reagent for 30 min. Horseradish peroxidase substrates DAB (Diaminobenzidine) or NovaRed were used to visualize the localization of the antibodies. Sections were then counter stained with hematoxylin, or methyl green, dehydrated through stepwise changes of alcohol (70%, 95%, 100%) to xylene and mounted using Permount. The slides were then examined using a Zeiss Axioscop 2 with a colour CCD camera.

For immunohistochemical staining with CD34 antibody, sections from zinc fixed tissues were deparaffinzed and hydrated back to water as described above. Surface antigens were unmasked using a citrate antigen retrieval protocol. The slides were placed in warm citrate buffer and then boiled for 30 min followed by cooling for 20 min at room temperature. The sections were then processed as described above for frozen sections using rat anti-CD34 (1:100) in dilution buffer overnight at 4°C, and visualizing it using the horseradish peroxidase VIP substrate.

III. 3.iv. Blood smears for Giemsa staining

Whole blood smears from *wt* and *SMCRT* mice (n=15) were prepared from blood taken from cardiac puncture for the examination and evaluation of cellular components. Blood smears were air dried, fixed with absolute methanol for 1 minute and then washed with distilled water. Blood smears were stained

using the May-Grunwald Giemsa method from Sigma-Aldrich (St. Louis, USA). Platelet aggregation was examined by screening 10 high power fields (HPF) for each sample. Each HPF contained a value of 200-300 Red Blood Cells (RBC).

III. 4. Explant technique for Vascular Smooth Muscle Cell isolation

Descending aortas were removed from *wt* and *SMCRT* mice for vascular smooth muscle cell isolation by explant culture. Briefly, aortas were excised aseptically, washed thoroughly with sterile PBS plus Penicillin/Streptomycin, and then cleaned of connective tissue and adherent fat in a tissue culture setting. Cleaned aortas were cut into small pieces with iris scissors and placed in 2 cm tissue culture plates containing DMEM plus 20% FBS, and 5% antibiotic solution. Pieces of artery were allowed to adhere to the tissue culture plates and cells began to migrate out at 5-10 days (day 1). Adherent cells were sub-cultured after approximately 7 days to a new 10 cm plate with pieces remaining in original plate. Colonies of cells having the appearance of smooth muscle cells were isolated to small welled plates and culture to confluence. The cell composition of colonies was determined by plating cells on coverslips and immunostaining using anti-smooth muscle actin (1:400) and Texas Red labeled anti-mouse secondary antibody (1:70). Coverslips were visualized using a Zeiss AxioSkop 2 fluorescent microscope. Pure smooth muscle cell colonies were immortalized by transfection with a plasmid containing SV40 large T-antigen using Lipofectamine 2000 transfection reagent according to the manufactures protocols. Cells were maintained in low serum medium (DMEM plus 5% FBS) prior to experiments.

III. 5. Gelatin Zymography

VSMCs isolated from *wt* and *SMCRT* mice were seeded at a density of 2 x 10^6 cells per 10 cm culture plate and were cultured in DMEM plus 10% FBS at 37°C overnight. The following day the media was changed to conditioned media containing DMEM plus 1% Insulin-Transferrin-SeleniumA and incubated for 48 hrs. Conditioned media was collected from plates containing *wt*, *SMCRT* cells and plates containing no cells (media control) and was concentrated using Centricon 30 protein concentrators. 20 μl of concentrated media was mixed with sample buffer (20% glycerol, 4% SDS, 0.13 M Tris, pH 6.8) and resolved on a 7.5% acrylamide gel containing 1 mg/ml porcine gelatin (Sigma). To reactivate the MMPs, SDS was removed from the gels by washing the gels with a 2.5% Triton X-100 solution for 30 min at room temperature. Gels were then incubated in zymogram activating solution (50mM Tris-HCl, 5mM CaCl2, 0.2 M NaCl, pH 7.6) for 24-48 hrs at 37°C with gentle shaking. To visualize and measure MMP activity, the gels were stained in Coomassie blue for 1 hr at room temperature followed by destaining (40% methanol and 10% acetic acid solution) overnight at room temperature. Gelatinase activity was seen as clear zones against a dark background and band density was quantified using a BioRad Densitomer and QuantityOne program.

III. 6. Pressure Myography

III. 6.i. Preparation of Resistance Arteries

Male mice were euthanized by an overdose of anesthetic, and the superior mesenteric arteries from the part of the vascular bed feeding the jejunum distal to the pylorus were isolated and immediately placed in ice cold Krebs' solution (in mmol/L : NaCl 120, NaHCO3 25, KCl 4.7, KH2PO4 1.2, MgSO4 1.2, CaCl2 2.5, EDTA 0.026 and glucose 5.5, pH 7.4). Using a dissecting microscope a third order branch (2 mm in length; 75-150 microns in diameter) of the mesenteric artery network was cleaned of adipose and connective tissues, and then carefully dissected 1 mm from the intestine. The arterial segment was mounted and tied onto two glass microcannulae in a pressure myography chamber as previously described [198, 199]. The cannulae were carefully adjusted so that the arterial walls were in parallel without stretch or buckle. Intraluminal pressure was set to 45 mmHg using a servocontrolled pump, and the vessels were equilibrated with Krebs' solution (gassed with 95% air and 5% CO_2) for 1 hr at 37°C. The myography chamber was placed on the stage of an upright microscope with attached microcomputer-based video imaging system, which allowed the measurement of the lumen diameter and media thickness of the arterial segment.

III. 6.ii. Assessments of vessel viability

The viability of arterial segments was confirmed prior to carrying out all experiments. Resting lumen diameter of the vessel was determined and then the

vessel was challenged by extraluminal perfusion with a high-potassium (125 mmol/L KCL) Krebs' solution containing 10^{-5} mol/L norepinephrine. If this treatment elicited more than a 50% constriction of the resting lumen diameter the vessel was considered to be viable.

III. 6.iii. Determination of vascular structure and mechanical properties (Stiffness)

Resistance arteries were perfused extraluminally with a Ca^{2+}-free Krebs' containing 10 mmol/L EGTA for 30 minutes. This treatment deactivates the vascular smooth muscle cells which allows for maximal dilation of the vessels allowing the structural and mechanical properties of the vessel wall to be assessed without interference of vascular tone [200]. Prior to experiments vessels were pressurized to 140 mmHg and the cannulae were readjusted to correct for the lengthening of the arterial segments. To obtain pressure-lumen diameter relationships, the servocontrolled pump was used to increase intraluminal pressure by increments of 10 mmHg (from 3 mmHg to pressure of 40 mmHg) and then by increments of 20 mmHg (to an intraluminal pressure of 140 mmHg). Media thickness and lumen diameter of the vessel wall were measured at each increment of pressure starting at 3 mmHg because at pressures below this the vessel collapsed. These data were used to calculate circumferential stress, circumferential strain and tangential elastic modulus using previously described formulae [199]. Circumferential stress was calculated as $\sigma = (PD)/(2M)$, where P is the intraluminal pressure (dyne/cm^2), and D and M are

lumen diameter and media thickness, respectively. Arterial pressures were converted from mmHg to dynes per centimeter squared (1 mmHg = 1.334 X 10^3 dynes/cm^2). Circumferential strain was calculated as $\varepsilon = (D-D_o)/D_o$, where D is the observed lumen diameter for a given intramural pressure and D_o is the original diameter at 3 mmHg. The stress-strain data from each animal were fitted to an exponential curve using the least squares analysis: $\sigma = \sigma_o e^{\beta\varepsilon}$, where σ_o is stress at the original diameter (D_o) and β is a constant related to the rate of increase of the stress-strain curve. The elastic modulus was calculated at several values of stress from the derivative of this exponential curve: elastic modulus = $d\sigma/d\varepsilon=\beta\sigma_o e^{\beta\varepsilon}$.

IV. Statistics

Mean and standard error were plotted for each individual experiment. The statistical differences between two values were assessed using Students's T-test and a P value <0.05 was considered as significant difference.

Two-way ANOVA with Bonferroni Post-hoc test was used to calculate statistical difference between the stress-strain data-points from the *wt* and *SMCRT* vessels. The strain was calculated from myography data as described above. The maximal strain was compared between the two animal groups (*wt* and *SMCRT*). The *wt* vessels had the lowest maximal strain and were denoted as the 100% strain value. This value was used to calculate the stress at 0, 20, 40, 60 and 80% values of strain. The calculated stress values from both *wt* and *SMCRT* mice were plotted using GraphPad Prism statistical software. The same

protocol was repeated to calculate statistical differences in elastic modulus vs. strain values.

D. Results

I. Generation and genotyping of the *SMCRT* mice

Transgenic mice over-expressing CRT in the vascular smooth muscle cells (*SMCRT* mice) were developed by pronuclear injection at the University of Alberta's Transgenic animal facility using the *SMCRT* transgene construct (schematic in Figure 2A). Four founder (F0) mice were confirmed to be transgenic using PCR screening of genomic DNA. These F0 founder mice were bred with *wt* FVB/N mice to propagate these lines. Three (FS5, FS18 and FS72) of the original four founder mice were successfully bred with the *wt* mice producing viable progeny (F1 generation). One of the founder mice (FS1) was unable to breed and was euthanized and its tissue was harvested for further investigation as described previously. The F1 progeny were screened for the transgene by PCR using genomic DNA as a template and the primers depicted in Figure 2A. The resulting 0.9 Kb amplification product was seen only in the transgenic mice and not their *wt* littermates (Figure 2B).

Expression of the transgene at the protein level was confirmed by western blot and immunohistochemical analysis using the HA antibody as described in "Materials and Methods". Western blot analysis of proteins isolated from *SMCRT* and *wt* littermates showed expression of HA-tagged CRT only in the tail biopsies of the *SMCR*T mice (Figure 3A). Expression of CRT-HA was higher in the descending aorta of these mice. Figure 3B shows immunohistochemical staining of arteries isolated from the *SMCRT* mice using the HA antibody. CRT-HA over-

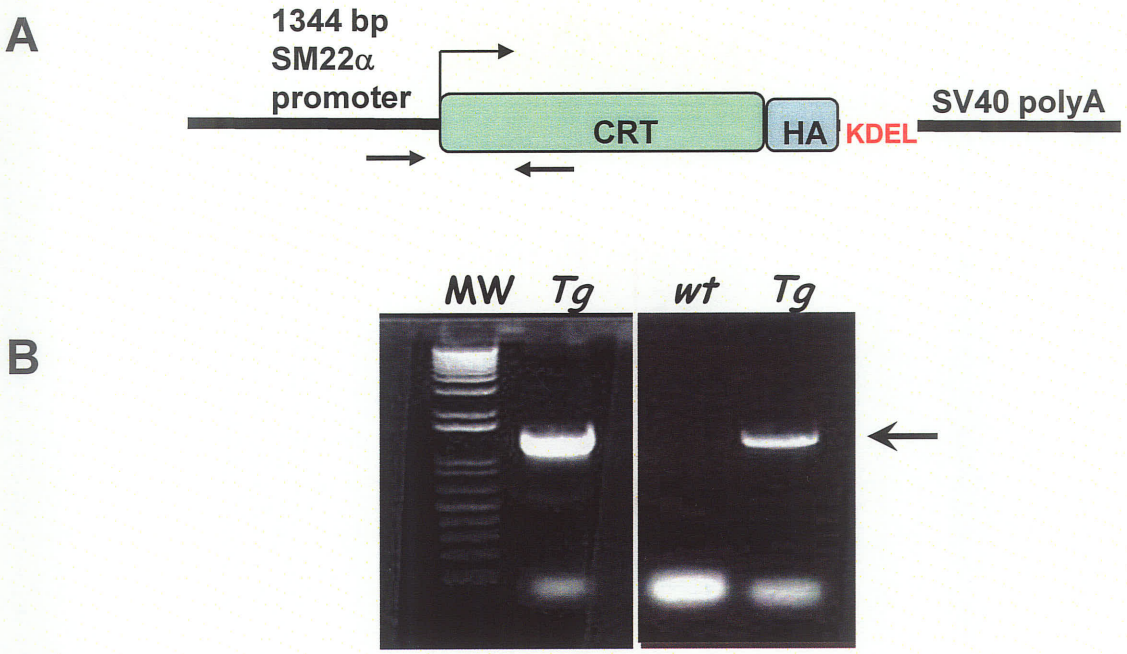

Figure 2: Generation of targeted over-expression of calreticulin in vascular smooth muscle cells.
(A) Schematic diagram (not to scale) showing the *SMCRT* transgene construct used to generate the *SMCRT* mice. The truncated 1344 bp SM22α promoter was cloned upstream of CRT-HA-KDEL fragment with transcription start point indicated. Small arrows indicated the location of primers used for genotyping. (B) PCR of genomic DNA isolated from *SMCRT* (*Tg*) and wild-type (*wt*) littermates demonstrates presence of transgene only in transgenic mice. Arrow indicates the location of the expected PCR product.

expression, as indicated by the red staining (Figure 3B), was present only in the smooth muscle layer of these vessels and was not observed in the endothelial cells (Figure 3B inset).

Two of the original founding lines (SF5 and SF18 lines), which expressed high levels of CRT-HA were bred for several generations in the FVB/N background for the purpose of characterizing the phenotype of the *SMCRT* mice.

II. Characterization of *SMCRT* Mice

II. 1. Skin phenotype in SMCRT male mice- Hemangioendothelioma

SMCRT mice were fertile, producing normal litter sizes, and *SMCRT* pups were indistinguishable from *wt* littermates. At 3 to 10 months of age, 38% of the male *SMCRT* mice from both the SF5 and SF18 lines developed skin abnormalities which appeared as roughened fur and bulging red skin on the lower back (Figure 4). The skin abnormality progressively developed into necrotic lesions that formed a scab. Eventually the necrotic area of skin was shed resulting in an open wound, which could heal when smaller in size (Figure 4). The skin abnormalities of the *SMCRT* mice were similar in appearance to spontaneously occurring vascular tumours, which develop in humans, called hemangiomas (or hemangioendotheliomas, a more aggressive form) [112, 114].

The skin hemangioendothelioma (HAE)-like abnormalities of the *SMCRT* male mice varied greatly in size between individual mice, with some being quite small in area (Figure 4A), while others covered almost the entire lower back (Figure 4B) and were raised in appearance (Figure 4C). Figure 4C shows the

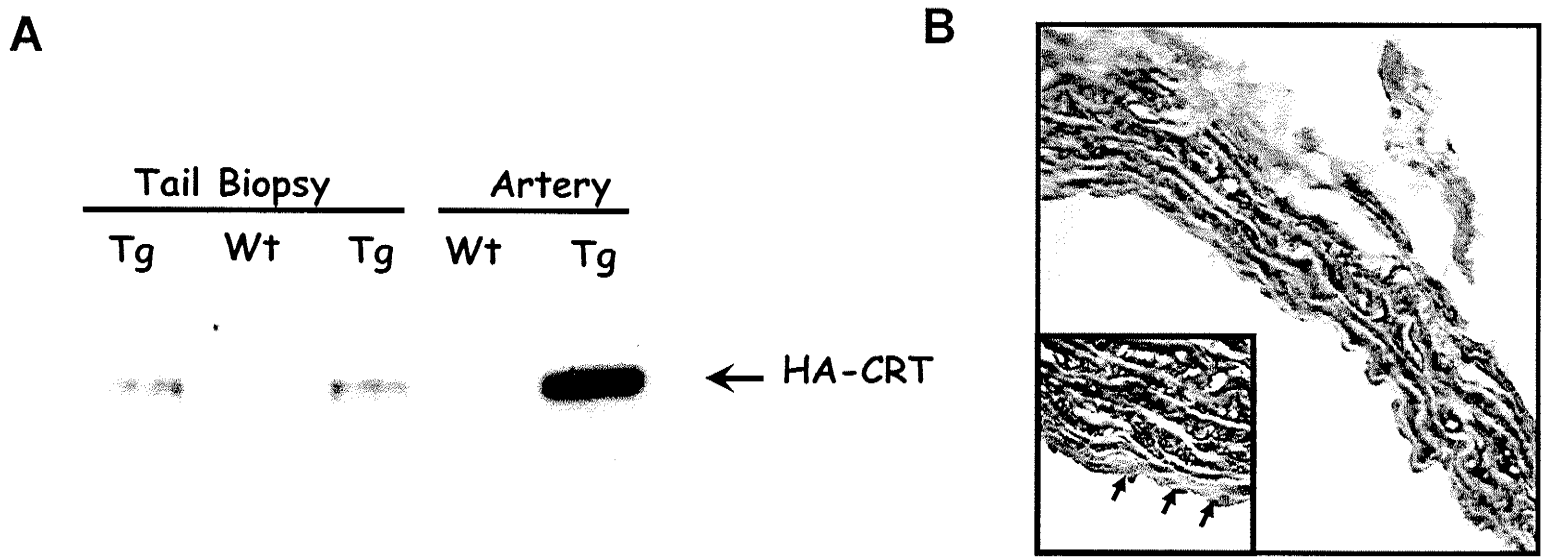

Figure 3: Transgene expression in the *SMCRT* mice. (A) Western blot analysis of proteins isolated from tail biopsies and descending aorta samples isolated from *SMCRT* and *wt* mice using anti-HA antibody to demonstrate transgene expression only in tissue from *SMCRT* mice.(B) Immunohistochemical staining demonstrates CRT-HA expression (red) only in the smooth muscle cell layer of the abdominal aorta from *SMCRT* mice. Inset is a higher magnification of the arterial section showing no HA staining in the endothelial cells (arrows).

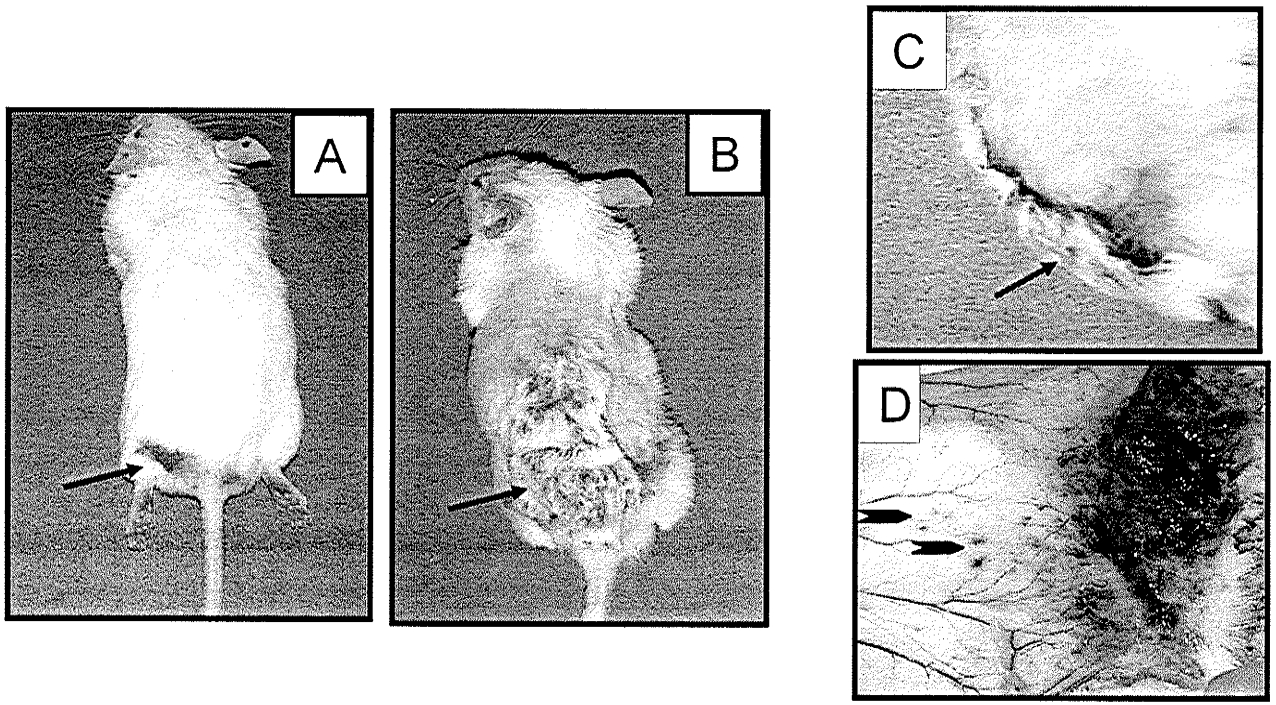

Figure 4: Skin phenotype of *SMCRT* Mice. A, B) Adult male *SMCRT* mice from two different transgenic lines showing the presence of cutaneous HAE of differing severity (arrows). (A) A *SMCRT* mouse in which tumor is small and the necrotic portion of skin has fallen and skin below has begun to heal. (B) A *SMCRT* male with large HAE on lower back, the mouse was anesthetized and shaved to show size of the tumor. Panel (C) shows raised appearance of HAE from mouse B in side-view. (D) Abnormal vasculature, ruptured microvessels (arrows) and appearance of thrombosis and necrosis in the skin lesion.

abnormal structure of the vasculature in the skin surrounding the lesion. In the lesion area, there was evidence of abnormal vascular structure, thrombosis and necrosis (Figure 4D). The skin immediately outside the area of the lesion had increased neovascularization and ruptured microvasculature as indicated by the arrows in Figure 4D. This phenotype was observed only in adult male *SMCRT* mice. No *wt* mice (male or female) *SMCRT* mice were seen to have this unique skin phenotype.

II. 2. Visceral Hemangioendotheliomas in male SMCRT mice

Following external examinations, *wt* and *SMCRT* mice were euthanized for gross anatomical examination. Large masses resembling blood clots were found associated with the heart and lungs (Figure 5A) of *SMCRT* male mice between the ages of 3 to 10 months of age. These masses were seen in both *SMCRT* males that had developed the skin HAE and in some that had not. Upon closer examination of these masses it was determined that they had distinct cellular borders and were not blood clots (Figure 5B). As shown in Figure 5C the HAEs associated with the heart and lungs developed as outgrowths from the base of the aorta. In addition to the HAE on the aorta, some *SMCRT* mice also developed vascular tumours originating from other arteries and tissues including the axillary arteries (Figure 5D), renal arteries (Figure 5E) and hepatic vessels (Figure 5F). Furthermore, the HAE of the *SMCRT* mice were also characterized by the presence of invasive vessels growing out of HAEs and infiltrating neighboring tissues (Figure 6). Figure 6A and inset show an invasive vessel

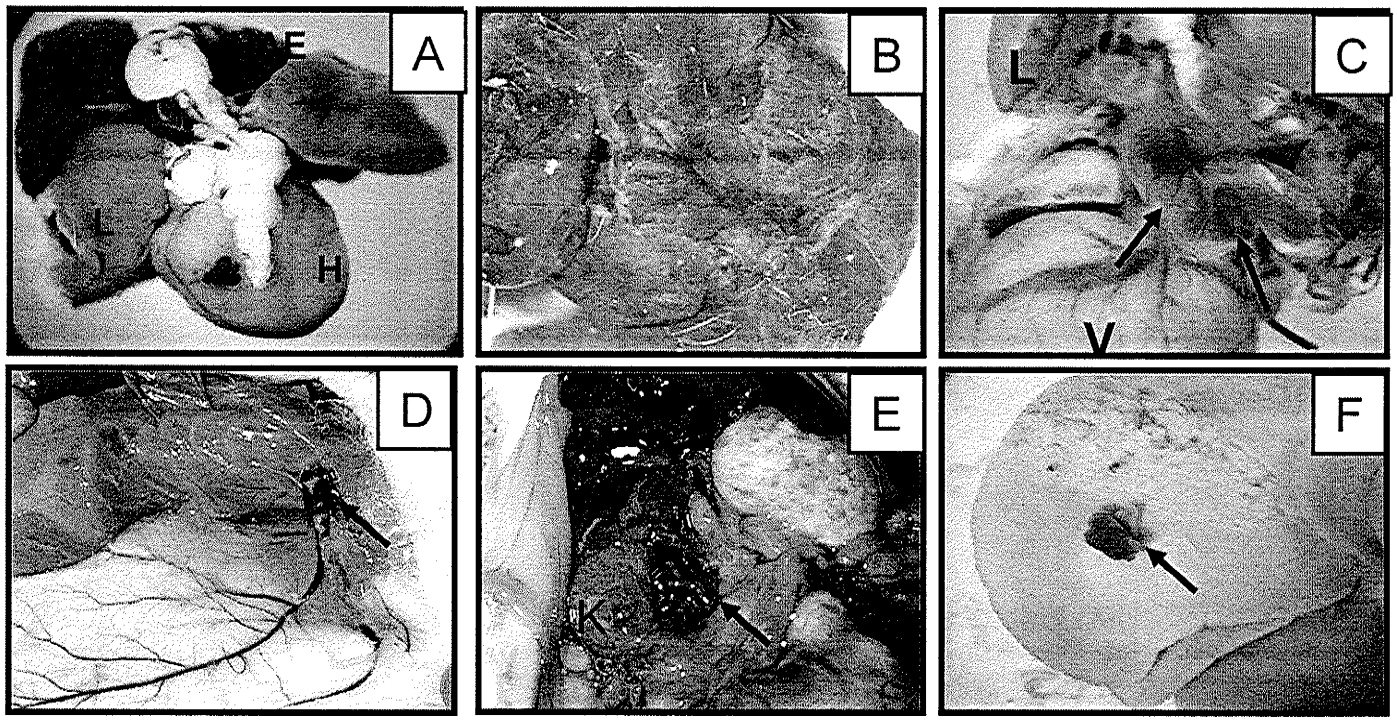

Figure 5: Localization of hemangioendothelioma (HAE) in *SMCRT* male mice (3-10 months). Panel (A) shows major phenotype of the male *SMCRT* mice, development of HAE associated with the heart (H) and lungs (L). (B) A photograph of HAE at higher magnification demonstrating the distinct borders of the tumor. In panel (C) arrows indicate the origin of the HAE from the base of the aorta (V, ventricle; L, lung). Panel (D) shows a HAE (arrow) growth on auxiliary artery beneath of the right forelimb of mouse. (E) HAE (arrow) growth from the renal artery and associated with the right kidney (K). (F) HAE (arrow) derived from the hepatic artery.

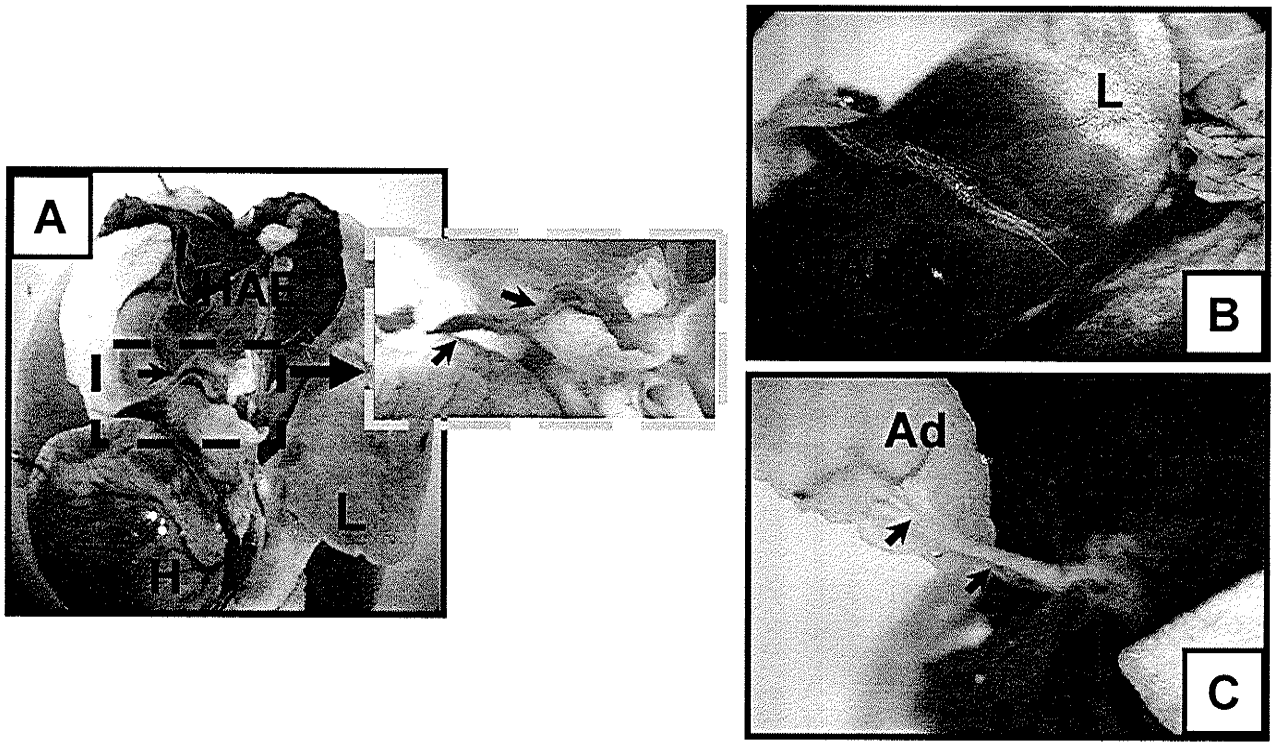

Figure 6: Invasive vessels associated with HAE in *SMCRT* mice (arrows). (A) Image of heart (H) and lungs (L) with attached HAE. A large vessel (arrow), an outgrowth of the aorta, is shown growing into the heart (green box). Inset shows enlarged view. (B) Image shows a large invasive vessel growing from a HAE that has infiltrated one lobe of lung of a *SMCRT* mouse. (C) Image shows vessel (arrows) growing out from a HAE and invading an adjacent adipose (Ad) tissue.

outgrowth from the HAE invading the heart. Figure 6B and 6C show invasive vessels from the HAE infiltrating the lungs and adjacent adipose tissues respectively.

II. 3. Cardiac Phenotype of SMCRT mice

Gross anatomical examination of hearts from the *SMCRT* mice showed increased angiogenesis of the coronary arteries as compared to *wt* hearts (Figure 7A). This was observed in the hearts of both male and female *SMCRT* mice. Male mice also frequently developed coronary aneurysms (arrows, Figure 7B) and occasionally aneurysms were observed associated with other organs such as the liver and kidneys (not shown).

SMCRT mice of both sexes frequently developed dilated cardiomyopathy that became more pronounced with age. In older mice, right ventricle dilation was more pronounced as demonstrated in Figure 7A. These mice also developed symptoms of congestive heart failure including edema, lung congestion, laboured breathing, kidney failure and lethargy. Figures 7A, B also show increased angiogenesis in the coronary arteries of both male and female *SMCRT* mice. There was also high incidence of coronary aneurysm in male *SMCRT* mice (Figure 7B).

Figure 8 shows H&E staining of tissue sections from a normal *wt* and a failing *SMCRT* kidney. The *SMCRT* kidneys show evidence of medullary necrosis and defects in the glomeruli structure in the cortex. Arrows in Figure 8 show thrombosis observed in the kidney capsule, cortex, and medulla of the

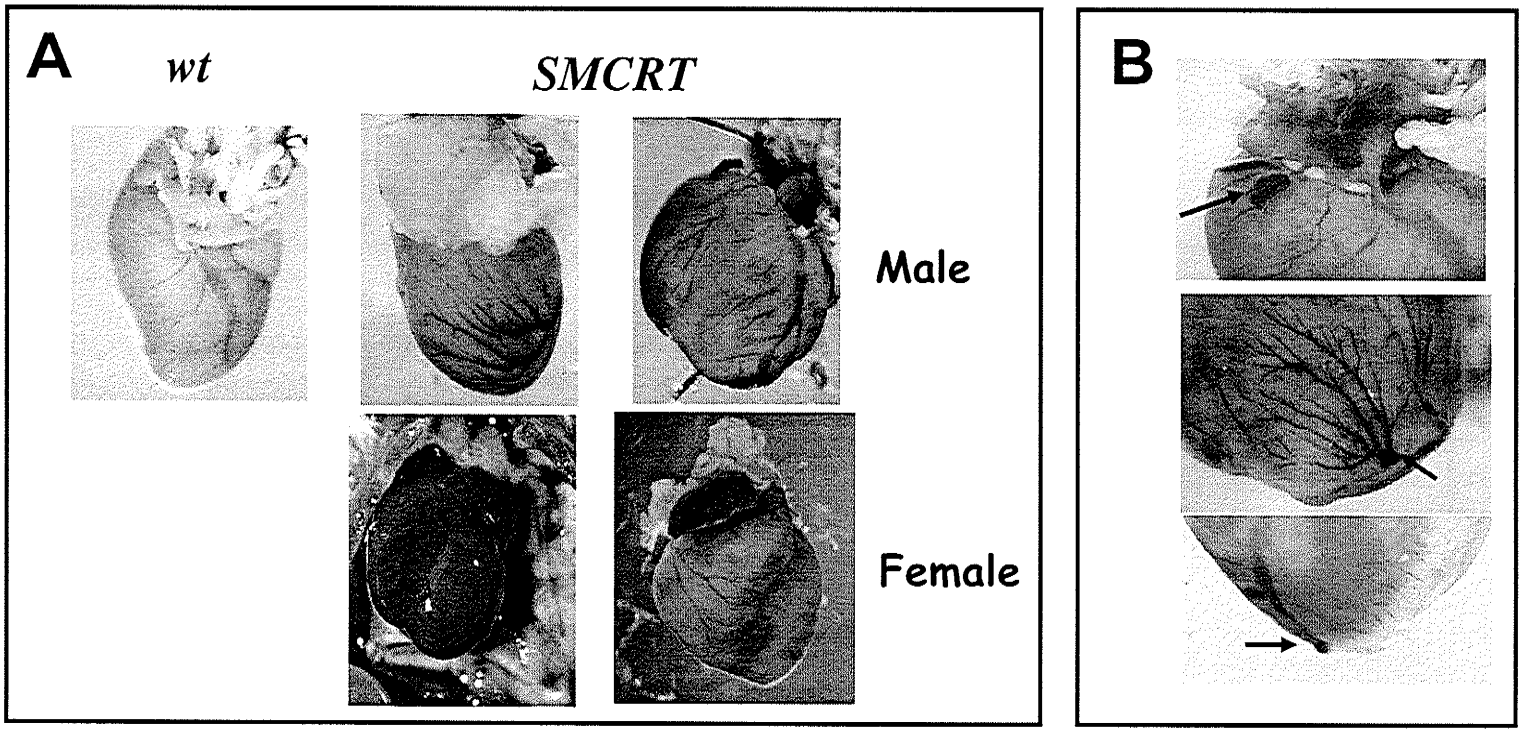

Figure 7: Heart and Coronary artery phenotype in *wt* and *SMCRT* mice. (A) Heart isolated from male and female *SMCRT* mice and *wt* mice. *SMCRT* hearts isolated from both males and females show increased coronary artery angiogenesis as compared to *wt* hearts (also seen in B). The *SMCRT* hearts show dilated cardiomyopathy in both male and females. However, the female *SMCRT* show more pronounced dilation in the right ventricles as compared to male *SMCRT* mice. (B) *SMCRT* hearts often had coronary aneurysms as indicated by the arrows.

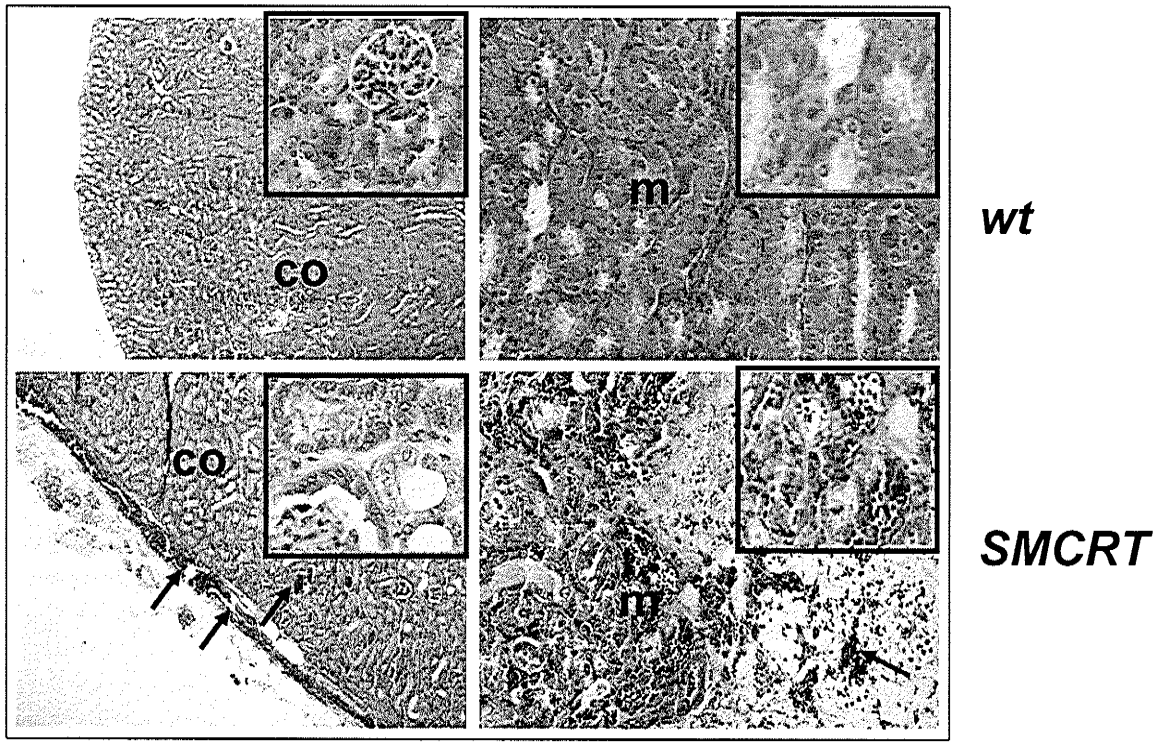

Figure 8: Histological analysis of the structure of kidneys from age matched *wt* and *SMCRT* mice. H&E stained sections (5 µm) of *wt* and *SMCRT* kidneys showing capsule, cortex (co) and medullary (m) region of kidneys. A sub-capsular bleed (arrows) is shown in a kidney section from *SMCRT* mouse, but not in the *wt* kidney. Medulla of *SMCRT* kidney shows areas of necrosis and thrombosis (arrow) disrupting normal tubule structure as seen in *wt* medulla (m).

SMCRT kidney. In non-failing kidneys of *SMCRT* mice, we frequently observed the presence of cysts in the cortex (data not shown).

Another phenotype of the *SMCRT* mice was the increased activation of blood coagulation. Figure 9 shows Giemsa staining of blood smears from *wt* and *SMCRT* mice. Interestingly, blood smears from *SMCRT* mice showed a marked increase in the number of platelet aggregates as compared to *wt* blood smears (Figure 9) indicating that coagulation pathways are upregulated in the *SMCRT* mice.

III. Characterization of the Hemangioendotheliomas

To characterize the HAE like vascular tumours of the *SMCRT* mice, sections from HAE were stained with H&E. Figure 10A show that the HAE of the *SMCRT* mice were composed of solid sheets of epitheliod and spindle shaped cells, which were often vacuolated (Figure 10A', A"). In addition, the HAE also contained vessel-like lumens filled with erythrocytes (Figure 10A', A"; black arrows). Masson's Trichrome staining sections of HAE associated with the lungs demonstrated that it contains little connective tissue and that a significant area of the tumour is made of thrombus (Figure 10B, B', B"). Previous reports showed that human HAE stain positively for the endothelial cell markers CD31 and CD34 [112, 201]. Thus to further characterize the HAE from the *SMCRT* mice we carried out immunohistochemical staining of the HAE section with antibodies to CD31 and CD34. Figure 11A shows a control showing positive staining of CD31 of endothelial cells lining the lumen of atria and aorta. Figure 11B shows staining

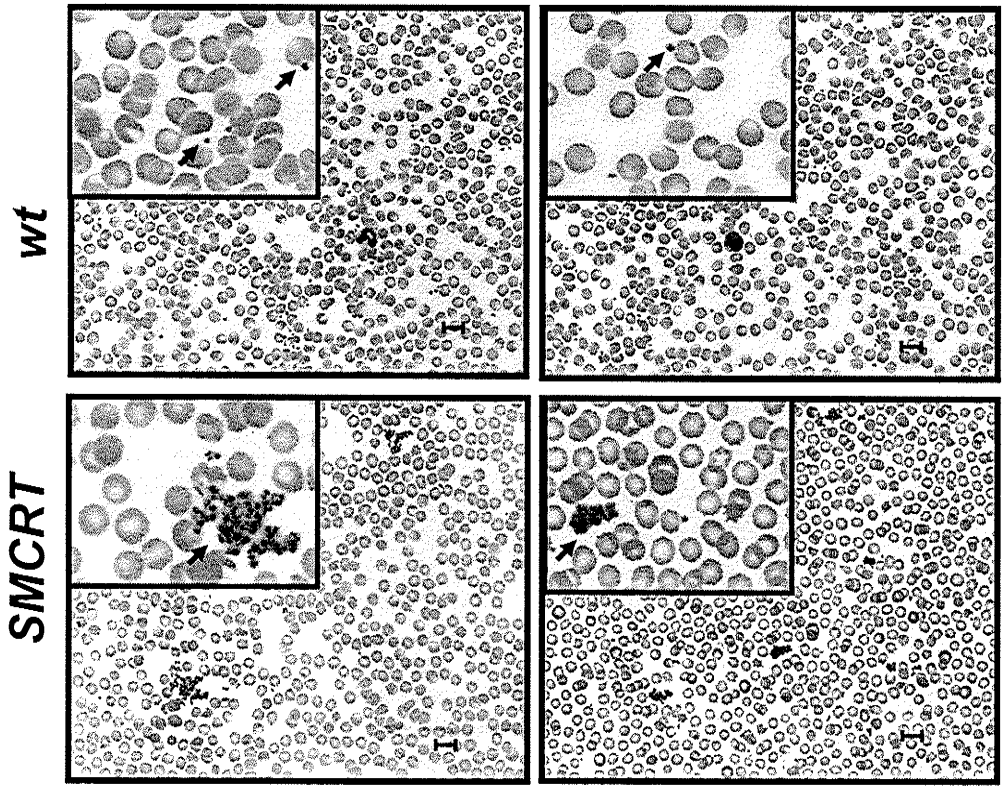

Figure 9: Giemsa staining of blood smears from *wt* mice (top panel) and *SMCRT* mice (lower panel). Arrows in each panel pointing to platelets in the blood smears. As seen in the *SMCRT* mice, platelets form large aggregates indicating that blood coagulation pathways are activated. No platelet aggregates seen in smears from *wt* mice. Scale bars indicate 20 μm.

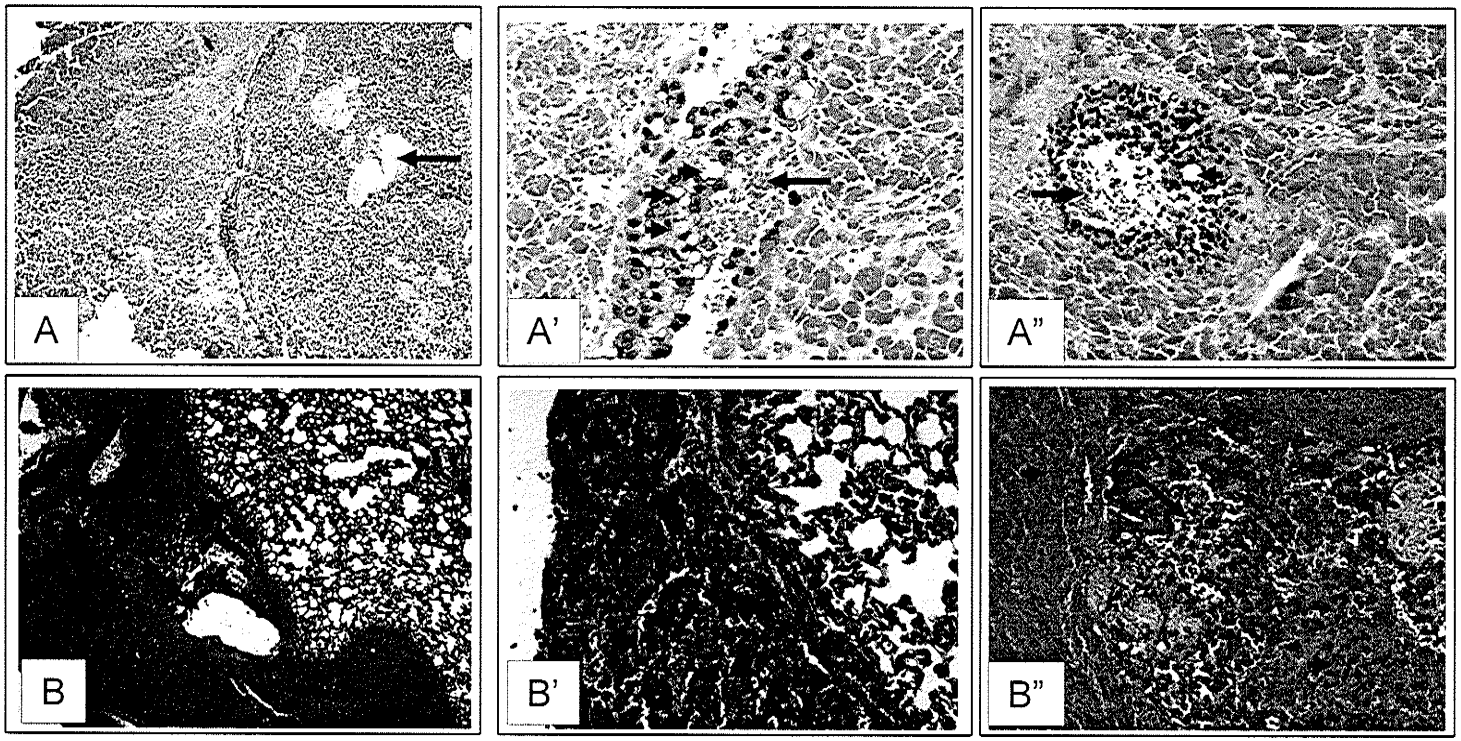

Figure 10: Histological analysis of HAE from male *SMCRT* mice. (A-A") Hematoxlin and eosin staining of an HAE demonstrates the variety of cell types in tumor including epitheliod and mesenchymal-like cells. (A', A") Arrows show lumen like structures lined containing erythrocytes, and lined with epitheliod cells that contain distinct vacuoles (green arrowheads). (B-B") Masson Trichrome staining of HAE associated with lung. The HAE is a very cellular structure containing little or no extracellular matrix components (lack blue staining). (B, B") Arrows point to lumen like compartments, and green arrowheads indicate the presence of thrombus in the HAE.

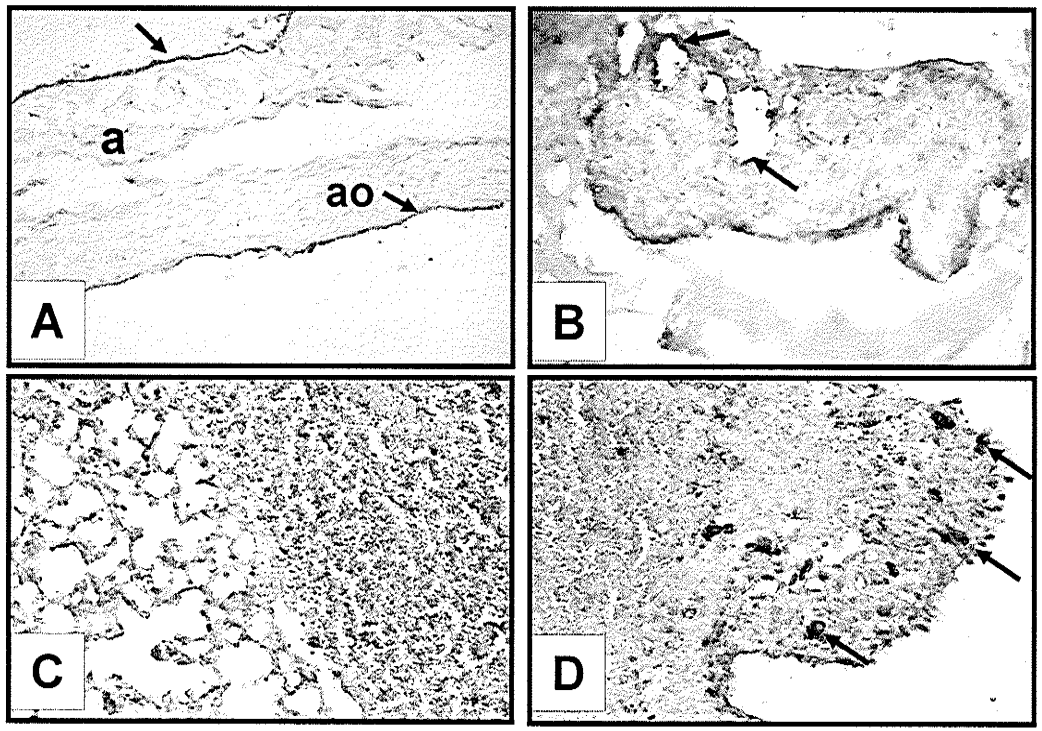

Figure 11: Immunohistochemical analysis of sections of HAE from male *SMCRT* mice. (A, B) Staining of HAE with anti-CD31 antibody. (A) Positive control shows dark brown stained endothelial cell layer (arrows) lining the aorta (ao) and atria (a). (B) Diffuse CD31 staining throughout the HAE with more intense staining lining borders and the lumen-like cavities in the HAE (arrows). (C), (D) HAE stained with anti-CD34 antibodies. (C) negative control (no primary antibody) showing no background staining. (D) shows CD34 positive cells stained purple within the tumor (arrows).

of the HAE section with CD31 antibody with the most intense staining of the cells lining the lumen-like cavities and the outside border of the tumour. The HAE tumours also contained CD34 positive cells (arrows, Figure 11D) as compared to the no antibody controls (Figure 11C).

IV. Mechanism for HAE development

HAE are endothelial derived vascular tumours resulting from abnormal angiogenesis [5, 115]. Histological analysis of sections from a *SMCRT* lung associated with a HAE shows increased angiogenesis of small arterioles even in sections without tumour present (Figure 12B). Figures 12B and C show the migration of EC through the smooth muscle layer producing a vessel sac, which will give rise to the HAE. We observed this phenotype in the lungs of *SMCRT*, but none in the lungs of the *wt* mice (Figure 12A).

The breakdown of the extracellular matrix is a key step in new blood vessel formation [17, 54]. Therefore we examined changes in the matrix composition of *SMCRT* tissues as compared to *wt*. *SMCRT* and *wt* arterial sections were stained with PicroSirius Red, which stains collagen fibers. The intensity of red staining was less in the medial layer of the *SMCRT* vessels (Figure 13) indicating decreased collagen content in these vessels as compared to *wt* vessels. As described in the literature review MMPs, particularly MMP-2 and MMP-9, play an important role in regulating collagen degradation in the vessel wall [17, 54]. Immunohistochemical staining of arteries from transgenic and *wt* (Figure 14) mice demonstrates that MMP-2 and MMP-9 protein levels are

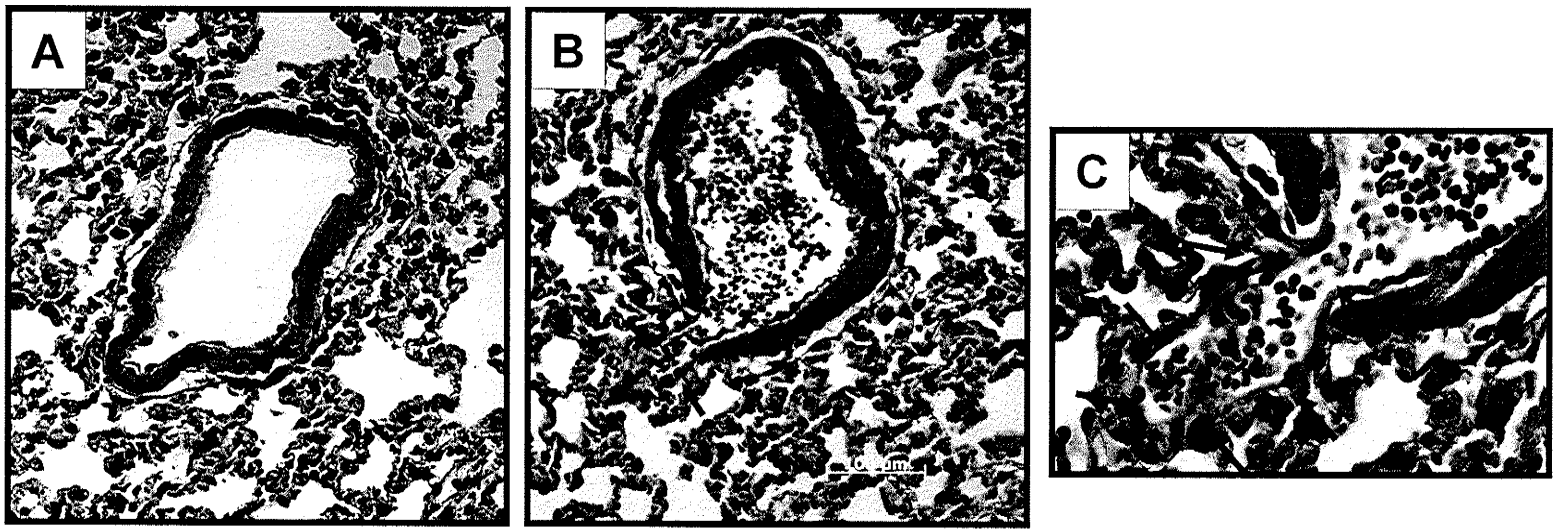

Figure 12: Histological analysis of arterioles in the lungs of *wt* (A) and *SMCRT* (B) mice. The arterial wall in the *SMCRT* mice shows disruption of the smooth muscle layer, and migration and outgrowth of the endothelial cells from the preexisting arteriole. Panel (C) shows an enlarged view of this endothelial migration (arrows) through the smooth muscle layer to form a sack-like structure in which blood has accumulated. Sections were stained with Masson's Trichrome stain as described in Materials and Methods.

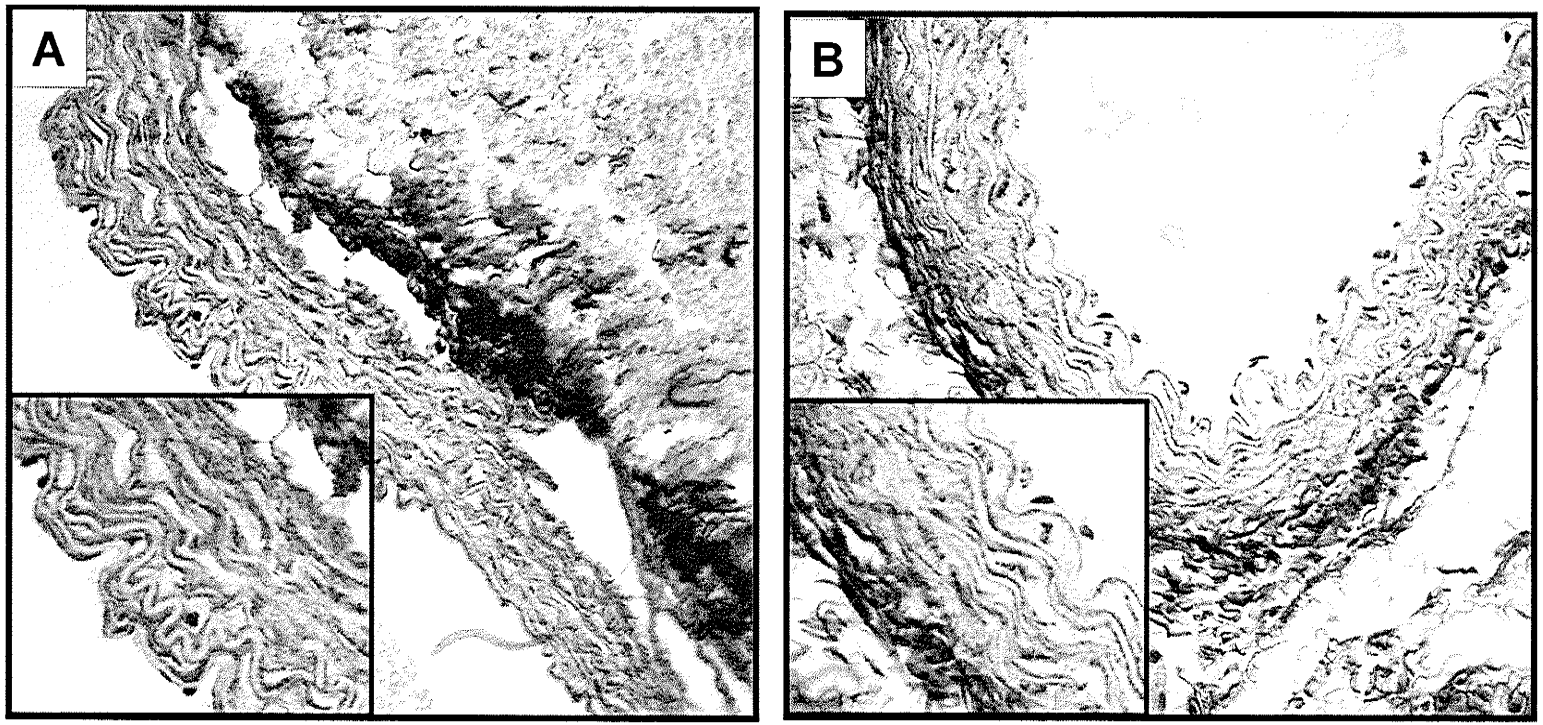

Figure 13: PicroSirius red staining of artery (A, B) sections from male *wt* and *SMCRT* mice, respectively. Sections were stained for collagen with Picrosirius red stain according to "Materials and Methods". *SMCRT* artery sections (B) show significantly less collagen staining (red) in the smooth muscle cell layer as compared to the *wt* artery (A) sections.

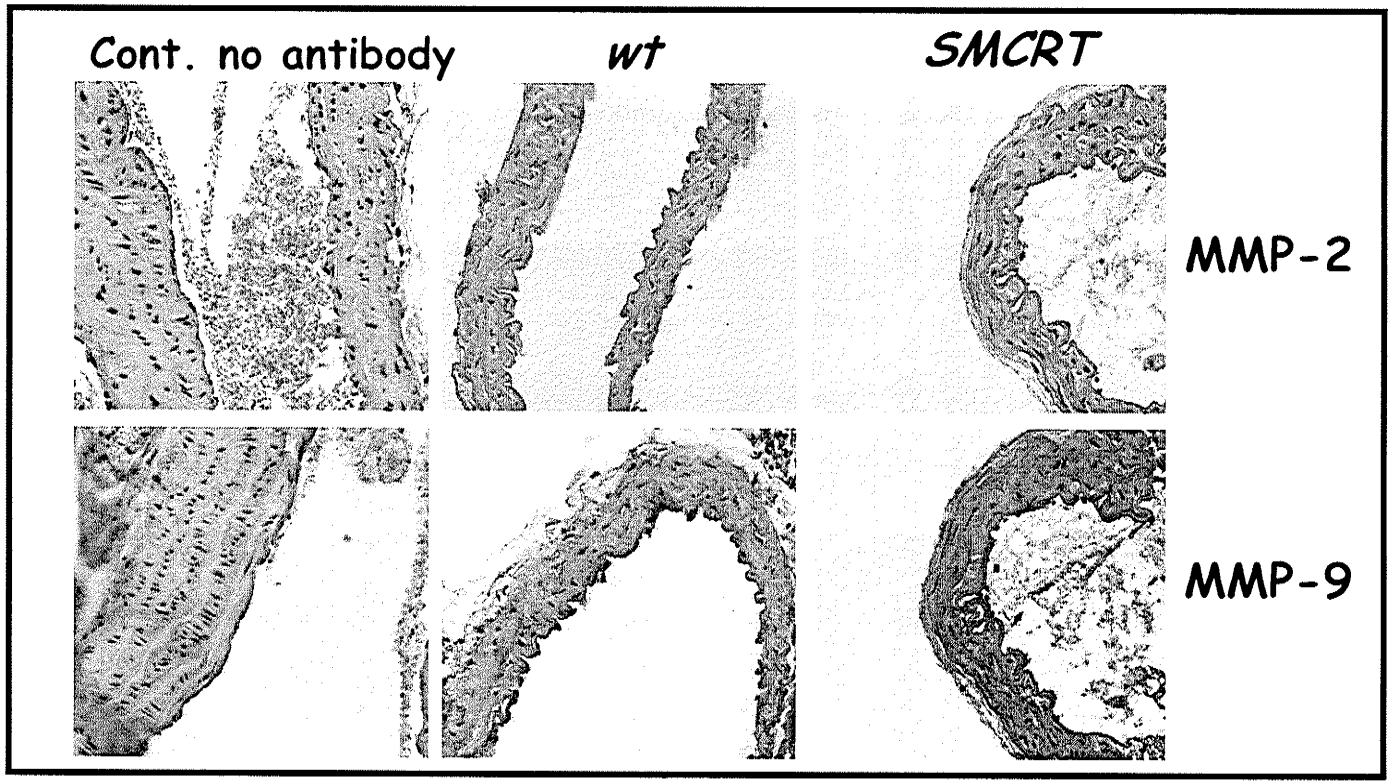

Figure 14: Analysis of MMP-2 and MMP-9 expression in *wt* and *SMCRT* arteries. Immunohistochemical staining of arterial sections from *wt* and *SMCRT* mice with MMP-2 and MMP-9 antibodies. MMP-2 and MMP-9 staining is seen as brown color in *wt* and *SMCRT* arterial sections compared with no staining in negative control without primary antibody (left panel).

present in the *SMCRT* and *wt* vessel walls. Figure 14 also demonstrates a slightly higher intensity of MMP-9 staining in the *SMCRT* arteries. To determine whether changes in collagen content of the vessel wall may be due to altered MMP-2 and -9 gelatinase activity, we carried out gelatin zymography experiments with media collected from VSMCs isolated from either *wt* or *SMCRT* aortas. Figure 15A shows significantly higher MMP-2 and MMP-9 activity in a representative zymograph from the media of *SMCRT* and *wt* VSMCs. Figure 15B illustrates the increase in the activity of MMP-2 and MMP-9, which was significantly higher in the *SMCRT* VSMCs as compared to *wt* cells.

Previous studies have demonstrated that CRT overexpression in cardiomyocytes results in decreased connexin 40 and 43 expression [184]. Additionally, decreased expression of connexins and functional gap junctions has been demonstrated in the development of a variety of tumours [202]. Thus we carried out western blot analysis of connexin 40 and 43 expression in tissue lysate isolated from arteries as described in "Materials and Methods". Figure 16 shows a significant decrease in the levels of gap junction proteins in the *SMCRT* vessels as compared to *wt* arteries. Similar data was also obtained in VSMCs (data not shown).

V. Mechanical Properties of *SMCRT* vessels

Pressure myography experiments were carried out to determine whether the observed changes in *SMCRT* vasculature (increased vessel branching, reduced collagen content) had resulted in altered vessel mechanics, such as

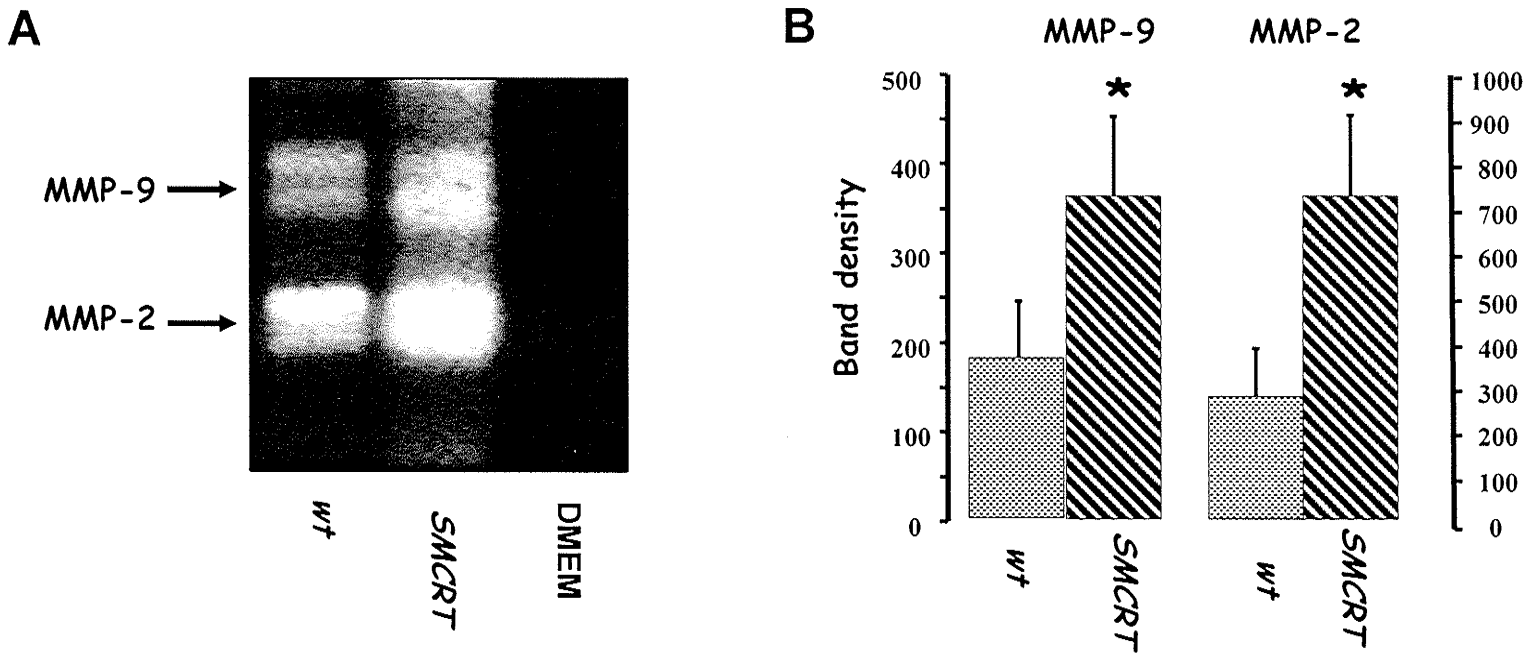

Figure 15: Gelatin zymography for the analysis of MMP-2 and MMP-9 enzyme activity. A) Representative gelatin zymograph with conditioned media collected from *wt* and *SMCRT* vascular smooth muscle cells (see Materials and Methods) and control (DMEM). MMP-2 and MMP-9 activity is seen as clear zones against dark background. (B) Bar graph shows densitometric quantification of bands corresponding to MMP-2 and MMP-9 activity. The values are the mean +/- SE of MMP-2 and MMP-9 from 5 separate experiments. * $P < 0.05$ significantly different compared to *wt*.

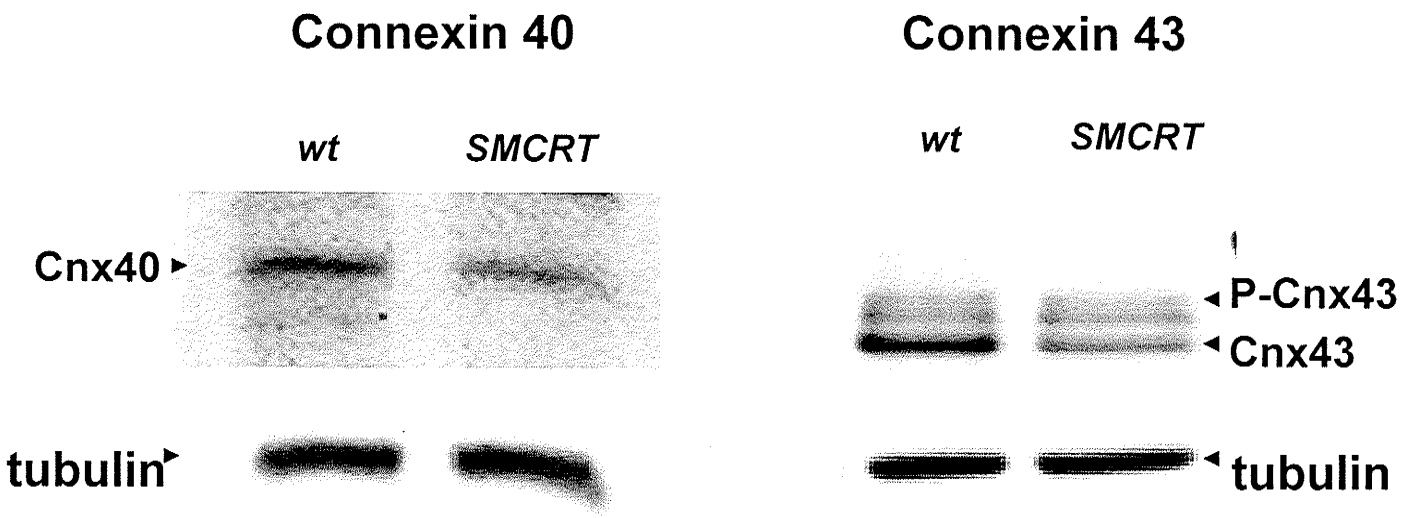

Figure 16: Protein expression levels of connexins (Cnx) 40 and 43 in *wt* and *SMCRT* arteries. Western blot analysis of lysates isolated from *wt* and *SMCRT* abdominal arteries using anti-cnx 43 and 40, and tubulin (loading control) antibodies demonstrating decreased expression in *SMCRT* arteries as compared to *wt*.

distensibility and stiffness, as compared to *wt* vessels. Figure 17A shows the relationship between media stress and media strain plotted for *SMCRT* and *wt* vessels. Stress values for *wt* and *SMCRT* vessels were calculated and compared at fixed percentages of strain (see "Materials and Methods"). There was no significant differences between *SMCRT* and *wt* vessels in calculated mean stress (dynes/cm2 ± SEM) at values at strain of 20% (0.0292 ± 0.0103 vs. 0.0116 ± 0.0025), 40% (0.1060 ± 0.0385 vs. 0.0419 ± 0.0080), 60% (0.4080 ± 0.1509 vs. 0.1550 ± 0.0263) and 80% (0.614 ± 0.0.0790 vs. 0.3550 ± 0.1981). At maximal strain, in the upward turn of the curves there is a significant difference in calculated stress (0.2225 ± 0.0921 vs. 0.2.980 ± 0.4616, $p<0.05$), with a rightward shift of the *SMCRT* curve in relation to *wt.* This trend suggests that less strain (stretch) is required to produce a given amount of stress in the *SMCRT* vessels as compared to *wt.* Elastic modulus which is calculated from the slope of the stress-strain curve is a measure of vessel wall stiffness. Elastic modulus plotted as a function of vessel strain describes vessel stiffness as a function of both vessel wall geometry and vessel wall ECM composition. We observed the same rightward trend of the *SMCRT* curve in relation to *wt* with significance only observed at maximal strain of 100% (1.0335 ± 0.1366 vs. 16.456 ± 2.8379, $p< 0.05$) that for a given strain the elastic modulus of the *SMCRT* vessels is skewed to the right compared to *wt* vessels indicating that the vessels from these transgenic mice are less stiff then normal mice (Figure17B).

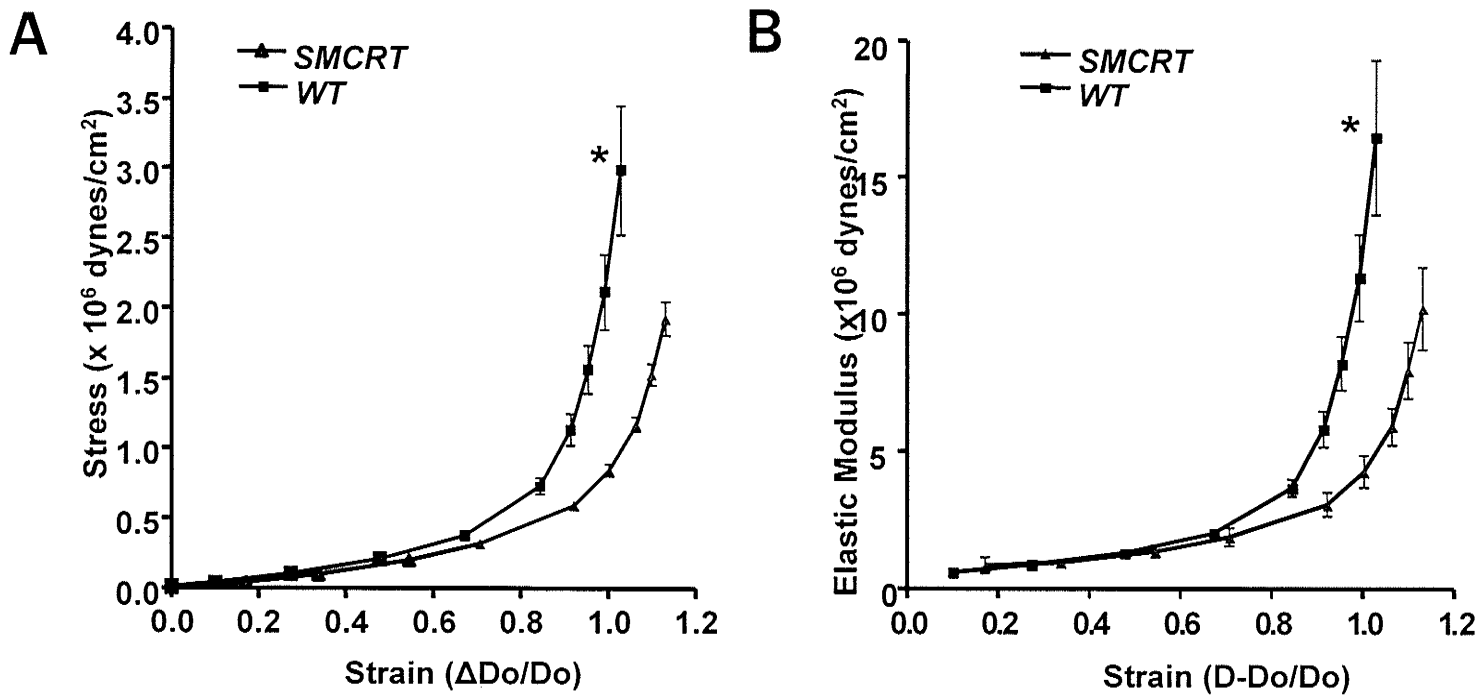

Figure 17 : Mechanical properties of mesenteric arteries from *wt* and *SMCRT* mice as determined by stress vs strain (A) and Elastic modulus vs strain (B) relationships. (A) Stress as a function of strain of vessels describes the distensibility of the vessels. The vessel walls of *SMCRT* arteries are more distensible as compared to *wt* vessels. (B) Elastic modulus as a function of increasing strain describes stiffness of vessel walls. *SMCRT* Vessels are less stiff than *wt* vessels. Values are mean +/- standard error of the mean, (* $p < 0.05$, n=8).

To differentiate between the effect of vessel ECM composition and vessel geometry on vessel stiffness we looked at elastic modulus vs. stress, lumen diameter vs. intraluminal pressure and media cross-sectional area (CSA) vs. intraluminal pressure (Figure 18). Elastic modulus in relation to wall stress describes vessel wall stiffness as a function of ECM components of the vessel wall alone. Figure 18A demonstrates that based on ECM components alone there is no difference between *wt* and *SMCRT* vessels. Figures 18B and C describe lumen and vessel wall dimensions as a function of pressure, respectively. We observed some change in vessel wall geometry of SMCRT vessels as compared to *wt*, but it is not a significant (Figure 18C).

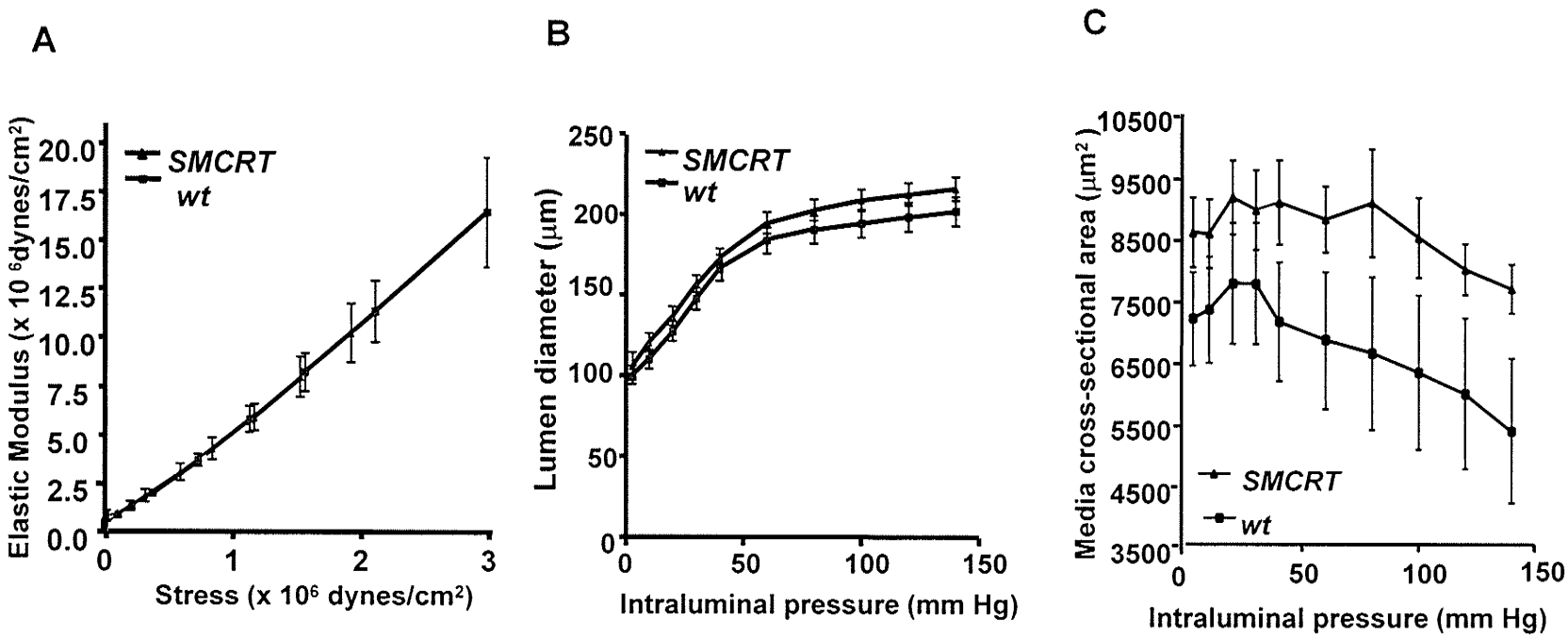

Figure 18: Changes in mesenteric artery stiffness and geometry in *wt* and *SMCRT* mice. (A) Elastic modulus as a function of stress describes stiffness of vessel wall ECM components. There are no differences in vessel stiffness as the result of ECM components alone. (B) Vessel lumen diameter vs intraluminal pressure and (C) media cross-sectional area vs. intraluminal pressure describe artery geometry. There is no significant difference in vessel geometry of *wt* and *SMCRT* vessels. Values are mean +/- standard error of the mean, (n=8).

E. Discussion

CRT is a ubiquitously expressed chaperone protein of the ER with roles in calcium handling protein folding and cell adhesion. CRT has been previously demonstrated to play a critical role in development of the heart, and is highly expressed in the cardiovascular system during embryogenesis [167, 168]. In adulthood,CRT expression is down regulated in the heart but it is expressed in the vascular wall [137, 167]. Studies using gene therapy or delivery of exogenous protein have demonstrated the potential of CRT as an anti-angiogenic agent, by its suppression of tumour growth [156, 189, 191, 194, 203]. In the current study we developed a transgenic mouse model overexpressing CRT in the vascular wall, specifically in the vascular smooth muscle layer (*SMCRT* mice) to elucidate the role of endogenous CRT in vascular remodeling and function. To our knowledge this is the first mouse model overexpressing CRT specifically in the blood vessel wall.

The *SMCRT* mice developed cardiovascular defects, which were not observed in the *wt* littermates. The major defect was the development of vascular anomalies in the skin (Figure 4), and associated with the heart and large arteries (Figure 5) in the male *SMCRT* mice. These vascular abnormalities were similar to skin hemangiomas, and visceral hemangioendotheliomas (HAE) seen in humans. Interestingly, only older female *SMCRT* mice (more then 18 months old) developed HAE. This suggests a role for sex hormones in the development of HAE in these mice. Both male and female mice developed increased coronary angiogenesis, dilated cardiomyopathy (Figure 7), edema and kidney failure

(Figure 8). Overall, the symptoms of these mice suggest major changes in vascular wall structure leading to secondary pathologies.

Hemangiomas and HAE represent a broad spectrum of vascular neoplasms ranging in severity from benign hemangiomas to locally aggressive epitheliod or Kaposiform HAE [111-115]. These vascular tumours are characterized by the rapid proliferation of endothelial cells forming vascularized masses of densely packed cells [112, 113, 115]. HAE can develop cutaneously, subcutaneously and viscerally in soft tissues such as the lungs and liver [112, 113, 115] where they often originate from an artery or vein [112]. These HAE developed in the male *SMCRT* mice at 3 to 10 months of age on the skin of the lower back (Figure 4). *SMCRT* mice also developed visceral HAE originating from the aorta, associated with the heart and lungs (Figure 5A-C), as well as associated with the axillary artery, renal artery and hepatic artery (Figure 5D-F), all of which have been described in humans [201, 204, 205]. HAE in humans have large associated vessels that feed and drain the tumours [114], similar to the large invasive vessels we observed associated with the *SMCRT* HAE (Figure 6).

Histologically and pathologically the *SMCRT* HAE have many features that are similar to the Kaposiform HAE, also called giant hemangiomas. The human lesions, like those found in the male *SMCRT* mice, are locally aggressive tumours characterized by irregular lobules and sheets of round, spindle or epitheliod shaped endothelial cells (Figure 10). Like Kaposiform HAE the *SMCRT* tumours were seen to infiltrate the surrounding tissues and frequently contain

microthrombi and trapped platelets [114, 117] (Figures 5, 6 & 10). This type of vascular lesion is associated with Kasabach-Merritt syndrome (KMS), a coagulopathy where the platelets and clotting factors are sequestered within the vascular lesions, leading to activation of local blood clots. The increased platelet aggregation seen in the *SMCRT* mice (Figure 9) could lead to intravascular coagulopathy, also observed in these mice (Figure 10). Similarly, KMS patients frequently have a tendency to develop intravascular blood clots, and have an increased risk of bleeding due to depletion of clotting factors [111, 117]. HAE characteristically expresses endothelial markers such as CD31 and CD34 [111, 117] which we have also to be expressed by the *SMCRT* lesions (Figure 11). These data illustrate that our mouse model phenocopies the human patients with KMS. However, further studies need to be carried out to examine changes in CRT expression in human patient samples to confirm this observation.

As *SMCRT* mice aged, they became lethargic, inactive and developed pulmonary and systemic edema. These symptoms in addition to the development of dilated cardiomyopathy (Figure 7), lung congestion and necrosis of the kidneys (Figure 8) could develop collectively as complications of heart failure. Similar symptoms have also been frequently found to be associated with Kaposiform HAE and large hemangiomas in human patients [111, 117]. Cardiovascular stress due to an increased blood flow, increased number of blood vessels and the development of the HAE in humans has been demonstrated to cause high-output cardiac failure and symptoms of heart failure [114, 115, 117].

HAE are described as endothelial derived vascular tumours that result from abnormal angiogenesis [5, 115]. The *SMCRT* mice demonstrated evidence of increased angiogenesis as seen in the increased vascularization of the coronary arteries (Figure 7) and the lungs (Figure 12). Additionally, Figure 11 shows that vascular tumours of the *SMCRT* mice are of endothelial cell origin as they stained positively for CD31 and CD34, common EC markers. There are several possible mechanisms for this increase in angiogenesis in the *SMCRT* model. The first mechanism leading to activation of angiogenesis in the *SMCRT* mice may be due to changes in ECM composition. Altered ECM composition has been shown to change the phenotype of EC from a quiescent to activated phenotype [17, 54, 103]. MMPs which are involved in the degradation of the ECM have been shown to increase the mobilization and proliferation of EC [17, 54, 103, 206]. The processes initiating angiogenesis include increased permeabilization of the vessel wall, deposition of fibrin into the subendothelial space, activation of proteases and degradation of the ECM [13, 54]. The breakdown of the ECM is mediated by many proteases including MMP-2 and 9 [54, 206]. These proteases digest ECM barriers thereby enabling EC migration and the release a number of matrix associated growth factors such as, FGF-2 and VEGF, that upregulate EC proliferation [17, 54]. In the *SMCRT* model, we showed evidence of decreased collagen in the VSMC layer of the vessels (Figure 13). We also demonstrated a significant increase in the activity of MMP-2 and MMP-9 secreted by *SMCRT* VSMCs (Figure 15). These changes in matrix composition and the increased activity of proteases that digest them could be

factors that lead to the activation of EC and inducing EC to migrate and proliferate resulting in the increased angiogenesis seen in the *SMCRT* animals (Figures 7A & 12).

Coagulation and angiogenesis are highly interrelated processes [13, 73, 107]. In the *SMCRT* mice we detected increased platelet activation as demonstrated by enhanced platelet aggregation (Figure 9). As mentioned previously, this increased activation of the platelets is commonly associated with Kaposiform HAE and KMS [111, 115, 117]. Activated platelets secrete a number of factors that stimulate the coagulation cascade and further induce platelet aggregation including vWF, factor V, factor XIII and calcium [26]. Platelet activation also results in the release of many proangiogenic factors including PDGF, VEGF, and FGF-2 [26, 107]. Thus, the coagulopathy associated with the HAE that develops in the *SMCRT* mice may be resulting in increased growth factor release from activated platelets. The release of these growth factors may induce further EC proliferation, migration and new vessel formation, thus contributing to enhanced angiogenesis and tumour formation in the *SMCRT* mice.

Finally, changes in VSMC adhesiveness and motility as a result of CRT overexpression may play a role in abnormal vessel development and HAE formation. Many studies indicate that CRT plays a role in cell adhesion. For instance, CRT over-expression in L-fibroblasts has been shown to modulate increased cell-cell and cell-matrix adhesiveness resulting in decreased cell motility [144, 145, 166]. Thus overexpression of CRT in the VSMC of the

SMCRT mice may also result in increased adhesion of the cells and an overall decrease in their motility. VSMC interaction with EC during blood vessel development is necessary for the proper maturation, and stabilization of vessels. Vessel stabilization is mediated by growth factor and receptor tyrosine kinase signaling through the Ang/Tie receptor and the PDGF-B/PDGFR-β pathways [92-94, 96, 98, 99]. Mice deficient for any of the genes encoding these receptors or their ligands are embryonic lethal due to leaky immature vasculature that lacks appropriate VSMC support [92, 93, 96, 98, 99]. In the case of PDGFR and PDGF-B mutants, the vessels have increased numbers of EC but lack VSMC/pericytes resulting in aneurysm development [98, 99]. Altered regulation of Ang-2 has been reported in hemangioma derived cells [125]. One of the phenotypes of the *SMCRT* mice is the development of aneurysms which were mostly associated with the coronary arteries (Figure 7B). Increased vessel rupture was also observed in the subcutaneous vessels, close to the hemangiomas (Figure 4). Interestingly, Figure 12 shows that lung arterioles branch to form sacs of EC cells. However, these new vessels do not recruit SMC (Figure 12). VSMC stabilize vessels by preventing EC proliferation [37, 46], migration [3, 37, 46], apoptosis [94] and promoting elaboration of the supportive ECM [33]. If the VSMC of the *SMCRT* mice are not as motile then they may not associate appropriately with the EC of the newly developing vessels. Without suitable VSMC recruitment to the nascent vessel wall, the vessel will be more prone to rupture. Furthermore, angiogenic EC may continue to proliferate and migrate unchecked especially in the presence of mitogenic stimuli such as

VEGF, PDGF and FGF-2 provided by activated platelets and increased release from ECM. Ultimately these changes may lead to the endothelial tumour formation.

Additionally, cell-cell contacts have been shown to play a role in tumour related metastasis and angiogenesis. Connexins are tumour suppressors and are found to be down-regulated in a variety of cancers. Up-regulation of connexins in different models of cancer have been shown to inhibit tumour related metastasis and angiogenesis [202]. It has been previously demonstrated that CRT overexpression in cardiomyocytes results in decreased expression of the connexins 40 and 43 [184]. Similarly, we report a significant decrease in the expression of connexin 40 and 43 proteins in the blood vessels of the *SMCRT* mice (Figure 16). This decreased expression of connexins 40 and 43 in the *SMCRT* vessels would be predicted to decrease intracellular communication between VSMC to VSMC and EC to VSMC. Loss of cell-cell contact could ultimately contribute to changes in the EC microenvironment and also provide less of a barrier for active EC migration resulting in the increased angiogenesis observed in the *SMCRT* mice. Loss of cell-cell contact in addition to altered EC composition could also contribute to increased vascular permeability leading to edema.

Altered ECM composition of the vessel wall, such as reduced collagen content, could affect vessel wall mechanics leading to changes in vascular resistance and hemodynamics. Indeed, our data showed a trend towards increased vessel distensibility (Figure 17A), and decreased vessel stiffness

(Figure 17B) of *SMCRT* mesenteric arteries as compared to *wt* arteries. At maximal strain there was a significant rightward shift in the *SMCRT* stress vs. strain curve (Figure 17A) as compared to *wt* suggesting that less strain is required to produce a given stress in *SMCRT* vessels. Elastic modulus plotted as a function of strain describes vessel stiffness as a function of both vessel wall geometry and vessel wall ECM composition. Our data showed that at maximal strain the *SMCRT* vessels had lower vessel wall stiffness (Figure 17B). We observed less PicroSirius red staining of collagen in the medial layer of the dorsal aorta (Figure 13). Thus, the mesenteric vessels may be more distensible and less stiff as a result of the decreased collagen content in their medial layer. For instance, in aging vessels and in some forms of hypertension, collagen content increases in the vessel media and may lead to stiffer, less distensible vessels [47, 207, 208]. To elucidate which of these vessel properties (ECM composition or vessel geometry) were responsible for the changes in vessel stiffness we examined the elastic modulus as a function of stress (Figure 18A), lumen diameter as a function of intraluminal pressure (Figure 18B) and media CSA as a function intraluminal pressure (Figure 18C). We observed no significant change in elastic modulus as a function of either ECM components, or vessel geometry (Figure 18). This finding suggests that altered vessel stiffness is due to a synergistic effect of both vessel geometry and wall ECM composition. The rightward shift in the stress vs. strain curve further indicates that the *SMCRT* vessels are more distensible possibly due to decreased collagen content of the medial layer. It is also possible that the pressure myography technique was not

sensitive enough to detect the changes in collagen composition that we observed.

. In conclusion our study shows that CRT overexpression in the vascular smooth muscle cells of mice results in significant vascular wall remodeling leading to increased angiogenesis and vascular tumour formation. Increased angiogenesis may result due to a combination of decreased expression of connexins 40 and 43, increased activity of MMP-2 and MMP-9 and the resulting decrease in extracellular matrix components. The *SMCRT* mice also suffer from defects in the cardiovascular system including increased vascularization of the coronary arteries and rupture of coronary aneurysms. However, the major defect in these mice is the presence of Giant Hemangioma (hemangioendothelioma) associated with coagulopathy similar to KMS. Finally, overexpression of CRT in the vascular wall leads to the generation of a vascular tumour similar to the human disease. This transgenic mouse is a unique animal model for the human HAE, which could be utilized to understand the molecular mechanism of the development of HAE in human patients.

F. REFERENCES

1. Gilbert, S.F., *Lateral plate mesoderm and endoderm*, in *Developmental Biology*. 2000, Sinauer associates, Inc. p. 471-501.
2. Risau, W. and I. Flamme, *Vasculogenesis.* Annu Rev Cell Dev Biol, 1995. **11**: p. 73-91.
3. Carmeliet, P. and D. Collen, *Transgenic mouse models in angiogenesis and cardiovascular disease.* J Pathol, 2000. **190**(3): p. 387-405.
4. Distler, J.H., et al., *Angiogenic and angiostatic factors in the molecular control of angiogenesis.* Q J Nucl Med, 2003. **47**(3): p. 149-61.
5. Roguin, A. and A.P. Levy, *Angiogenesis--an update.* Pediatr Endocrinol Rev, 2005. **2**(3): p. 391-8.
6. Standing, S., ed. *Gray's Anatomy: The anatomical basis of clinical practice*. Thirty Ninth Edition ed. 2005, Elsevier Churchill Livingston.
7. Kumar, S., D.C. West, and A. Ager, *Heterogeneity in endothelial cells from large vessels and microvessels.* Differentiation, 1987. **36**(1): p. 57-70.
8. Huang, H., J. McIntosh, and D.G. Hoyt, *An efficient, nonenzymatic method for isolation and culture of murine aortic endothelial cells and their response to inflammatory stimuli.* In Vitro Cell Dev Biol Anim, 2003. **39**(1-2): p. 43-50.
9. McGuire, P.G. and R.W. Orkin, *Isolation of rat aortic endothelial cells by primary explant techniques and their phenotypic modulation by defined substrata.* Lab Invest, 1987. **57**(1): p. 94-105.

10. Nicosia, R.F., S. Villaschi, and M. Smith, *Isolation and characterization of vasoformative endothelial cells from the rat aorta.* In Vitro Cell Dev Biol Anim, 1994. **30A**(6): p. 394-9.

11. Cines, D.B., et al., *Endothelial cells in physiology and in the pathophysiology of vascular disorders.* Blood, 1998. **91**(10): p. 3527-61.

12. Carmeliet, P., et al., *Abnormal blood vessel development and lethality in embryos lacking a single VEGF allele.* Nature, 1996. **380**(6573): p. 435-9.

13. Dvorak, H.F., *Angiogenesis: update 2005.* J Thromb Haemost, 2005. **3**(8): p. 1835-42.

14. Ferrara, N., et al., *Heterozygous embryonic lethality induced by targeted inactivation of the VEGF gene.* Nature, 1996. **380**(6573): p. 439-42.

15. van der Rest, M. and R. Garrone, *Collagen family of proteins.* Faseb J, 1991. **5**(13): p. 2814-23.

16. Esparza, J., et al., *Fibronectin upregulates gelatinase B (MMP-9) and induces coordinated expression of gelatinase A (MMP-2) and its activator MT1-MMP (MMP-14) by human T lymphocyte cell lines. A process repressed through RAS/MAP kinase signaling pathways.* Blood, 1999. **94**(8): p. 2754-66.

17. Iivanainen, E., et al., *Endothelial cell-matrix interactions.* Microsc Res Tech, 2003. **60**(1): p. 13-22.

18. Michaux, G. and D.F. Cutler, *How to roll an endothelial cigar: the biogenesis of Weibel-Palade bodies.* Traffic, 2004. **5**(2): p. 69-78.

19. Ilan, N. and J.A. Madri, *PECAM-1: old friend, new partners.* Curr Opin Cell Biol, 2003. **15**(5): p. 515-24.

20. Wood, H.B., et al., *CD34 expression patterns during early mouse development are related to modes of blood vessel formation and reveal additional sites of hematopoiesis.* Blood, 1997. **90**(6): p. 2300-11.

21. Peichev, M., et al., *Expression of VEGFR-2 and AC133 by circulating human CD34(+) cells identifies a population of functional endothelial precursors.* Blood, 2000. **95**(3): p. 952-8.

22. Fina, L., et al., *Expression of the CD34 gene in vascular endothelial cells.* Blood, 1990. **75**(12): p. 2417-26.

23. Baumhueter, S., et al., *Global vascular expression of murine CD34, a sialomucin-like endothelial ligand for L-selectin.* Blood, 1994. **84**(8): p. 2554-65.

24. Cheng, J., et al., *Hematopoietic defects in mice lacking the sialomucin CD34.* Blood, 1996. **87**(2): p. 479-90.

25. Stankevicius, E., et al., *[Role of nitric oxide and other endothelium-derived factors].* Medicina (Kaunas), 2003. **39**(4): p. 333-41.

26. Meisenberg, G.S., W. H., *Plasma Proteins*, in *Principles of Medical Biochemistry*. 1998, Mosby.

27. Aird, W.C., *Endothelium and Hemostasis*, in *Endothelial Cells in Health and Disease*, W.C. Aird, Editor. 2005, Taylor & Francis: Cambridge, Massachusetts.

28. Nachman, R.L., *Review: Stratton Lecture. Thrombosis and atherogenesis: molecular connections.* Blood, 1992. **79**(8): p. 1897-906.

29. Hodivala-Dilke, K.M., A.R. Reynolds, and L.E. Reynolds, *Integrins in angiogenesis: multitalented molecules in a balancing act.* Cell Tissue Res, 2003. **314**(1): p. 131-44.

30. Brooks, P.C., et al., *Disruption of angiogenesis by PEX, a noncatalytic metalloproteinase fragment with integrin binding activity.* Cell, 1998. **92**(3): p. 391-400.

31. Brooks, P.C., et al., *Localization of matrix metalloproteinase MMP-2 to the surface of invasive cells by interaction with integrin alpha v beta 3.* Cell, 1996. **85**(5): p. 683-93.

32. Young, B.H., J., *Wheater's Functional Histology.* 2002.

33. Hungerford, J.E. and C.D. Little, *Developmental biology of the vascular smooth muscle cell: building a multilayered vessel wall.* J Vasc Res, 1999. **36**(1): p. 2-27.

34. Hirschi, K.K. and P.A. D'Amore, *Pericytes in the microvasculature.* Cardiovasc Res, 1996. **32**(4): p. 687-98.

35. de Ruiter, M.C., et al., *The early development of the tunica media in the vascular system of rat embryos.* Anat Embryol (Berl), 1990. **181**(4): p. 341-9.

36. Hungerford, J.E., et al., *Development of the aortic vessel wall as defined by vascular smooth muscle and extracellular matrix markers.* Dev Biol, 1996. **178**(2): p. 375-92.

37. Hellstrom, M., et al., *Role of PDGF-B and PDGFR-beta in recruitment of vascular smooth muscle cells and pericytes during embryonic blood vessel formation in the mouse.* Development, 1999. **126**(14): p. 3047-55.

38. Li, L., et al., *SM22 alpha, a marker of adult smooth muscle, is expressed in multiple myogenic lineages during embryogenesis.* Circ Res, 1996. **78**(2): p. 188-95.

39. Li, L., et al., *Expression of the SM22alpha promoter in transgenic mice provides evidence for distinct transcriptional regulatory programs in vascular and visceral smooth muscle cells.* J Cell Biol, 1996. **132**(5): p. 849-59.

40. Zhang, J.C., et al., *Analysis of SM22alpha-deficient mice reveals unanticipated insights into smooth muscle cell differentiation and function.* Mol Cell Biol, 2001. **21**(4): p. 1336-44.

41. Berne, R.L., MN., ed. *Physiology*. Fourth Edition ed. 1998, Mosby.

42. Miyauchi, T., et al., *Involvement of endothelin in the regulation of human vascular tonus. Potent vasoconstrictor effect and existence in endothelial cells.* Circulation, 1990. **81**(6): p. 1874-80.

43. Narumiya, S., Y. Sugimoto, and F. Ushikubi, *Prostanoid receptors: structures, properties, and functions.* Physiol Rev, 1999. **79**(4): p. 1193-226.

44. Dudzinski, D.M., et al., *The regulation and pharmacology of endothelial nitric oxide synthase.* Annu Rev Pharmacol Toxicol, 2006. **46**: p. 235-76.

45. Diaz-Flores, L., et al., *Microvascular pericytes: a review of their morphological and functional characteristics.* Histol Histopathol, 1991. **6**(2): p. 269-86.

46. Benjamin, L.E., I. Hemo, and E. Keshet, *A plasticity window for blood vessel remodelling is defined by pericyte coverage of the preformed endothelial network and is regulated by PDGF-B and VEGF.* Development, 1998. **125**(9): p. 1591-8.

47. Diez, J., *Arterial stiffness and extracellular matrix.* Adv Cardiol, 2007. **44**: p. 76-95.

48. Egeblad, M. and Z. Werb, *New functions for the matrix metalloproteinases in cancer progression.* Nat Rev Cancer, 2002. **2**(3): p. 161-74.

49. Vassalli, J.D., A.P. Sappino, and D. Belin, *The plasminogen activator/plasmin system.* J Clin Invest, 1991. **88**(4): p. 1067-72.

50. Collen, D. and H.R. Lijnen, *Basic and clinical aspects of fibrinolysis and thrombolysis.* Blood, 1991. **78**(12): p. 3114-24.

51. Lijnen, H.R., *Plasmin and matrix metalloproteinases in vascular remodeling.* Thromb Haemost, 2001. **86**(1): p. 324-33.

52. Visse, R. and H. Nagase, *Matrix metalloproteinases and tissue inhibitors of metalloproteinases: structure, function, and biochemistry.* Circ Res, 2003. **92**(8): p. 827-39.

53. Snoek-van Beurden, P.A. and J.W. Von den Hoff, *Zymographic techniques for the analysis of matrix metalloproteinases and their inhibitors.* Biotechniques, 2005. **38**(1): p. 73-83.

54. Heissig, B., et al., *Angiogenesis: vascular remodeling of the extracellular matrix involves metalloproteinases.* Curr Opin Hematol, 2003. **10**(2): p. 136-41.

55. Pyo, R., et al., *Targeted gene disruption of matrix metalloproteinase-9 (gelatinase B) suppresses development of experimental abdominal aortic aneurysms.* J Clin Invest, 2000. **105**(11): p. 1641-9.

56. Creemers, E.E., et al., *Matrix metalloproteinase inhibition after myocardial infarction: a new approach to prevent heart failure?* Circ Res, 2001. **89**(3): p. 201-10.

57. Rajavashisth, T.B., et al., *Membrane type 1 matrix metalloproteinase expression in human atherosclerotic plaques: evidence for activation by proinflammatory mediators.* Circulation, 1999. **99**(24): p. 3103-9.

58. Spinale, F.G., et al., *A matrix metalloproteinase induction/activation system exists in the human left ventricular myocardium and is upregulated in heart failure.* Circulation, 2000. **102**(16): p. 1944-9.

59. Nagase, H. and J.F. Woessner, Jr., *Matrix metalloproteinases.* J Biol Chem, 1999. **274**(31): p. 21491-4.

60. Van Wart, H.E. and H. Birkedal-Hansen, *The cysteine switch: a principle of regulation of metalloproteinase activity with potential applicability to the entire matrix metalloproteinase gene family.* Proc Natl Acad Sci U S A, 1990. **87**(14): p. 5578-82.

61. Springman, E.B., et al., *Multiple modes of activation of latent human fibroblast collagenase: evidence for the role of a Cys73 active-site zinc*

complex in latency and a "cysteine switch" mechanism for activation. Proc Natl Acad Sci U S A, 1990. **87**(1): p. 364-8.

62. Gomis-Ruth, F.X., et al., *The helping hand of collagenase-3 (MMP-13): 2.7 A crystal structure of its C-terminal haemopexin-like domain.* J Mol Biol, 1996. **264**(3): p. 556-66.

63. Gohlke, U., et al., *The C-terminal (haemopexin-like) domain structure of human gelatinase A (MMP2): structural implications for its function.* FEBS Lett, 1996. **378**(2): p. 126-30.

64. Chung, L., et al., *Collagenase unwinds triple-helical collagen prior to peptide bond hydrolysis.* Embo J, 2004. **23**(15): p. 3020-30.

65. Strongin, A.Y., et al., *Mechanism of cell surface activation of 72-kDa type IV collagenase. Isolation of the activated form of the membrane metalloprotease.* J Biol Chem, 1995. **270**(10): p. 5331-8.

66. Lafleur, M.A., A.M. Tester, and E.W. Thompson, *Selective involvement of TIMP-2 in the second activational cleavage of pro-MMP-2: refinement of the pro-MMP-2 activation mechanism.* FEBS Lett, 2003. **553**(3): p. 457-63.

67. Bornstein, P., A. Agah, and T.R. Kyriakides, *The role of thrombospondins 1 and 2 in the regulation of cell-matrix interactions, collagen fibril formation, and the response to injury.* Int J Biochem Cell Biol, 2004. **36**(6): p. 1115-25.

68. Maquoi, E., et al., *Type IV collagen induces matrix metalloproteinase 2 activation in HT1080 fibrosarcoma cells.* Exp Cell Res, 2000. **261**(2): p. 348-59.

69. Ellerbroek, S.M., Y.I. Wu, and M.S. Stack, *Type I collagen stabilization of matrix metalloproteinase-2.* Arch Biochem Biophys, 2001. **390**(1): p. 51-6.

70. Ito, H., Y. Seyama, and S. Kubota, *Calreticulin is directly involved in anti-alpha3 integrin antibody-mediated secretion and activation of matrix metalloprotease-2.* Biochem Biophys Res Commun, 2001. **283**(2): p. 297-302.

71. Hofmann, U.B., et al., *Expression of integrin alpha(v)beta(3) correlates with activation of membrane-type matrix metalloproteinase-1 (MT1-MMP) and matrix metalloproteinase-2 (MMP-2) in human melanoma cells in vitro and in vivo.* Int J Cancer, 2000. **87**(1): p. 12-9.

72. Bornstein, P., et al., *Thrombospondin 2 modulates collagen fibrillogenesis and angiogenesis.* J Investig Dermatol Symp Proc, 2000. **5**(1): p. 61-6.

73. Zucker, S., et al., *Thrombin induces the activation of progelatinase A in vascular endothelial cells. Physiologic regulation of angiogenesis.* J Biol Chem, 1995. **270**(40): p. 23730-8.

74. Galis, Z.S., et al., *Thrombin promotes activation of matrix metalloproteinase-2 produced by cultured vascular smooth muscle cells.* Arterioscler Thromb Vasc Biol, 1997. **17**(3): p. 483-9.

75. Lohi, J. and J. Keski-Oja, *Calcium ionophores decrease pericellular gelatinolytic activity via inhibition of 92-kDa gelatinase expression and decrease of 72-kDa gelatinase activation.* J Biol Chem, 1995. **270**(29): p. 17602-9.

76. Mukhopadhyay, S., et al., *Calcium-induced matrix metalloproteinase 9 gene expression is differentially regulated by ERK1/2 and p38 MAPK in oral keratinocytes and oral squamous cell carcinoma.* J Biol Chem, 2004. **279**(32): p. 33139-46.

77. Wu, M., et al., *Differential expression and activity of matrix metalloproteinase-2 and -9 in the calreticulin deficient cells.* Matrix Biol, 2007.

78. Yoon, A. and R.A. Hurta, *Insulin like growth factor-1 selectively regulates the expression of matrix metalloproteinase-2 in malignant H-ras transformed cells.* Mol Cell Biochem, 2001. **223**(1-2): p. 1-6.

79. Shin, I., et al., *H-Ras-specific activation of Rac-MKK3/6-p38 pathway: its critical role in invasion and migration of breast epithelial cells.* J Biol Chem, 2005. **280**(15): p. 14675-83.

80. Ogawa, K., et al., *Suppression of matrix metalloproteinase-9 transcription by transforming growth factor-beta is mediated by a nuclear factor-kappaB site.* Biochem J, 2004. **381**(Pt 2): p. 413-22.

81. Bellairs, R., *The primitive streak.* Anat Embryol (Berl), 1986. **174**(1): p. 1-14.

82. Risau, W., *Mechanisms of angiogenesis.* Nature, 1997. **386**(6626): p. 671-4.

83. Poole, T.J., E.B. Finkelstein, and C.M. Cox, *The role of FGF and VEGF in angioblast induction and migration during vascular development.* Dev Dyn, 2001. **220**(1): p. 1-17.

84. Ema, M. and J. Rossant, *Cell fate decisions in early blood vessel formation.* Trends Cardiovasc Med, 2003. **13**(6): p. 254-9.

85. Eichmann, A., et al., *Vascular development: from precursor cells to branched arterial and venous networks.* Int J Dev Biol, 2005. **49**(2-3): p. 259-67.

86. Pardanaud, L., et al., *Vasculogenesis in the early quail blastodisc as studied with a monoclonal antibody recognizing endothelial cells.* Development, 1987. **100**(2): p. 339-49.

87. Shalaby, F., et al., *Failure of blood-island formation and vasculogenesis in Flk-1-deficient mice.* Nature, 1995. **376**(6535): p. 62-6.

88. Choi, K., et al., *A common precursor for hematopoietic and endothelial cells.* Development, 1998. **125**(4): p. 725-32.

89. Kitajima, S., et al., *Transgenic rabbits with increased VEGF expression develop hemangiomas in the liver: a new model for Kasabach-Merritt syndrome.* Lab Invest, 2005. **85**(12): p. 1517-27.

90. Fong, G.H., et al., *Role of the Flt-1 receptor tyrosine kinase in regulating the assembly of vascular endothelium.* Nature, 1995. **376**(6535): p. 66-70.

91. Ward, N.L. and D.J. Dumont, *The angiopoietins and Tie2/Tek: adding to the complexity of cardiovascular development.* Semin Cell Dev Biol, 2002. **13**(1): p. 19-27.

92. Dumont, D.J., et al., *Dominant-negative and targeted null mutations in the endothelial receptor tyrosine kinase, tek, reveal a critical role in vasculogenesis of the embryo.* Genes Dev, 1994. **8**(16): p. 1897-909.

93. Suri, C., et al., *Requisite role of angiopoietin-1, a ligand for the TIE2 receptor, during embryonic angiogenesis.* Cell, 1996. **87**(7): p. 1171-80.

94. Morris, P.N., et al., *Functional analysis of a mutant form of the receptor tyrosine kinase Tie2 causing venous malformations.* J Mol Med, 2005. **83**(1): p. 58-63.

95. Maisonpierre, P.C., et al., *Angiopoietin-2, a natural antagonist for Tie2 that disrupts in vivo angiogenesis.* Science, 1997. **277**(5322): p. 55-60.

96. Puri, M.C., et al., *The receptor tyrosine kinase TIE is required for integrity and survival of vascular endothelial cells.* Embo J, 1995. **14**(23): p. 5884-91.

97. Gale, N.W., et al., *Angiopoietin-2 is required for postnatal angiogenesis and lymphatic patterning, and only the latter role is rescued by Angiopoietin-1.* Dev Cell, 2002. **3**(3): p. 411-23.

98. Leveen, P., et al., *Mice deficient for PDGF B show renal, cardiovascular, and hematological abnormalities.* Genes Dev, 1994. **8**(16): p. 1875-87.

99. Lindahl, P., et al., *Pericyte loss and microaneurysm formation in PDGF-B-deficient mice.* Science, 1997. **277**(5323): p. 242-5.

100. Fredriksson, L., H. Li, and U. Eriksson, *The PDGF family: four gene products form five dimeric isoforms.* Cytokine Growth Factor Rev, 2004. **15**(4): p. 197-204.

101. Hellstrom, M., et al., *Lack of pericytes leads to endothelial hyperplasia and abnormal vascular morphogenesis.* J Cell Biol, 2001. **153**(3): p. 543-53.

102. Reigstad, L.J., J.E. Varhaug, and J.R. Lillehaug, *Structural and functional specificities of PDGF-C and PDGF-D, the novel members of the platelet-derived growth factors family.* FEBS J, 2005. **272**(22): p. 5723-41.

103. Bergers, G., et al., *Matrix metalloproteinase-9 triggers the angiogenic switch during carcinogenesis.* Nat Cell Biol, 2000. **2**(10): p. 737-44.

104. Zhou, Z., et al., *Impaired endochondral ossification and angiogenesis in mice deficient in membrane-type matrix metalloproteinase I.* Proc Natl Acad Sci U S A, 2000. **97**(8): p. 4052-7.

105. Holmbeck, K., et al., *MT1-MMP-deficient mice develop dwarfism, osteopenia, arthritis, and connective tissue disease due to inadequate collagen turnover.* Cell, 1999. **99**(1): p. 81-92.

106. Lafleur, M.A., et al., *Perivascular cells regulate endothelial membrane type-1 matrix metalloproteinase activity.* Biochem Biophys Res Commun, 2001. **282**(2): p. 463-73.

107. Stoller, G.L. and S.A. Mousa, *Angiogenesis, choroidal neovascularization, and the coagulation system.* Retina, 2005. **25**(1): p. 19-25.

108. Carmeliet, P., et al., *Role of tissue factor in embryonic blood vessel development.* Nature, 1996. **383**(6595): p. 73-5.

109. Zhang, Y., et al., *Tissue factor controls the balance of angiogenic and antiangiogenic properties of tumor cells in mice.* J Clin Invest, 1994. **94**(3): p. 1320-7.

110. Hunt, S.J. and D.J. Santa Cruz, *Vascular tumors of the skin: a selective review.* Semin Diagn Pathol, 2004. **21**(3): p. 166-218.

111. Lyons, L.L., et al., *Kaposiform hemangioendothelioma: a study of 33 cases emphasizing its pathologic, immunophenotypic, and biologic uniqueness from juvenile hemangioma.* Am J Surg Pathol, 2004. **28**(5): p. 559-68.

112. Tsang, W.Y. and J.K. Chan, *The family of epithelioid vascular tumors.* Histol Histopathol, 1993. **8**(1): p. 187-212.

113. Weiss, S.W. and F.M. Enzinger, *Epithelioid hemangioendothelioma: a vascular tumor often mistaken for a carcinoma.* Cancer, 1982. **50**(5): p. 970-81.

114. Gampper, T.J. and R.F. Morgan, *Vascular anomalies: hemangiomas.* Plast Reconstr Surg, 2002. **110**(2): p. 572-85; quiz 586; discussion 587-8.

115. Drolet, B.A., N.B. Esterly, and I.J. Frieden, *Hemangiomas in children.* N Engl J Med, 1999. **341**(3): p. 173-81.

116. Fishman, S.J. and J.B. Mulliken, *Hemangiomas and vascular malformations of infancy and childhood.* Pediatr Clin North Am, 1993. **40**(6): p. 1177-200.

117. Maguiness, S. and L. Guenther, *Kasabach-merritt syndrome.* J Cutan Med Surg, 2002. **6**(4): p. 335-9.

118. Takahashi, K., et al., *Cellular markers that distinguish the phases of hemangioma during infancy and childhood.* J Clin Invest, 1994. **93**(6): p. 2357-64.

119. Razon, M.J., et al., *Increased apoptosis coincides with onset of involution in infantile hemangioma.* Microcirculation, 1998. **5**(2-3): p. 189-95.

120. North, P.E., et al., *A unique microvascular phenotype shared by juvenile hemangiomas and human placenta.* Arch Dermatol, 2001. **137**(5): p. 559-70.

121. Burton, B.K., et al., *An increased incidence of haemangiomas in infants born following chorionic villus sampling (CVS).* Prenat Diagn, 1995. **15**(3): p. 209-14.

122. Walter, J.W., et al., *Genetic mapping of a novel familial form of infantile hemangioma.* Am J Med Genet, 1999. **82**(1): p. 77-83.

123. Walter, J.W., et al., *Somatic mutation of vascular endothelial growth factor receptors in juvenile hemangioma.* Genes Chromosomes Cancer, 2002. **33**(3): p. 295-303.

124. Yu, Y., et al., *Increased Tie2 expression, enhanced response to angiopoietin-1, and dysregulated angiopoietin-2 expression in hemangioma-derived endothelial cells.* Am J Pathol, 2001. **159**(6): p. 2271-80.

125. Perry, B.N., et al., *Pharmacologic blockade of angiopoietin-2 is efficacious against model hemangiomas in mice.* J Invest Dermatol, 2006. **126**(10): p. 2316-22.

126. Ostwald, T.J. and D.H. MacLennan, *Isolation of a high affinity calcium-binding protein from sarcoplasmic reticulum.* J Biol Chem, 1974. **249**(3): p. 974-9.

127. Fliegel, L., et al., *Molecular cloning of the high affinity calcium-binding protein (calreticulin) of skeletal muscle sarcoplasmic reticulum.* J Biol Chem, 1989. **264**(36): p. 21522-8.

128. Smith, M.J. and G.L. Koch, *Multiple zones in the sequence of calreticulin (CRP55, calregulin, HACBP), a major calcium binding ER/SR protein.* Embo J, 1989. **8**(12): p. 3581-6.

129. Johnson, S., et al., *The ins and outs of calreticulin: from the ER lumen to the extracellular space.* Trends Cell Biol, 2001. **11**(3): p. 122-9.

130. McCauliffe, D.P., et al., *The 5'-flanking region of the human calreticulin gene shares homology with the human GRP78, GRP94, and protein disulfide isomerase promoters.* J Biol Chem, 1992. **267**(4): p. 2557-62.

131. Rooke, K., et al., *Mapping of the gene for calreticulin (Calr) to mouse chromosome 8.* Mamm Genome, 1997. **8**(11): p. 870-1.

132. Waser, M., et al., *Regulation of calreticulin gene expression by calcium.* J Cell Biol, 1997. **138**(3): p. 547-57.

133. Persson, S., M. Rosenquist, and M. Sommarin, *Identification of a novel calreticulin isoform (Crt2) in human and mouse.* Gene, 2002. **297**(1-2): p. 151-8.

134. Baksh, S. and M. Michalak, *Expression of calreticulin in Escherichia coli and identification of its Ca2+ binding domains.* J Biol Chem, 1991. **266**(32): p. 21458-65.

135. Opas, M., et al., *Regulation of expression and intracellular distribution of calreticulin, a major calcium binding protein of nonmuscle cells.* J Cell Physiol, 1991. **149**(1): p. 160-71.

136. Fliegel, L., et al., *The high-affinity calcium binding protein of sarcoplasmic reticulum. Tissue distribution, and homology with calregulin.* Biochim Biophys Acta, 1989. **982**(1): p. 1-8.

137. Tharin, S., et al., *Widespread tissue distribution of rabbit calreticulin, a non-muscle functional analogue of calsequestrin.* Cell Tissue Res, 1992. **269**(1): p. 29-37.

138. Leung-Hagesteijn, C.Y., et al., *Cell attachment to extracellular matrix substrates is inhibited upon downregulation of expression of calreticulin, an intracellular integrin alpha-subunit-binding protein.* J Cell Sci, 1994. **107 (Pt 3)**: p. 589-600.

139. Dedhar, S., *Novel functions for calreticulin: interaction with integrins and modulation of gene expression?* Trends Biochem Sci, 1994. **19**(7): p. 269-71.

140. Burns, K., et al., *Modulation of gene expression by calreticulin binding to the glucocorticoid receptor.* Nature, 1994. **367**(6462): p. 476-80.

141. Afshar, N., B.E. Black, and B.M. Paschal, *Retrotranslocation of the chaperone calreticulin from the endoplasmic reticulum lumen to the cytosol.* Mol Cell Biol, 2005. **25**(20): p. 8844-53.

142. Holaska, J.M., et al., *Calreticulin Is a receptor for nuclear export.* J Cell Biol, 2001. **152**(1): p. 127-40.

143. Michalak, M., et al., *Endoplasmic reticulum form of calreticulin modulates glucocorticoid-sensitive gene expression.* J Biol Chem, 1996. **271**(46): p. 29436-45.

144. Fadel, M.P., et al., *Calreticulin affects beta-catenin-associated pathways.* J Biol Chem, 2001. **276**(29): p. 27083-9.

145. Opas, M., et al., *Calreticulin modulates cell adhesiveness via regulation of vinculin expression.* J Cell Biol, 1996. **135**(6 Pt 2): p. 1913-23.

146. Michalak, M., et al., *Calreticulin: one protein, one gene, many functions.* Biochem J, 1999. **344 Pt 2**: p. 281-92.

147. Coppolino, M.G., et al., *Calreticulin is essential for integrin-mediated calcium signalling and cell adhesion.* Nature, 1997. **386**(6627): p. 843-7.

148. Coppolino, M.G. and S. Dedhar, *Calreticulin.* Int J Biochem Cell Biol, 1998. **30**(5): p. 553-8.

149. Matsuoka, K., et al., *Covalent structure of bovine brain calreticulin.* Biochem J, 1994. **298 (Pt 2)**: p. 435-42.

150. Baksh, S., et al., *Identification of the Zn2+ binding region in calreticulin.* FEBS Lett, 1995. **376**(1-2): p. 53-7.

151. Baksh, S., et al., *Interaction of calreticulin with protein disulfide isomerase.* J Biol Chem, 1995. **270**(52): p. 31338-44.

152. Spiro, R.G., et al., *Definition of the lectin-like properties of the molecular chaperone, calreticulin, and demonstration of its copurification with endomannosidase from rat liver Golgi.* J Biol Chem, 1996. **271**(19): p. 11588-94.

153. Thomson, S.P. and D.B. Williams, *Delineation of the lectin site of the molecular chaperone calreticulin.* Cell Stress Chaperones, 2005. **10**(3): p. 242-51.

154. Kapoor, M., et al., *Mutational analysis provides molecular insight into the carbohydrate-binding region of calreticulin: pivotal roles of tyrosine-109 and aspartate-135 in carbohydrate recognition.* Biochemistry, 2004. **43**(1): p. 97-106.

155. Leach, M.R., et al., *Localization of the lectin, ERp57 binding, and polypeptide binding sites of calnexin and calreticulin.* J Biol Chem, 2002. **277**(33): p. 29686-97.

156. Pike, S.E., et al., *Calreticulin and calreticulin fragments are endothelial cell inhibitors that suppress tumor growth.* Blood, 1999. **94**(7): p. 2461-8.

157. Burns, K., et al., *Calreticulin: from Ca2+ binding to control of gene expression.* Trends Cell Biol, 1994. **4**(5): p. 152-4.

158. Ellgaard, L., et al., *NMR structure of the calreticulin P-domain.* Proc Natl Acad Sci U S A, 2001. **98**(6): p. 3133-8.

159. Otteken, A. and B. Moss, *Calreticulin interacts with newly synthesized human immunodeficiency virus type 1 envelope glycoprotein, suggesting a chaperone function similar to that of calnexin.* J Biol Chem, 1996. **271**(1): p. 97-103.

160. Michalak, M., J.M. Robert Parker, and M. Opas, *Ca2+ signaling and calcium binding chaperones of the endoplasmic reticulum.* Cell Calcium, 2002. **32**(5-6): p. 269-78.

161. Nakamura, K., et al., *Functional specialization of calreticulin domains.* J Cell Biol, 2001. **154**(5): p. 961-72.

162. Zapun, A., et al., *Enhanced catalysis of ribonuclease B folding by the interaction of calnexin or calreticulin with ERp57.* J Biol Chem, 1998. **273**(11): p. 6009-12.

163. Corbett, E.F., et al., *Ca2+ regulation of interactions between endoplasmic reticulum chaperones.* J Biol Chem, 1999. **274**(10): p. 6203-11.

164. Mery, L., et al., *Overexpression of calreticulin increases intracellular Ca2+ storage and decreases store-operated Ca2+ influx.* J Biol Chem, 1996. **271**(16): p. 9332-9.

165. Kuwabara, K., et al., *Calreticulin, an antithrombotic agent which binds to vitamin K-dependent coagulation factors, stimulates endothelial nitric oxide production, and limits thrombosis in canine coronary arteries.* J Biol Chem, 1995. **270**(14): p. 8179-87.

166. Fadel, M.P., et al., *Calreticulin affects focal contact-dependent but not close contact-dependent cell-substratum adhesion.* J Biol Chem, 1999. **274**(21): p. 15085-94.

167. Mesaeli, N., et al., *Calreticulin is essential for cardiac development.* J Cell Biol, 1999. **144**(5): p. 857-68.

168. Rauch, F., et al., *Heart, brain, and body wall defects in mice lacking calreticulin.* Exp Cell Res, 2000. **256**(1): p. 105-11.

169. Li, J., et al., *Calreticulin reveals a critical Ca(2+) checkpoint in cardiac myofibrillogenesis.* J Cell Biol, 2002. **158**(1): p. 103-13.

170. Ellgaard, L. and A. Helenius, *Quality control in the endoplasmic reticulum.* Nat Rev Mol Cell Biol, 2003. **4**(3): p. 181-91.

171. Jorgensen, C.S., et al., *Polypeptide binding properties of the chaperone calreticulin.* Eur J Biochem, 2000. **267**(10): p. 2945-54.

172. Saito, Y., et al., *Calreticulin functions in vitro as a molecular chaperone for both glycosylated and non-glycosylated proteins.* Embo J, 1999. **18**(23): p. 6718-29.

173. Nauseef, W.M., S.J. McCormick, and R.A. Clark, *Calreticulin functions as a molecular chaperone in the biosynthesis of myeloperoxidase.* J Biol Chem, 1995. **270**(9): p. 4741-7.

174. McDonnell, J.M., et al., *Calreticulin binding affinity for glycosylated laminin.* J Biol Chem, 1996. **271**(14): p. 7891-4.

175. Pipe, S.W., et al., *Differential interaction of coagulation factor VIII and factor V with protein chaperones calnexin and calreticulin.* J Biol Chem, 1998. **273**(14): p. 8537-44.

176. Bastianutto, C., et al., *Overexpression of calreticulin increases the Ca2+ capacity of rapidly exchanging Ca2+ stores and reveals aspects of their lumenal microenvironment and function.* J Cell Biol, 1995. **130**(4): p. 847-55.

177. Liu, N., et al., *Decreasing calreticulin expression lowers the Ca2+ response to bradykinin and increases sensitivity to ionomycin in NG-108-15 cells.* J Biol Chem, 1994. **269**(46): p. 28635-9.

178. Meldolesi, J. and T. Pozzan, *The endoplasmic reticulum Ca2+ store: a view from the lumen.* Trends Biochem Sci, 1998. **23**(1): p. 10-4.

179. Michikawa, T., et al., *Transmembrane topology and sites of N-glycosylation of inositol 1,4,5-trisphosphate receptor.* J Biol Chem, 1994. **269**(12): p. 9184-9.

180. John, L.M., J.D. Lechleiter, and P. Camacho, *Differential modulation of SERCA2 isoforms by calreticulin.* J Cell Biol, 1998. **142**(4): p. 963-73.

181. Lynch, J., et al., *Calreticulin signals upstream of calcineurin and MEF2C in a critical Ca(2+)-dependent signaling cascade.* J Cell Biol, 2005. **170**(1): p. 37-47.

182. Camacho, P. and J.D. Lechleiter, *Calreticulin inhibits repetitive intracellular Ca2+ waves.* Cell, 1995. **82**(5): p. 765-71.

183. Lozyk, M.D., et al., *Ultrastructural analysis of development of myocardium in calreticulin-deficient mice.* BMC Dev Biol, 2006. **6**: p. 54.

184. Nakamura, K., et al., *Complete heart block and sudden death in mice overexpressing calreticulin.* J Clin Invest, 2001. **107**(10): p. 1245-53.

185. Guo, L., et al., *COUP-TF1 antagonizes Nkx2.5-mediated activation of the calreticulin gene during cardiac development.* J Biol Chem, 2001. **276**(4): p. 2797-801.

186. Olson, E.N., *Gene regulatory networks in the evolution and development of the heart.* Science, 2006. **313**(5795): p. 1922-7.

187. Lin, Q., et al., *Control of mouse cardiac morphogenesis and myogenesis by transcription factor MEF2C.* Science, 1997. **276**(5317): p. 1404-7.

188. Dai, E., et al., *Calreticulin, a potential vascular regulatory protein, reduces intimal hyperplasia after arterial injury.* Arterioscler Thromb Vasc Biol, 1997. **17**(11): p. 2359-68.

189. Xiao, F., et al., *A gene therapy for cancer based on the angiogenesis inhibitor, vasostatin.* Gene Ther, 2002. **9**(18): p. 1207-13.

190. Wu, P.C., et al., *Inhibition of corneal angiogenesis by local application of vasostatin.* Mol Vis, 2005. **11**: p. 28-35.

191. Yao, L., et al., *Effective targeting of tumor vasculature by the angiogenesis inhibitors vasostatin and interleukin-12.* Blood, 2000. **96**(5): p. 1900-5.

192. Lange-Asschenfeldt, B., et al., *The angiogenesis inhibitor vasostatin does not impair wound healing at tumor-inhibiting doses.* J Invest Dermatol, 2001. **117**(5): p. 1036-41.

193. Ma, L., et al., *Complete eradication of hepatocellular carcinomas by combined vasostatin gene therapy and B7H3-mediated immunotherapy.* J Hepatol, 2007. **46**(1): p. 98-106.

194. Yao, L., S.E. Pike, and G. Tosato, *Laminin binding to the calreticulin fragment vasostatin regulates endothelial cell function.* J Leukoc Biol, 2002. **71**(1): p. 47-53.

195. Palmiter, R.D. and R.L. Brinster, *Germ-line transformation of mice.* Annu Rev Genet, 1986. **20**: p. 465-99.

196. McElroy, D., *Chapter 17: Connective Tissue*, in *Laboratory Methods in Histotechnology*, E. Prophet, Mills, B., Arrington, JB, Sobin, LH, Editor. 1994, American Registry of Pathology: Washington, DC. p. 127-146.

197. Kiernan, J., *Histological and Histochemical Methods.* 1999, Oxford, England, &Woburn, MA. USA: Butterworth Heinemann.

198. Falloon, B.J., et al., *In vitro perfusion studies of resistance artery function in genetic hypertension.* Hypertension, 1993. **22**(4): p. 486-95.

199. Intengan, H.D., G. He, and E.L. Schiffrin, *Effect of vasopressin antagonism on structure and mechanics of small arteries and vascular expression of endothelin-1 in deoxycorticosterone acetate salt hypertensive rats.* Hypertension, 1998. **32**(4): p. 770-7.

200. Baumbach, G.L., et al., *Mechanics of cerebral arterioles in hypertensive rats.* Circ Res, 1988. **62**(1): p. 56-64.

201. Palsson, B., *Epitheloid hemangioendothelioma.* Acta Oncol, 1999. **38**(5): p. 659-61.

202. McLachlan, E., et al., *Connexins act as tumor suppressors in three-dimensional mammary cell organoids by regulating differentiation and angiogenesis.* Cancer Res, 2006. **66**(20): p. 9886-94.

203. Pike, S.E., et al., *Vasostatin, a calreticulin fragment, inhibits angiogenesis and suppresses tumor growth.* J Exp Med, 1998. **188**(12): p. 2349-56.

204. Chatterjee, D. and A. Powell, *Renal hemangioendothelioma.* Int Surg, 1982. **67**(4): p. 373-5.

205. Brizard, C., et al., *Cardiac hemangiomas.* Ann Thorac Surg, 1993. **56**(2): p. 390-4.

206. Stetler-Stevenson, W.G., *Matrix metalloproteinases in angiogenesis: a moving target for therapeutic intervention.* J Clin Invest, 1999. **103**(9): p. 1237-41.

207. Intengan, H.D. and E.L. Schiffrin, *Vascular remodeling in hypertension: roles of apoptosis, inflammation, and fibrosis.* Hypertension, 2001. **38**(3 Pt 2): p. 581-7.

208. Intengan, H.D., et al., *Resistance artery mechanics, structure, and extracellular components in spontaneously hypertensive rats : effects of angiotensin receptor antagonism and converting enzyme inhibition.* Circulation, 1999. **100**(22): p. 2267-75.